The (Mis)Allocation Channel of Climate Change

Evidence from Global Firm-level Microdata *

Tianzi Liu †
Cornell University

Zebang Xu ‡
Cornell University

January 2025

Click here for the latest version

Abstract

An extensive literature has documented the negative effect of global warming on aggregate productivity, but we know little about the micro origins of this relationship. This paper identifies and quantifies a novel channel—*the impact of extreme temperature on capital misallocation*—as a key driver of aggregate climate damage. Using global firm-level microdata from 32 countries, we provide causal evidence that a day with extreme heat (>30°C) increases the dispersion of marginal revenue products of capital (MRPK) across firms by 0.31 log points, implying a 0.11% annual aggregate TFP loss for an average region-sector. This effect is more pronounced in hotter and more economically developed regions. Taking future adaptation and development into account, our estimates suggest a global aggregate TFP loss of 36.73% from the misallocation channel by the end of the century under the SSP3-4.5 scenario, relative to 2019. To explain the mechanisms, we develop a firm dynamics model featuring heterogeneous temperature sensitivities both within and across firms. The model predicts that inaccurate temperature forecasts and heightened productivity volatility in extreme climates jointly exacerbate capital misallocation. We find strong evidence for these mechanisms in the data. The estimated model reveals that climate-induced misallocation costs 9% of global TFP annually and accounts for 9% of cross-country productivity differences as well as 15% of income inequality. These findings emphasize the importance of incorporating firm-level heterogeneity into climate policies and highlight improving mid-range weather forecast accuracy as a cost-effective adaptation strategy.

*We are grateful to our advisors, Ryan Chahrour, Kristoffer Nimark, Ivan Rudik, Ezra Oberfield and Mathieu Taschereau-Dumouchel for their continued guidance and support. This paper has also benefited from discussions with Levon Barseghyan, Julieta Caunedo, Luming Chen, Tomás Domínguez-Iino, Pablo Ottonello, Diego Restuccia, Jeffrey Shrader, and seminar participants at Columbia Climate School, Cornell Macro Lunch and Cornell SEERE Seminar, the 2024 Econometric Society NASM, CU Environmental & Resource Economics Workshop and SED Winter Meeting 2024. We thank the Structural Transformation and Economic Growth (STEG) Research programme for supporting this research. First draft was circulated on February 16th, 2024.

†Department of Applied Economics and Management, Cornell University (email:tl567@cornell.edu).

‡Department of Economics, Cornell University (email:zx88@cornell.edu).

1 Introduction

Rising temperatures due to climate change have been estimated to cause sizable aggregate economic losses. A natural question then is: what are the underlying drivers of these large economic losses from temperature? Research on this question has largely focused on how temperature worsens production technology, often interpreted as damages to physical productivity. At the micro level, empirical work has shown that extreme temperature conditions can affect within-firm productivity, especially labor productivity (e.g. Zhang et al. 2018; Somanathan et al. 2021). At the macro level, a mix of structural and empirical studies prioritizes aggregate productivity damage as the primary effect of climate change (e.g. Barrage and Nordhaus 2023; Cruz and Rossi-Hansberg 2023; Nath 2023). These studies benchmark their results in models of efficient economies, with little to no role for micro-level distortions.

Our paper adopts a different approach. Instead of focusing solely on physical productivity losses due to rising temperatures, we study how climate change results in aggregate TFP losses by increasing capital misallocation across firms, in the spirit of the seminal work by Hsieh and Klenow (2009). The misallocation channel should come as no surprise. For instance, consider a regional economy consisting of firms with varying degrees of heat sensitivity: some are heat-loving, while others are heat-sensitive. Although all firms endure the same regional heat shocks, the impact may vary significantly. Heat-loving firms tend to be less affected and remain more productive compared to heat-sensitive firms. Given that capital is generally hard to adjust in the short term, a heat shock affecting all firms would lead to dispersion in capital returns across firms, with heat-loving firms having higher marginal revenue products of capital (MRPK) than heat-sensitive ones. This is a clear case of climate-induced misallocation: aggregate productivity and output could increase if more capital was reallocated from heat-sensitive firms to heat-loving ones that have higher marginal products. Therefore, the *across-firm* misallocation channel of climate change could result in depressed aggregate TFP. The misallocation channel has direct implications for adaptation policy: policies should aim not only to mitigate average damage but also to reduce disparities in firms' adaptability to climate change.

Our goals in this paper are threefold: first, to causally identify the misallocation channel using temperature shocks and assess its quantitative impact under future climate change scenarios; second, to understand the drivers of climate-induced misallocation from a firm dynamics perspective; and third, to uncover novel implications for climate mitigation and adaptation policies suggested by the misallocation channel.

We begin by developing a climate-TFP accounting framework, reminiscent of Hsieh and Klenow (2009). Our accounting model features heterogeneous firms with climate-driven input distortions that can unevenly affect the marginal products of factors across firms. This framework allows us to decompose the region-sector level aggregate TFP into a set of firm-level sufficient statistics, which measure the efficient frontier (i.e., technology) and losses from capital misallocation. Specifically, the cost of capital misallocation is measured by the variance of (log) MRPK across firms in a given year at the region-sector level. We can thus exploit panel variations in across-firm MRPK dispersion resulting from exogenous temperature shocks to causally identify the extent of misallocation stemming from temperature-related distortions.

To measure the dispersion in the marginal products within individual sectors in each subnational region annually, we use firm-level data from 30 European countries extracted from the BvD Orbis dataset, as well as data from China and India obtained from government-conducted surveys. We construct historical climate variables and temperature forecasts for each region using the ERA5-Land gridded daily temperature data from the European Centre for Medium-Range Weather Forecasts (ECMWF). Our sample covers regions with a wide range of economic and climatic conditions. Our estimation reveals a U-shaped pattern: both extreme heat and cold increase measured capital misallocation. Notably, an extra hot day with a temperature above 30°C (86°F) relative to a day in the 5-10°C (41-50°F) range within a year increases MRPK dispersion by about 0.31 log points, which translates to a 0.11% annual aggregate TFP loss. Our findings also suggest that the misallocation channel is a dominant force in aggregate climate damage, given that technical efficiency losses from heat are estimated to be only one-fifth as large as misallocation losses. Importantly, we estimate the heterogeneous effects of temperature on misallocation across long-run regional climates and income levels. We find that the effect of heat shocks on capital misallocation is more pronounced in hotter and more economically developed regions, indicating limited potential for market adaptation to mitigate aggregate misallocation losses as economies develop and climates warm over the long run. Moreover, the estimated heterogeneous effects based on our microdata align remarkably well with estimates derived from aggregate data (i.e., country-level GDP per capita).

What do our estimates imply for the misallocation cost of future climate change? We project the impact of global warming on misallocation-induced TFP loss by the end of the century using our estimates of the heterogeneous temperature-misallocation effect. Coupled with the climate projections from the CMIP6 model and income projections from the OECD Env-Growth model under the SSP3-4.5 scenario, our estimates indicate that, compared to current income and climate levels, the global cost of climate-induced misallocation will amount to 36.73% of aggregate TFP by the end of the century. Empirically, the projected loss can be decomposed into three channels: a 2.13% contribution from the shifted daily temperature distribution, 19.46% from the income effect of projected economic development, and 11.34% from the level effect of the long-run average temperature increase. The projected losses are large and growing over time as more regions transition into richer and hotter economies with more extreme temperature realizations. The magnitude of these estimates is comparable to the projected impacts reported by Burke, Hsiang, and Miguel (2015) and Bilal and Känzig (2024).

The second goal of our paper is to understand the drivers of the identified climate-induced misallocation. To explain why both the shock distributions and levels of temperature are relevant for the dispersion in capital returns, we develop a firm dynamics model featuring time-to-build capital and rich temperature-productivity interactions. Specifically, we allow firms' productivity to be heterogeneous in their persistent and idiosyncratic sensitivities to temperature. The *persistent* sensitivity reflects a firm's specific characteristics and whether it is heat-loving or heat-averse by nature of its production (or demand). Persistent sensitivity is assumed to be known by the firm and to affects its capital investment decisions. For example, when anticipating future heat, a heat-averse firm will invest less than an average firm due to its relatively lower expected productivity. The *idiosyncratic* sensitivity, on the other hand, is randomly as-

signed to each firm at each period. It reflects the increased likelihood of severe disruptions at the firm level, such as plant-level fire hazards, equipment failures, or operational shutdowns, associated with extreme climates. As idiosyncratic sensitivity is unknown to the firm ex-ante, it does not affect the firm's capital investment decisions (to the first order). However, it generates unexpected productivity shocks and, consequently, affects the firm's MRPK upon realization.

The heterogeneity in persistent and idiosyncratic sensitivities across firms shapes two channels through which temperature affects misallocation. First, shifts in the *level* of temperature (toward extreme heat or cold), operating through idiosyncratic sensitivities, would increase the probability of experiencing extreme events across all firms. Such regions experience higher temperature-induced damage volatility across firms and, consequently, greater capital misallocation. Second, unexpected *shocks* in temperature impact investment returns differentially across firms based on their persistent sensitivities. For example, an unexpected heat shock reduces the MRPK for heat-averse firms but might raise the return for heat-loving ones. From an ex-post perspective, heat-averse firms, anticipating higher productivity than realized, over-invested in capital. Therefore, greater temperature forecast accuracy could lead to more efficient capital allocation across firms and raise aggregate TFP. Overall, these two channels closely explain our reduced-form results: the *level effect* of temperature, through damage volatility, explains why a region-sector's geographical location and long-run climates matter for capital misallocation, while the *forecast error effect* explains why larger weather shocks lead to increased misallocation.

We empirically test the mechanisms of our model by exploiting variations at both the firm and region-sector levels. First, we examine the link between heterogeneous sensitivities and differential MRPK responses to temperature shocks using firm-level panel data. As firm-specific sensitivities are hard to measure directly, we use firm size and AC installation as proxies. This approach allows us to test how firms' MRPKs respond heterogeneously to identical heat shocks within a region-sector. Our estimates reveal that heat shocks significantly lower the MRPK for smaller firms and firms without AC but have minimal impact on the MRPK for larger firms and AC-equipped firms, as they are less sensitive to temperature. Additionally, the role of firm size as a determinant of heterogeneous sensitivities helps rationalize the income effect identified in our reduced-form regression. We find that regions with higher levels of economic development exhibit greater dispersion in firm sizes, leading to greater differences in adaptability to shocks among firms. This, in turn, results in higher dispersion of persistent sensitivity across firms and increased susceptibility to misallocation due to temperature shocks at the aggregate level.

Next, we estimate and evaluate the quantitative implications of the level and forecast error effects using model-implied regressions. We empirically test the level effect by estimating how temperature levels non-linearly affect TFP volatility and MRPK dispersion across firms at the region-sector level. Our findings confirm the model's predictions that temperature extremes increase damage volatility: TFP volatility exhibits a U-shaped relationship with temperature. We identify an optimal temperature of around 12-13°C, at which point TFP volatility reaches its lowest level, thereby imposing the least burden on allocative efficiency and aggregate TFP through the level effect of misallocation. We also provide direct evidence of the

forecast error effect using forecast data from the monthly long-range temperature forecasts released by ECMWF (Copernicus Climate Change Service and Climate Data Store 2018). By aggregating these monthly long-run temperature forecast errors at the region-year level, the model-induced regression shows that, conditional on realized temperature, a 1°C error in temperature forecasts for all months leads to at least a 1.6 log-point increase in MRPK dispersion. Such an increase in capital misallocation is equivalent to an approximate 0.58% annual aggregate TFP loss when compared to the perfect information counterfactual. Our findings suggest that temperature forecast errors are costly: unexpected temperature shocks lead to dispersion in investment mistakes among firms due to their varying sensitivity to heat. Therefore, our model highlights the aggregate importance of accurate temperature forecasts as they increase the allocative efficiency of capital.

Using the model parameters identified in the model-induced regression, we quantitatively assess the global cost of climate-induced capital misallocation, demonstrating that permanent climate differences and imperfect weather forecasts together impose substantial productivity losses. Combining the estimated model with granular climate and forecast data from around 4,000 regions since 1981, we find that eliminating climate-related dispersion in firm-level MRPK would raise global TFP by about 8.9%. Most of this loss arises from persistent climate deviations from the optimum, contributing around 8.34% to the TFP gap, while forecast errors account for only 0.56%. Over time, rising global temperatures since 1981 have further displaced regions to be more volatile, lowering aggregate TFP by an additional 2.49%. Although improvements in weather forecasts have offset some of these adverse effects, the dominant force remains the ongoing rise in global temperatures. Furthermore, our model effectively fits the cross-country dispersion and within-country evolution of the observed aggregate TFP data, and the climate-misallocation channel explains about 9% of cross-country TFP differences. Holding climate-induced misallocation at its 1981 level would have raised cumulative TFP growth since 1981 by an additional 2.36 percentage points—equivalent to roughly 36% of the observed increase of 8.9 percentage points. Our results also uncovers the role of climate in global income inequalities. Although the dispersion of global income fell from 2.09 to 0.83 from 1981 to 2019, the share attributable to climate-induced misallocation rose from about 3% to 14%, indicating that a warming climate slows the pace of income convergence and entrenches inequality by reducing aggregate productivity in hot and poor countries.

Lastly, we discuss how our findings shed new light on the design and effects of climate mitigation and adaptation policies. Specifically, we explore three types of policies that could potentially reduce the cost of climate-induced misallocation. First, we consider mitigation policies that reduce the end-of-century temperature rise from 4°C to 2°C. Our results project an avoidable TFP loss of 22% globally under RCP 2.6 compared to RCP 7.0. Compared to the benefits of avoided misallocation losses, the estimated cost of optimal mitigation policy from DICE-2016R is very moderate and largely outweighed by the benefits by 2100. Second, we evaluate the potential of improving mid-range weather forecast accuracy as an adaptation policy, which has already seen success since the 1980s and demonstrates a large benefit-cost ratio according to our model estimates. Finally, from a micro perspective, our results broadly suggest that policies reducing the "climate inequality" of impact sensitivity among firms could

mitigate the misallocation losses from extreme climate events. Policies should be directed to identifying and subsidizing firms that are productive but lack the resources to defend against heat. Our results also highlight that there need not be an equity-efficiency trade-off in the context of heterogeneous firms. If firms exhibit more uniform adaptability to temperature, the aggregate economy also achieves greater allocative efficiency.

We conclude that capital misallocation is a quantitatively important channel through which climate change affects the aggregate economy. Climate-induced misallocation stems from substantial cross-sectional firm-level heterogeneity in temperature sensitivity. The estimated loss due to misallocation across firms is considerable, indicating that the average effect of firm-level productivity loss alone is insufficient to capture the aggregate cost of climate change in the economy. Our results suggest that climate policies that solely target the average effect, while overlooking firm heterogeneity, may have limited efficacy.

Contributions to the Literature. This paper relates to a large literature on measuring the economic damages from temperature shocks and climate change. One canonical approach is to directly estimate the effect of temperature shocks on aggregate region-sector, country, or global outcomes (See Dell, Jones, and Olken 2012; Burke, Hsiang, and Miguel 2015; Lemoine 2018; Carleton et al. 2022; Nath, Ramey, and Klenow 2023; Bilal and Känzig 2024, among others). Another strand of work estimates the *average* firm- or worker-level productivity damages from climate change and explores the underlying micro-level mechanisms (Somanathan et al. 2021; Acharya, Bhardwaj, and Tomunen 2023; Ponticelli, Xu, and Zeume 2023). Most studies interpret their findings as physical productivity losses resulting from climate shocks. This paper contributes to this literature by taking a conceptually different approach: we focus on how climate change could drive down aggregate productivity by causing the *across-firm* misallocation of capital. We show that a sizable portion of aggregate climate impact is *allocative* rather than purely *physical*. Our approach estimates a large causal effect of the misallocation channel from climate shocks and projects substantial TFP loss across all future climate change scenarios. Quantitatively, we uncover novel heterogeneity in climate-induced misallocation losses across regions with different levels of development and climates.

Second, regarding the macroeconomic modeling of climate change, the existing studies have incorporated climate change into workhorse macro and trade models of efficient economies (Nath 2023; Cruz and Rossi-Hansberg 2023; Bakkensen and Barrage 2021; Casey, Fried, and Gibson 2022; Rudik et al. 2021). Naturally, these models remain silent on the causes and effects of how climate change drives distortions and misallocation of productive factors in the economy. This paper provides a static general equilibrium framework to measure the costs of the temperature-induced misallocation channel using an easy-to-implement sufficient statistics approach. We also build a firm dynamics model to better understand the endogenous mechanisms behind climate-induced misallocation, which stem from *firm-level heterogeneity*, a previously overlooked but quantitatively significant dimension in the climate-macro literature. Very few studies have explored the allocative effect of climate change. Perhaps the closest to our paper is the contemporaneous work by Caggese et al. (2023). They project how the future geographical distribution of temperature shocks in Italy might lead to differential factor

productivity of firms across micro-regions under future global warming, and thus allocative efficiency losses could be predicted. In contrast, our paper provides a direct causal estimate of climate impacts on within-region *marginal product dispersion* across firms using historical regional climate variations and firm-level data drom 32 countries globally. It is a direct measure of misallocation (as in Hsieh and Klenow 2009 and Sraer and Thesmar 2023) and captures *all channels* of climate-induced misallocation, not just those stemming from the geographical distribution of temperature.

Third, our research contributes to the burgeoning literature on the impacts and economic value of weather forecasts. Recent work evaluates the market internalization of weather forecasts (Schlenker and Taylor 2021), agents updating beliefs in response to forecasts (Shrader 2023; Kala 2017), and the economic values of reducing mortality with more accurate forecasts (Shrader, Bakkensen, and Lemoine 2023). We show evidence that inaccuracies in forecasts result in more frequent investment mistakes in the cross-section of firms and thus reduce aggregate productivity. Our research supports micro-level findings at the macro level and emphasizes the vital role of accurate weather forecasting in reducing economic disruptions and boosting productivity.

Finally, we contribute to the literature on misallocation. Since the seminal contributions by Restuccia and Rogerson (2008) and Hsieh and Klenow (2009), a large body of work has studied the aggregate (e.g., Gopinath et al. 2017, David and Zeke 2021) and firm-level (e.g., Asker, Collard-Wexler, and De Loecker 2014, David and Venkateswaran 2019, Baqaee and Farhi 2019) drivers of misallocation. Our paper adds to this literature by demonstrating that environmental factors, such as temperature variations and climate change, are also sources of misallocation and might become increasingly important as global warming worsens. Additionally, our paper connects to a small but growing body of literature that studies the causal identification of the drivers of misallocation using (quasi-)natural experiments (Sraer and Thesmar 2023, Bau and Matray 2023, among others). These studies employ exogenous shocks to explore the causes and consequences of misallocation. We expand on this literature by using exogenous temperature variations to examine the impacts of climate change as a driver of misallocation.

The structure of the paper is organized as follows. In Section 2, we develop our climate growth accounting framework. Our data sources and methodology for constructing variables are detailed in Section 3. Section 4 presents our empirical identification strategy and reduced-form results. Section 5 introduces the firm dynamics model to explain the underlying mechanisms. Evidence at the firm level, which tests the proposed channels, is provided in Section 6. Section 7 offers evidence and quantitative results of the model at the aggregate level. We discuss implications for mitigation and adaptation policies in Section 8, and we conclude in Section 9.

2 A Framework for Climate TFP Accounting

In this section, we develop a climate-TFP accounting framework by extending Hsieh and Klenow (2009)'s distorted closed-economy model of heterogeneous firms to flexibly capture climate's firm-specific effects on productivity, demand, and wedges, and to quantify their

aggregate implications. We show how climate shocks might affect aggregate productivity through two distinct channels in a distorted economy: lowering micro-level productivity (technology) and increasing the dispersion in marginal products (misallocation). We derive measurable sufficient statistics for both channels, guiding our empirical strategy in Section 4. We deliberately abstract from the exact mechanisms driving climate-related wedges to keep the accounting framework general. This allows our empirical strategy to measure *all* channels through which climate might lead to across-firm marginal product dispersions. We will return to the question of *why* in Sections 5, 6, and 7.

2.1 Model Preliminaries

Consider an economy comprised of R regions indexed by r, and S sectors indexed by s. We use $n = (r, s)$ to denote a region-sector pair and there are $N = R \cdot S$ region-sector pairs. We focus on the aggregation of firm-level economic activities within a region-sector pair. We allow all fundamentals of firm i in the market $n = (r, s)$ to be arbitrary functions of a general array of (current and past) regional climate conditions, $\tilde{\mathbf{T}}_{rt}$, the aggregate states of the economy, $\tilde{\mathbf{X}}_{nt}$, and the idiosyncratic states of firm i, $\tilde{\mathbf{Z}}_{nit}$. [1] This general representation accommodates a wide range of structural models in our accounting framework.

2.2 Aggregation Model with Micro Effects of Climate Conditions

We now describe the aggregation model and how we incorporate the micro effects of climate conditions into the model.

Aggregate Region-Sector Production. Total output Y_{nt} for region-sector n is given by a constant elasticity of substitution (CES) production function of differentiated products of measure J_n:[2]

$$Y_{nt} = \left(\int_0^{J_n} B_{nit}^{\frac{1}{\sigma_n}} Y_{nit}^{\frac{\sigma_n - 1}{\sigma_n}} di \right)^{\frac{\sigma_n}{\sigma_n - 1}}, \tag{1}$$

where B_{nit} is a good-specific preference shifter, Y_{nit} denotes the output of firm i and $\sigma_n > 1$ is the elasticity of substitution between products within region-sector n. Profit maximization of industry output producers leads to the inverse demand function for the output of each firm, Y_{nit}:

$$Y_{nit} = B_{nit} Y_{nt} \left[\frac{P_{nit}}{P_{nt}} \right]^{-\sigma_n}, \tag{2}$$

where $P_{nt} = \left(\int_0^{J_n} B_{nit} P_{nit}^{1-\sigma_n} di \right)^{\frac{1}{1-\sigma_n}}$ is the price index in region-sector n. The demand shifter $B_{nit} \equiv B_{ni}(\tilde{\mathbf{T}}_{rt}, \tilde{\mathbf{X}}_{nt}, \tilde{\mathbf{Z}}_{nit})$ is a firm-specific function of climate and economic conditions, cap-

1. For concreteness, one can think of current climate conditions, $\mathbf{T}_{rt}$, as realizations of daily temperature, precipitation, and other types of extreme weather events. $\mathbf{X}_{nt}$ and $\mathbf{Z}_{nit}$ can be interpreted as other aggregate and firm-specific productivity or demand shocks. The data generating process of $(\tilde{\mathbf{T}}_{rt}, \tilde{\mathbf{X}}_{nt}, \tilde{\mathbf{Z}}_{nit})$ could be stochastic. We use the tilde notation, $(\tilde{\mathbf{T}}_{rt}, \tilde{\mathbf{X}}_{nt}, \tilde{\mathbf{Z}}_{nit})$, to denote the history of realizations up to date t. Also, we do not take a stance on whether $\mathbf{X}_{nt}$ and $\mathbf{Z}_{nit}$ depend on $\mathbf{T}_{rt}$.

2. In theory, J_n, the local variety, could also vary over time to capture how climate might affect firm entry and exit. However, accurately measuring these dynamics within a granular region-sector pair over time is challenging due to data limitations, particularly for cross-country analysis. Therefore, the model does not address this aspect.

turing how certain goods or services may be less desirable in hotter climates.[3]

Firm-level Production. Each product is produced by a single firm with a constant returns-to-scale Cobb-Douglas production function

$$Y_{nit} = A_{nit}\, K_{nit}^{\alpha_{Kn}} L_{nit}^{\alpha_{Ln}}, \tag{3}$$

where $A_{nit} \equiv A_{ni}(\tilde{\mathbf{T}}_{rt}, \tilde{\mathbf{X}}_{nt}, \tilde{\mathbf{Z}}_{nit})$ denotes physical productivity of firm i, and K_{nit} and L_{nit} are capital stock and labor input employed by i.[4] The parameters satisfy $\alpha_{Kn} + \alpha_{Ln} = 1$. The physical productivity of firm i is modeled as a firm-specific function, $A_{nit} \equiv A_{ni}(\tilde{\mathbf{T}}_{rt}, \tilde{\mathbf{X}}_{nt}, \tilde{\mathbf{Z}}_{nit})$, to capture the different sensitivity to heat (or cold) among different firms within and across various region-sectors. Such heterogeneity can be potentially attributed to the distinct nature of production processes across firms and varying levels of adaptability to climate conditions.[5] Even within the same region-sector, heterogeneity arises: in agriculture, rainfed farms endure more heat stress than irrigated farms (Piao et al. 2010), while in manufacturing, workers with AC installations are less vulnerable to heat than those without (Somanathan et al. 2021).

Wedges. Each firm faces a variety of frictions, including climate-related ones. Regardless of their structural origins and for pure accounting purposes, we describe them as time-varying and firm-specific wedges that distort the static equilibrium decisions of firms operating in otherwise (monopolistically) competitive markets. Subject to the inverse demand and wedges, each firm i engages in monopolistic competition and optimally chooses its quantity of inputs and price to maximize profits:

$$\max_{P_{nit}, K_{nit}, L_{nit}} \left(1 - \tau_{nit}^{Y}\right) P_{nit} \underbrace{A_{nit} K_{nit}^{\alpha_{Kn}} L_{nit}^{\alpha_{Ln}}}_{Y_{nit}} - \left(1 + \tau_{nit}^{K}\right) R_{nt} K_{nit} - \left(1 + \tau_{nit}^{L}\right) W_{nt} L_{nit} \tag{4}$$

$$\text{subject to : } Y_{nit} = B_{nit} Y_{nt} \left[\frac{P_{nit}}{P_{nt}}\right]^{-\sigma_n},$$

where R_{nt} is the user cost of capital and W_{nt} is the wage. The output wedge τ_{nit}^{Y} distorts output prices, while the input wedges τ_{nit}^{F} for $F \in \{K, L\}$ changes the effective marginal cost of each factor from its market rate. We assume all firms take these wedges as given for now and turn to model the endogenous nature of these frictions and their relationship with climate change in Section 5. As with demand shifters and productivity, we assume they are firm-specific functions of climate and of the region-sector and firm states.

What might appear as wedges in this accounting exercise? For instance, the output wedge $\tau_{nit}^{Y} \equiv \tau_{ni}^{Y}(\tilde{\mathbf{T}}_{rt}, \tilde{\mathbf{X}}_{nt}, \tilde{\mathbf{Z}}_{nit})$ reflects potential heterogeneity in revenue taxes and markups rela-

3. This is particularly evident in service industries where climate can sharply affect consumer behavior. For example, Zivin and Neidell (2014) find that heat shocks shift Americans from outdoor to indoor recreational activities (e.g., away from recreational fishing as found by Dundas and Haefen 2020). Anecdotal examples in food services include ice-cream parlors versus hot tea shops.

4. A_{nit} is a measure of quantity-based total factor productivity (TFPQ), reflecting the overall efficiency with which the firm uses its inputs to produce units of *physical output*. TFPQ cannot be directly measured in the absence of price or quantity data, barring any additional structural assumptions (see, for example, Bils, Klenow, and Ruane 2021).

5. For the cross-country heterogeneity in productivity damage due to adaptation, see Nath (2023).

tive to the Dixit-Stigliz benchmark. These market imperfections could potentially be amplified by temperature shocks changing the local market structure (Ponticelli, Xu, and Zeume 2023). Similarly, input wedges, $\tau^F_{nit} \equiv \tau^F_{ni}(\tilde{\mathbf{T}}_{rt}, \tilde{\mathbf{X}}_{nt}, \tilde{\mathbf{Z}}_{nit})$, capture all channels through which firms are disincentivized from using inputs $F \in \{K, L\}$, as if they were effectively paying higher factor prices.[6] For instance, firms with more exposure to adverse climate conditions may encounter worse financing frictions (Ginglinger and Moreau 2023). Importantly, in the context of dynamic input choices with adjustment frictions, such as capital, the wedge function $\tau^K_{ni}(\tilde{\mathbf{T}}_{rt}, \cdot)$ also accounts for ex-post investment mistakes triggered by unanticipated temperature shocks (e.g. when a heat-averse firm invested too much capital before a severe heat wave), in reminiscence of Asker, Collard-Wexler, and De Loecker (2014) and David, Hopenhayn, and Venkateswaran (2016).

Equilibrium. The total factor supply in the region-sector n are given by $K_{nt} = \sum_i K_{nit}$ and $L_{nt} = \sum_i L_{nit}$.[7] The equilibrium allocations in a region-sector depend on the set of fundamentals $(\{B_{nit}\}_i, \{A_{nit}\}_i, \{\tau^Y_{nit}\}_i, \{\tau_{nit}\}_{F;i}, \{F_{nt}\}_F)$. Given preference shifter B_{nit}, physical productivity A_{nit}, output distortions τ^Y_{nit}, factor distortions $\{\tau^F_{nit}\}_F$ for all firms i, aggregate prices P_{nt}, and total factor supply of K_{nt} and L_{nt}, an equilibrium in region-sector n consists of goods prices P_{nit}, factor prices $\{P^F_{nt}\}_F$, and a set of factor allocation $\{F_{nit}\}_{F,i}$ that solves all firms' problems in (4) and all markets clear. We call the equilibrium defined by $(\{B_{nit}\}_i, \{A_{nit}\}_i, \{\tau^Y_{nit}\}_i, \{\tau_{nit}\}_{F;i}, \{F_{nt}\}_F)$ the *distorted equilibrium* and the equilibrium defined by $(\{B_{nit}\}_i, \{A_{nit}\}_i, \{0\}_i, \{0\}_{F;i}, \{F_{nt}\}_F)$ the *efficient equilibrium*.[8] We will use an asterisk (*) to denote the efficient equilibrium outcomes.

Wedges and Misallocation of Inputs. As these wedges distort firm-level input choices, they also create measurable differences in marginal products across firms. For any input $F \in \{K, L\}$, the firm's optimality condition implies that the marginal revenue product of factor F (MRPF),

$$\text{MRPF}_{nit} = \alpha_{F_n} \frac{\sigma_n - 1}{\sigma_n} \frac{P_{nit} Y_{nit}}{F_{nit}} = \frac{1 + \tau^F_{ni}(\tilde{\mathbf{T}}_{rt}, \cdot)}{1 - \tau^Y_{ni}(\tilde{\mathbf{T}}_{rt}, \cdot)} P^F_{nt}, \tag{5}$$

is proportional to the firm's revenue-to-factor ratio and must equal the wedge-adjusted market price, $\frac{1+\tau^F_{ni}(\tilde{\mathbf{T}}_{rt}, \cdot)}{1-\tau^Y_{ni}(\tilde{\mathbf{T}}_{rt}, \cdot)} P^F_{nt}$. A higher input wedge $1 + \tau^F_{ni}(\tilde{\mathbf{T}}_{rt}, \cdot)$ increases the effective cost of factor F, discouraging its use and thus elevating MRPF. Conversely, a lower output wedge $\tau^Y_{ni}(\tilde{\mathbf{T}}_{rt}, \cdot)$ raises the effective price of the firm's output, encouraging the use of factor F and consequently lowering MRPF. Therefore, heterogeneity in how wedges respond to climate change can alter the cross-sectional dispersion of MRPF—often termed "misallocation"—as inputs may not flow to the firms that would use them most efficiently. The wedges would thus also change

6. Naturally, for a firm to be active, it is necessary that all prices are positive, which requires $1 - \tau^Y_{nit} > 0$ and $1 + \tau^F_{nit} > 0$.

7. The total factor supply is treated as exogenously given every period. We could also model the total factor supply to be region-sector specific functions of the form: $L_{nt} := L_n(\tilde{\mathbf{T}}_{rt}, \cdot), K_{nt} := K_n(\tilde{\mathbf{T}}_{rt}, \cdot)$, but this plays little role in our TFP accounting.

8. Again, we stress that, in the accounting framework, efficiency is defined in a static and unconstrained sense.

the size of the firm. By writing down firm i's sales share θ_{nit} in n,

$$\theta_{nit} = \frac{P_{nit}Y_{nit}}{\int_0^{J_n} P_{nit}Y_{nit}di} = \frac{B_{nit}A_{nit}^{\sigma_n-1}\frac{\left(1-\tau_{nit}^{Y}\right)^{(\sigma_n-1)}}{\prod_{F\in\{K,L\}}\left(1+\tau_{nit}^{Fn}\right)^{\alpha_{Fn}(\sigma_n-1)}}}{\int_0^{J_n} B_{nit}A_{nit}^{\sigma_n-1}\frac{\left(1-\tau_{nit}^{Y}\right)^{(\sigma_n-1)}}{\prod_{F\in\{K,L\}}\left(1+\tau_{nit}^{Fn}\right)^{\alpha_{Fn}(\sigma_n-1)}}di}, \tag{6}$$

we see that, unsurprisingly, a positive input wedge makes the firm inefficiently small and negative output wedge makes the firm inefficiently large. We proceed to explicitly characterize how these wedges lead to the equilibrium (mis-)allocation of factors as follows.

Proposition 1 ***Equilibrium (Mis)Allocation.*** *The (log) ratio of firm i's distorted and efficient equilibrium allocation of factor, $\frac{F_{nit}}{F_{nit}^*}$,*

$$\log(\frac{F_{nit}}{F_{nit}^*}) = \underbrace{-\log(\frac{1+\tau_{nit}^F}{1+\tau_{nt}^F})}_{\substack{\textit{relative wedge}\\ \textit{effect}}} + \underbrace{\log(\frac{\theta_{nit}}{\theta_{nit}^*})}_{\substack{\textit{size}\\ \textit{effect}}}$$

is decreasing in the ratio of firm i's own factor wedge comparing to the aggregate factor wedge $1+\tau_{nt}^F \equiv \left(\int_0^{J_n}\frac{1}{(1+\tau_{nit}^F)}\theta_{nit}di\right)^{-1}$, and increasing in the ratio of the firm's sales share θ_{nit} comparing to its efficient counterfactual θ_{nit}^*. Moreover, the efficient allocation of inputs, $\frac{F_{nit}^*}{F_{nt}} = \theta_{nit}^* = \frac{B_{nit}A_{nit}^{\sigma_n-1}}{\int_0^{J_n} B_{nit}A_{nit}^{\sigma_n-1}di}$, is entirely determined by firm i's relative preference shifter and physical productivity within the region-sector and aligns with sales share θ_{nit}^*.

Proof. See Appendix A.2. ■

Proposition 1 highlights the two effects through which wedges distorts the equilibrium allocation of factor F. The *relative wedge effect* captures how a higher input wedge on F makes it more expensive firm i pays for factor F relative to the region-sector's average. Firm i is more discouraged from employing factor F and thus ends up with using less of it than under the efficient benchmark. The *size effect* captures how any wedges firm i faces would make the firm inefficiently small, leading to a smaller sales share θ_{nit} compared to efficient level θ_{nit}^* and thus suppresses the usage of all inputs.

First, they shift the efficient allocation by directing more capital to firms that suffer less heat damage or produce goods with higher demand under hot conditions. Second, they can introduce heterogeneous frictions in the capital market—such as adjustment costs or financing constraints—that distort firms' cost structures and potentially prevent some productive firms from securing an optimal amount of capital.

2.3 Aggregation, TFP Decomposition and Cost of Misallocation

We proceed to perform aggregation in this accounting framework. We adopt a widely-used assumption in the misallocation literature (Hsieh and Klenow 2009 and Sraer and Thesmar 2023) that productivity, demand shifter and all associated wedges follow a joint log-normal distribution across firms in any region-sector-year pair, which holds very well in the data.

More formally, we assume that for any given set of arguments $\left(\tilde{\mathbf{T}}_{rt}, \tilde{\mathbf{X}}_{nt}, \left\{\tilde{\mathbf{Z}}_{nit}\right\}_i\right)$, the joint distribution of the realized values of the sets of functions, $\mathbf{S}_{nit} = (B_{ni}(\cdot), A_{ni}(\cdot), 1+\tau^Y_{ni}(\cdot), 1+\tau^K_{ni}(\cdot), 1+\tau^L_{ni}(\cdot))$, can be characterized as follows:

$$\log(\mathbf{S}_{nit}) \sim \mathcal{N}\left(\boldsymbol{\mu}_n(\tilde{\mathbf{T}}_{rt}, \tilde{\mathbf{X}}_{nt}), \boldsymbol{\Sigma}_n(\tilde{\mathbf{T}}_{rt}, \tilde{\mathbf{X}}_{nt})\right). \tag{7}$$

Here, $\boldsymbol{\mu}_n(\tilde{\mathbf{T}}_{rt}, \tilde{\mathbf{X}}_{nt})$ represents the mean vector of firm-level fundamentals, while $\boldsymbol{\Sigma}_n(\tilde{\mathbf{T}}_{rt}, \tilde{\mathbf{X}}_{nt})$ is the covariance matrix of these fundamentals across firms. Each element of these are smooth functions of their respective arguments, since they are population moments of $\mathbf{S}_{nit}$ and each element of which themselves are smooth in its arguments. For tractability, we adopt the aggregation notation of Krusell and Smith (1998) that the distribution of firm-level fundamentals $\tilde{\mathbf{Z}}_{nit}$ (over i) can be summarized by a finite set of moments and stacked into the aggregate states of the economy $\tilde{\mathbf{X}}_{nt}$. Thus, $\boldsymbol{\mu}_n$ and $\boldsymbol{\Sigma}_n$ are region-sector-specific functions of only $\tilde{\mathbf{T}}_{rt}$ and $\tilde{\mathbf{X}}_{nt}$. The log-normality assumption allows us to transparently show how micro-level wedges are translated into losses in aggregate productivity:

Proposition 2 ***Aggregation and TFP Decomposition.*** *Under the log-normality assumption, each region-sector n admits an aggregate production function of the form*

$$Y_{nt} = TFP_{nt} K_{nt}^{\alpha_{Kn}} L_{nt}^{\alpha_{Ln}}, \tag{8}$$

where the region-sectoral aggregate Total Factor Productivity $TFP_{nt} := TFP_n\left(\tilde{\mathbf{T}}_{rt}, \tilde{\mathbf{X}}_{nt}\right)$ can be decomposed as follows:

$$\log TFP_n(\tilde{\mathbf{T}}_{rt}, \cdot) = \underbrace{\frac{1}{\sigma_n - 1}\log\left[J_n \mathbb{E}_i\left[B_{ni}(\tilde{\mathbf{T}}_{rt}, \cdot)\left(A_{ni}(\tilde{\mathbf{T}}_{rt}, \cdot)\right)^{\sigma_n - 1}\right]\right]}_{\text{Technology}(\log TFP^E_{nt})}$$

$$\text{Misallocation Loss} \begin{cases} \underbrace{-\frac{\sigma_n}{2}\operatorname{var}_{\log\left(1-\tau^Y_{ni}\right)}(\tilde{\mathbf{T}}_{rt}, \cdot)}_{\text{Output Wedge Dispersion}} \underbrace{-\sum_{F\in\{K,L\}} \frac{\alpha_{Fn} + \alpha^2_{Fn}(\sigma_n - 1)}{2}\operatorname{var}_{\log\left(1+\tau^F_{ni}\right)}(\tilde{\mathbf{T}}_{rt}, \cdot)}_{\text{Factor Wedge Dispersion}} \\ \underbrace{+\sigma_n \sum_{F\in\{K,L\}} \alpha_{Fn}\operatorname{cov}_{\log\left(1-\tau^Y_{ni}\right),\log\left(1+\tau^F_{ni}\right)}\left(\tilde{\mathbf{T}}_{rt}, \cdot\right)}_{\text{Output-Factor Mixed Distortion}} \\ \underbrace{-(\sigma_n - 1)\alpha_{Kn}\alpha_{Ln}\operatorname{cov}_{\log\left(1+\tau^K_{ni}\right),\log\left(1+\tau^L_{ni}\right)}\left(\tilde{\mathbf{T}}_{rt}, \cdot\right)}_{\text{Factor Mixed Distortion}}. \end{cases} \tag{9}$$

Proof. See Appendix A.3. ■

Proposition 2 decomposes the aggregate TFP into two terms: *technology* and *misallocation loss*. The technology component, $\log \text{TFP}^E_{nt} = \frac{1}{\sigma_n - 1}\log\left[J_n \mathbb{E}_i\left[B_{ni}(\tilde{\mathbf{T}}_{rt}, \cdot)\left(A_{ni}(\tilde{\mathbf{T}}_{rt}, \cdot)\right)^{\sigma_n - 1}\right]\right]$, is a CES aggregation of demand shifter and physical productivity of all firms. This represents

the production possibility frontier of the economy. We label this term *technology* in the spirit of Basu and Fernald (2002) and Baqaee and Farhi (2019).

The rest of the terms represent the TFP cost of wedges in the economy, referred to as *misallocation loss*. All the variance and covariance terms are elements in the variance matrix $\mathbf{\Sigma}_n(\tilde{\mathbf{T}}_{rt}, \tilde{\mathbf{X}}_{nt})$ in Equation 7, and are thus themselves functions of climate and other economic fundamentals. They describe how these conditions would alter the distribution of wedges over the cross-section of firms. Dispersion in output wedges $\text{var}_{\log\left(1-\tau_{ni}^{Y}\right)}$ and factor input wedges $\text{var}_{\log\left(1+\tau_{ni}^{F}\right)}$ will both lead to dispersion in the marginal revenue products across firms, creating more misallocation of factors and lowering region-sector TFP. The impact of $\text{var}_{\log\left(1+\tau_{ni}^{F}\right)}$ on TFP are increasing in σ_n and α_{F_n}, as higher product substitutability and larger factor share both imply larger gains of reallocation for a given factor wedge dispersion. Furthermore, the interactions of wedges also impact productivity. All else being equal, more productivity losses occur when (1) firms facing higher tax on output are also those enduring higher input prices ($\text{cov}_{\log\left(1-\tau_{ni}^{Y}\right),\log\left(1+\tau_{ni}^{F}\right)} < 0$), and (2) firms experiencing capital distortions are also more likely to face higher labor distortions ($\text{cov}_{\log\left(1+\tau_{ni}^{K}\right),\log\left(1+\tau_{ni}^{L}\right)} > 0$). These interactions are often referred to as "mixed" distortions.

2.4 Decomposing the Impact of Climate Change on Aggregate TFP

Since all moments in Equation 9 are smooth functions of climate conditions $\tilde{\mathbf{T}}_{rt}$, we can decompose the (first-order) total impact of climate change on TFP via a set of measurable derivatives for each relevant moment. We formalize this in a case when only capital wedges are present.

Benchmark case: only capital wedges are present. We now consider a benchmark case where only capital wedges are present, as is common in the misallocation literature (see, for example, Asker, Collard-Wexler, and De Loecker 2014, David and Venkateswaran 2019, and Sraer and Thesmar 2023). This focus stems from the view that capital, unlike labor, is a more dynamic input that is often financed externally, requires significant adjustment costs, and typically cannot be reallocated on short notice. These features magnify distortions in capital usage—such as through credit frictions or investment irreversibility—and lead to potentially larger and more persistent misallocation relative to labor (Gorodnichenko et al. 2018). Consequently, how and why capital misallocation is affected by climate conditions will be the main focal point throughout the paper.

When the capital wedge is the only source of distortions in the economy within region-sector n, the MRPK of each firm i satisfies that: $\text{MRPK}_{nit} = \alpha_{Kn}\frac{\sigma_n-1}{\sigma_n}\frac{P_{it}Y_{it}}{K_{it}} \propto (1+\tau_{nit}^{K})R_{nt}$. The dispersion of capital wedges is therefore given by the variance of log(MRPK) across firms,

$$\text{var}(\log(1+\tau_{nit})) = \text{var}(mrpk_{nit}) = \text{var}\left(\log\left(\frac{P_{it}Y_{it}}{K_{it}}\right)\right), \tag{10}$$

where we define $mrpk_{nit} = \log(\text{MRPK}_{nit})$. Equation 10 shows that the cross-sectional variance of (log) capital wedges across firms is identical to the dispersion of (log) MRPK, which can be computed via the variance of log sales over capital stock given the common Cobb-Douglas technology within the region-sector-year. We can now formalize how climate conditions affect

aggregate TFP via the following Lemma:

Lemma 1 *With only capital wedges, the (first-order)impact of climate conditions on the aggregate TFP of region-sector $n = (r, s)$ can be decomposed as:*

$$\begin{aligned}\frac{d\log TFP_n(\tilde{\mathbf{T}}_{rt},\cdot)}{d\tilde{\mathbf{T}}_{rt}} &= \frac{d\ Technology_{nt}}{d\tilde{\mathbf{T}}_{rt}} - \frac{d\ Misallocation\ Loss_{nt}}{d\tilde{\mathbf{T}}_{rt}} \\ &= \frac{1}{\sigma_n-1}\frac{d\log \mathbb{E}_i\left[B_{ni}(\tilde{\mathbf{T}}_{rt},\cdot)\left(A_{ni}(\tilde{\mathbf{T}}_{rt},\cdot)\right)^{\sigma_n-1}\right]}{d\tilde{\mathbf{T}}_{rt}} \\ &\quad \underbrace{-\frac{\alpha_{Kn}+\alpha_{Kn}^2(\sigma_n-1)}{2}\frac{d\,\mathrm{var}_{mrpk_{ni}}(\tilde{\mathbf{T}}_{rt},\cdot)}{d\tilde{\mathbf{T}}_{rt}}}_{\textit{The Misallocation Channel}},\end{aligned} \tag{11}$$

where $\mathrm{var}_{mrpk_{ni}}(\tilde{\mathbf{T}}_{rt},\tilde{\mathbf{X}}_{rt}) \equiv \mathrm{var}_{\log(1+\tau_{ni}^K)}(\tilde{\mathbf{T}}_{rt},\tilde{\mathbf{X}}_{rt})$ *denotes a function capturing how n's (log)MRPK dispersion across firms changes with climate and economic conditions.*

Lemma 1 shows that the total first-order effect of climate on aggregate TFP can be fully described by changes in (i) *technology* and (ii) *capital misallocation*. The technology channel boils down to the estimation of the (semi-)elasticity of the average firm's demand-adjusted productivity to climate. More importantly to the focus of our paper, measuring the cost of climate-induced misallocation reduces to estimating $\frac{d\,\mathrm{var}_{mrpk_{ni}}(\tilde{\mathbf{T}}_{rt},\cdot)}{d\tilde{\mathbf{T}}_{rt}}$—"the misallocation channel." This result also offers practical guidance for the reduced-form approach in Section 4, which focuses on the causal estimation of $\frac{d\,\mathrm{var}_{mrpk_{ni}}(\tilde{\mathbf{T}}_{rt},\cdot)}{d\tilde{\mathbf{T}}_{rt}}$.

In theory, the derivatives of our structural objects with respect to climate conditions are globally well-defined and could vary with the long-run evolution of climate and development. However, in practice, they can only be well estimated with respect to the observed equilibrium allocations. We will address this limitation explicitly in Section 4.4 to capture the heterogeneous effect arising from long-term climate conditions and economic development.

3 Data

3.1 Global Firm-level Microdata

We compile a global sample of firm-level microdata from both developed and developing economies that include 30 European countries, China and India, which covers 38.6% of world GDP. The firm-level data for the 30 European countries are sourced from Bureau van Dijk's (BvD) Orbis database, while the data for China and India are obtained from government-conducted surveys, the China National Bureau of Statistics (NBS) Annual Survey of Industrial Firms, and the India Annual Survey of Industries (ASI). These datasets provide comprehensive financial accounting information, including revenue, fixed assets, wage bills, and employment figures. The three datasets are widely utilized in the literature and could be regarded as nationally representative.[9]

9. A significant advantage of using the Orbis database for European countries is that company reporting is regulatory, ensuring comprehensive coverage even for small private firms. The China NBS surveys cover all industrial

Table B.1 provides a comprehensive list of countries, year coverage, and data sources for the three datasets. For all datasets, we harmonize the sectoral classifications of all firms into eight major divisions according to the U.S. Standard Industrial Classification (USSIC) code.[10] Regions are defined to be the NUTS 3 regions in Europe, prefectures in China, and districts in India. The size of these regions is close to the size of a county in the US.

Our primary economic variables of interest are the sufficient statistics of firm-level activities that map directly into aggregate TFP at the region-sector-year level, in particular, the variance of marginal revenue product of capital across firms. Thus, for all datasets we use, we restrict ourselves to work with firm-year observations that report data on both revenue and capital stock. We measure revenue $P_{it}Y_{it}$ with the reported operating revenue in both Orbis and China NBS data, and the reported total sales in India ASI. We use the book value of gross fixed assets as a measure of firm-level capital stock K_{it}.[11] For each country, we trim the observations of extreme values of MRPK at 0.1%.

For all reduced-form analysis using region-sector-year level sufficient statistics, we restrict our sample to the region-sector-year pairs with more than 30 firm-year observations of revenue and capital stock data, to minimize the noises in the variance measures and preserve log-normality in the data. To make sure variations in these sufficient statistics are not due to changes in data collection patterns and measurement errors, we also drop the observations after which there are sudden jumps in the number of firms and aggregate sales in the region-sector. The final region-sector sample is an unbalanced sample consisting 124,567 of region-sector-year observations, covering 76,826,956 firm-year observations. For the firm-level analysis in Section 6, we include all firm-year observations in the raw data after trimming the 0.1% extreme values of all firm-level dependent variables and covariates. Below, we provide a brief overview of each of the datasets.

BvD Orbis. The firm-level data for the 30 European countries are drawn from Orbis, a database maintained by Bureau van Dijk (BvD). Orbis originates from administrative records collected at the firm level, primarily by each country's local Chambers of Commerce. A significant advantage of focusing on European countries with Orbis is that company reporting is regulatory, even for small private firms. It covers firms from all sectors and approximately 99 percent of the companies included are private entities.

To organize and clean the Orbis dataset, we follow the approach in Kalemli- Özcan et al. (2024), Gopinath et al. (2017), and Nath (2023). A notable departure from the papers cited earlier lies in our method for expanding MRPK's coverage. We include firms that have complete data on revenue and capital (fixed assets) while allowing for variability in the extent of

firms with annual sales exceeding nominal CNY 5 million (approximately USD 0.61 million) from 1998 to 2007, representing over 90.7% of total output. The India ASI includes large plants employing more than 100 workers and a random sample of smaller plants registered under the Indian Factories Act, ensuring representativeness at the state and industry levels.

10. The industries included are agriculture, mining, construction, manufacturing, transportation & utilities, wholesale trade, retail trade, finance, insurance, and real estate(FIRE) and Services. We choose the SIC classification mainly due to its availability in the Orbis Data.

11. The only exception is India ASI, which reports the book value of net fixed assets in a much more consistent manner while the gross values are reported with a major amount of missing values.

coverage for other variables such as material costs, wage bills, and employee numbers.[12] Each firm in the Orbis data has its associated USSIC sector code, and its various address information can be matched with a NUTS3 region in Europe. Different countries in Orbis have different years of data coverage, detailed in Table B.1. We use the sample period of 1998-2018.

China NBS. The annual firm-level data for China is derived from surveys conducted by the National Bureau of Statistics (NBS) in China. These surveys encompass all industrial firms with annual sales exceeding nominal CNY 5 million (approximately USD 0.61 million) from 1998 to 2007. Such firms are commonly referred to as "above-scale" industrial firms.[13] The NBS data includes sectors such as mining, manufacturing, and utilities, with manufacturing constituting more than 90% of the total observations in the dataset. In processing the NBS data, we follow the methodology outlined in Zhang et al. (2018). Each firm in the dataset is categorized using a four-digit Chinese Industry Classification (CIC) code and is harmonized to the USSIC division level. Each firm's reported location can be mapped into a prefecture-level division. We only use the sample period of 1998-2007 due to inconsistent reporting after 2008 as discussed in Brandt, Van Biesebroeck, and Zhang (2014) and Nath (2023).

India ASI. Our data for India is drawn from India's Annual Survey of Industries (ASI). ASI is a census of large plants employing more than 100 workers and a random sample of about one-fifth of smaller plants that are registered under the Indian Factories Act.[14] The sampling procedure assures representativeness at the state and industry levels. Almost all plants included in the ASI data are in the manufacturing sector. We match the plants to the Indian districts following the approach of Somanathan et al. (2021). From 2001 to 2014, ASI also collects whether the plant is AC equipped which we will utilize as a proxy variable for a firm's adaptability. We use the sample period of 1998 to 2018.

3.2 Weather and Forecast Data

Climate. For climate data, we use the land component of the European ReAnalysis, known as ERA5-Land (Sabater 2019), produced by the European Centre for Medium-Range Weather Forecasts (ECMWF). ERA5-Land is a reanalysis dataset that combines historical observations with models to create a consistent time series of various climate variables. A main advantage of ERA5-Land is its enhanced temporal and horizontal resolution. It provides hourly data on surface variables at a spatial resolution of 0.1°longitude $\times$ 0.1°latitude (approximately 9 km), covering the entire world. Such high resolution allows for a clearer depiction of the spatial patterns of surface temperature between neighboring locations.

12. Nath (2023) keeps the firms with complete revenue and labor data, while Gopinath et al. (2017) use a more restrictive sample that only preserves observations having all production-related information in south European countries.

13. Brandt, Van Biesebroeck, and Zhang (2014) shows that when comparing to the 2004 NBS census of industrial firms that covers all industrial plants in China, these above-scale firms in the sample account for over 90.7% of the total output.

14. As noted by Allcott, Collard-Wexler, and O'Connell (2016), large plants in the census scheme are defined as factories with 100 or more workers in all years except 1997-2003 when it included only factories with 200 or more workers. The sampling scheme for smaller registered plants included one-third of factories until 2004 and one-fifth since then.

Our analysis uses variables of air temperature at 2 meters above the land surface. We aggregate daily average temperatures[15] up to the annual level. Specifically, in our main specification, we bin daily temperature every 5°C from -5°C to 30°C. Each temperature bin counts the number of days in a year when the daily average temperature falls within specific temperature ranges. This is calculated for every region in each year.

Figure 1a plots the difference of the number of hot days above 25°C in a year between periods of our sample firm coverage, 1999-2008 and 2009-2018, and the baseline periods, from 1951 to 1980. The dark red color represents an increase of more than 13.2 days in a year with temperatures above 25°C. Figure 1b depicts the daily temperature distributions in baseline periods, sample periods, and the projection year of 2100. The global warming trend reveals that the number of days above 25 has increased, and the number of days below 10 has reduced in each country in the past decades. The temperature distribution shifts rightward when we compare across and within countries, as climates grow warmer.

The use of temperature bins in our analysis better conceptualizes climate. Because climate change represents a long-term shift in weather patterns, the year-to-year variation in the whole temperature distribution offers a more accurate depiction of climate change than merely examining year-to-year variations in mean temperature. A key feature of climate change is the increased frequency of extreme heat events (Oudin Åström et al. 2013; Christidis, Mitchell, and Stott 2023), therefore the increase in the number of extreme hot bins, indicative of a rightward shift in the tail of the weather distribution, captures the idea of global warming more accurately.

Projection and Forecast. We collect global projection data computed by the sixth phase of the Coupled Model Intercomparison Project (CMIP6).[16] We use the SSP3-4.5 experiment in our main analysis, which is based on the SSP3 scenario that involves high mitigation and adaptation challenges, along with the RCP4.5 pathway with a radiative forcing of 4.5 $\mathrm{W/m^2}$ in the year 2100. The SSP3-4.5 scenario represents the intermediate greenhouse gas emissions level with modest mitigation policy and is described as a more likely path (O'Neill et al. 2016). We use SSP3-4.5 projection in the main analysis and present results from other scenarios in Appendix C.4.

For weather forecast data, we collect the long-range (seasonal) forecast from ECMWF (Copernicus Climate Change Service and Climate Data Store 2018), which provides information about atmospheric and oceanic conditions up to seven months into the future. The forecast data have a spatial resolution of 1°longitude by 1°latitude.[17] We collect forecast daily maximum and minimum 2m temperature from the first day of each month from January to December with forecasts up to 30 days measured in 724 lead-hours.

15. The daily average temperature is the simple geometric average of the maximum and minimum temperatures. The daily maximum temperature is identified by the highest value among the hourly temperatures, and the daily minimum temperature is the lowest recorded value.

16. We use the GFDL-ESM4 model with a 1-degree nominal horizontal resolution produced by the National Oceanic and Atmospheric Administration, Geophysical Fluid Dynamics Laboratory (NOAA-GFDL).

17. From 1981 to 2016, the forecast values were hindcasts generated with a 25-member ensemble. Starting in 2017, they are forecasts produced monthly with a 51-member ensemble. These ensembles are run on the first day of each month, providing forecasts for up to seven months ahead.

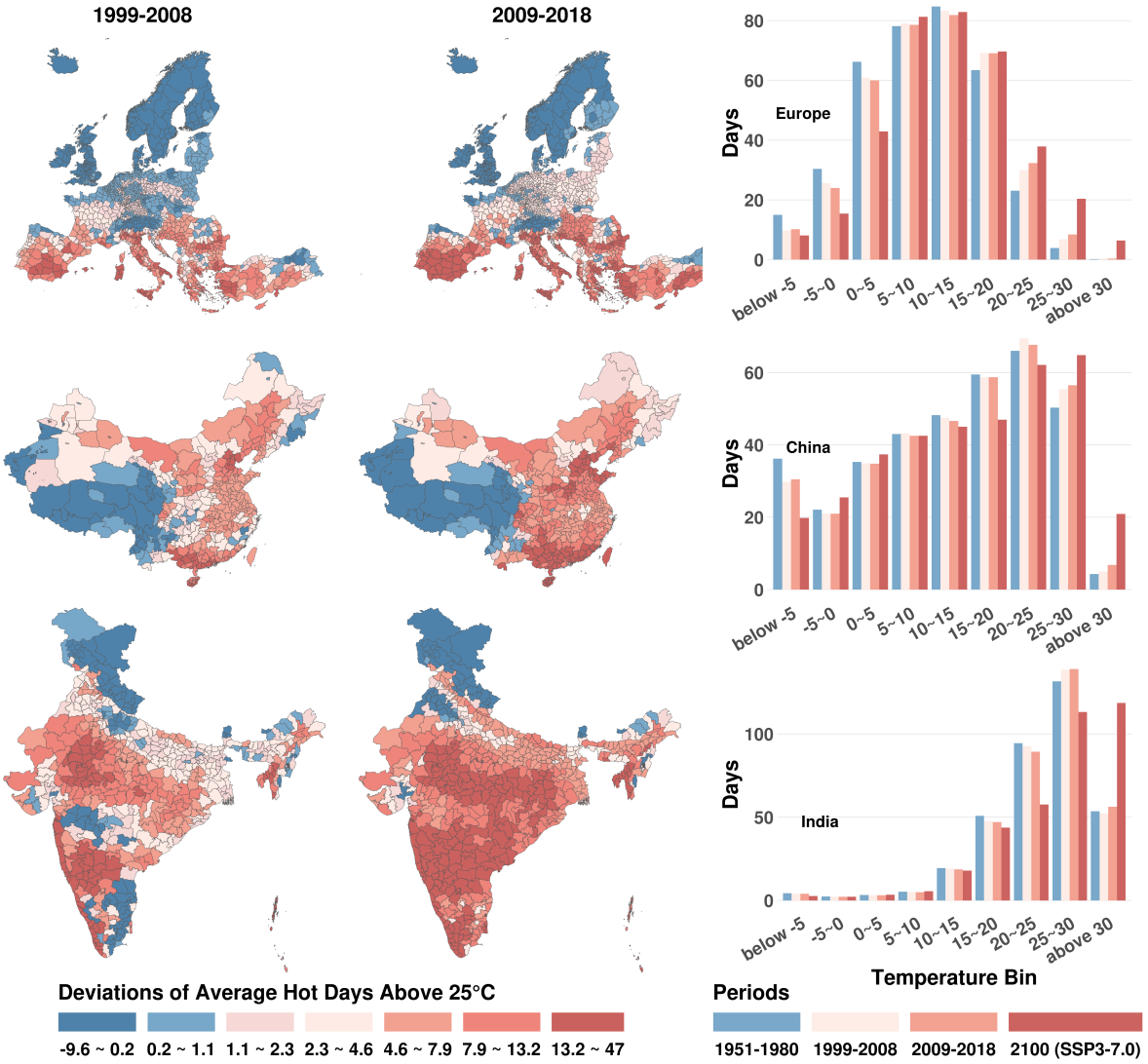
3.3 Other Data

Regional GDP. We collect regional-level global GDP data from DOSE (Wenz et al. 2023). We then clean and map global GDP data to our firm and weather datasets using spatial coordinates. This involves aligning different geographical units with administrative divisions like NUTS, prefectures, and districts.

Income Projection Projections of national income per capita are collected from the SSP Database, using the OECD EnvGrowth model (Dellink et al. 2017) hosted by the International Institute for Applied Systems Analysis.

Figure 1: Climates of our sample regions

(a) Number of Hot Days Deviation Relative to 1951-1980 (b) Average Daily Temperature Distribution



Notes: Figure 1a plots the difference of average number of days above 25°C between sample periods and baseline periods. The baseline period is from 1950 to 1980. The sample periods consist of two parts, 1999 to 2008, and 2009 to 2018. We calculate the 10-year average number of days above 25°C and deduct the 30-year baseline average number of days to obtain the difference. Figure 1b plots the average daily temperature distributions for baseline periods 1950-1980, two sample periods, and the projection year of 2100 under the SSP3-7.0 scenario.

4 Estimating the Misallocation Channel of Climate Change

4.1 Identification Strategy

We seek to estimate the *total* causal effect of climate shocks on capital misallocation, $\frac{d\ \mathrm{var}_{mrpk_{ni}}\left(\tilde{\mathbf{T}}_{rt},\tilde{\mathbf{X}}_{nt}\right)}{d\,\tilde{\mathbf{T}}_{rt}}$. Because $\tilde{\mathbf{X}}_{nt}$ may itself be influenced by climate as well, we consider a general function g such that $\tilde{\mathbf{X}}_{rt} = g(\tilde{\mathbf{W}}_{rt}, \tilde{\mathbf{T}}_{rt})$ where $\tilde{\mathbf{W}}_{rt}$ is a set of variables that are not affected by climate. Note that for each region-sector $n = (r, s)$, combining the Taylor expansions around the observed steady-state $(\overline{\mathrm{var}_{mrpk_{(s,r)i}}}, \overline{\tilde{\mathbf{T}}_r}, \overline{\tilde{\mathbf{X}}_{s,r}})$ of $\mathrm{var}_{mrpk_{(s,r)i}}(\tilde{\mathbf{T}}_{r,t}, \tilde{\mathbf{X}}_{s,r,t})$ and $\tilde{\mathbf{X}}_{rt} = g(\tilde{\mathbf{W}}_{rt}, \tilde{\mathbf{T}}_{rt})$ yields:

$$\begin{aligned}\mathrm{var}_{mrpk_{(s,r)i}}(\tilde{\mathbf{T}}_{r,t}, \tilde{\mathbf{X}}_{s,r,t}) &= \overline{\mathrm{var}_{mrpk_{(s,r)i}}} + \boldsymbol{\lambda}^{s,r}_{\sigma^2_{mrpk}} \cdot (\tilde{\mathbf{T}}_{r,t} - \overline{\tilde{\mathbf{T}}_r}) + \boldsymbol{\delta}^{s,r}_{\sigma^2_{mrpk}} \cdot (\tilde{\mathbf{W}}_{s,r,t} - \overline{\tilde{\mathbf{W}}_{s,r}}) + H.O.T. \\ &\approx \boldsymbol{\lambda}^{s,r}_{\sigma^2_{mrpk}} \cdot \tilde{\mathbf{T}}_{r,t} + \boldsymbol{\delta}^{s,r}_{\sigma^2_{mrpk}} \cdot \tilde{\mathbf{W}}_{s,r,t} + \eta_{s,r},\end{aligned} \tag{12}$$

where $\eta_{s,r}$ is a sector-region specific constant. For our benchmark exercise, we first estimate the average causal effect $\boldsymbol{\lambda}_{\sigma^2_{mrpk}} \equiv \mathbb{E}[\boldsymbol{\lambda}^{s,r}_{\sigma^2_{mrpk}}]$ across all region-sectors and years and will revisit the heterogeneous effects in Section 4.4.

We define current climate conditions, $\mathbf{T}_{r,t}$, in terms of temperature bins, following the approach by Deschênes and Greenstone (2011) and Carleton et al. (2022). Specifically, $\mathbf{T}_{r,t}$ is a vector, $\mathbf{T}_{r,t} = \left\{\mathrm{Tbin}^{<-5°C}_{r,t}, \mathrm{Tbin}^{-5\sim0°C}_{r,t}, \mathrm{Tbin}^{0\sim5°C}_{r,t}, ..., \mathrm{Tbin}^{25\sim30°C}_{r,t}, \mathrm{Tbin}^{>30°C}_{r,t}\right\}$, where each element $\mathrm{Tbin}^{b}_{r,t}$ counts the number of days in year t whose average temperature in region r falls into bin b. These bins, structured in 5-degree Celsius increments, cover a wide spectrum of daily temperature variations, including extreme heat and cold. As noted in Deschênes and Greenstone (2011), daily temperature data enable us to capture the nonlinear effects of weather using linear regression models.

To estimate the causal effect of temperature on MRPK dispersion (i.e., misallocation), we exploit interannual variation in the daily temperature distribution via the following panel regression:

$$\mathrm{var}_{mrpk_{(s,r),t}} = \sum_{b \in B/(5\sim10°C)} \lambda^{b}_{\sigma^2_{mrpk}} \times \mathrm{Tbin}^{b}_{r,t} + \boldsymbol{\delta}_{\sigma^2_{mrpk}} \mathbf{X}_{s,r,t} + \alpha_{c(r),t} + \eta_{s,r} + \varepsilon_{r,s,t}, \tag{13}$$

where $\eta_{s,r}$ is the region-sector fixed effects, accounting for the unvarying attributes of MRPK dispersion specific to each region-sector pair over time, consistent with the formulation in Equation 12. $\alpha_{c(r),t}$ is the country-by-year fixed effects, capturing the aggregate shocks to the country c that region r resides in. Standard errors are clustered at the region level to account for both serial and spatial correlations between all sectors across all years within each region (NUTS 3 in Europe, province in China, first-level administrative divisions in India).

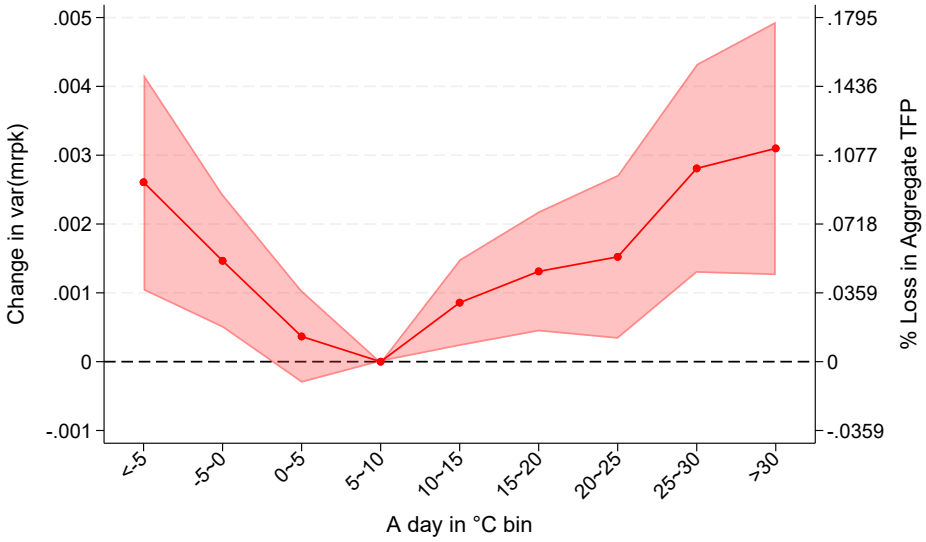
$\lambda^{b}_{\sigma^2_{mrpk}}$ are coefficients measuring the causal effect of one additional day in temperature bin b on contemporaneous MRPK dispersion, relative to a day in the 0°C to 5°C range. We use the $0 \sim 5$°C range as the reference category, so that the coefficient for this category is normalized to zero. $\mathbf{X}_{s,r,t}$ is a vector of logged control variables at the region-sector-year level, including the total number of observed firms, average firm-level sales, and average (log) MRPK. The first two control for sample size and business-cycle fluctuations, respectively. By including

average (log) MRPK, we aim to show that climate's impact on MRPK *dispersion* is mostly not driven by the mechanisms through which climate affects *average* productivity.[18] However, in our preferred specification, we exclude these controls because $\frac{d\mathbf{X}_{s,r,t}}{d\mathbf{T}_{r,t}} \neq 0$, which could bias $\lambda^b_{\sigma^2_{mrpk}}$ as an estimate of the total effect. In practice, adding these controls has minimal impact on our results.

4.2 Average Effects of Temperature on Capital Misallocation

The baseline estimates and implied TFP losses are reported in Table 1, columns (1) and (5), and depicted in Figure 2. In that figure, the left y-axis provides the scale of the estimated coefficients $\hat{\lambda}^b_{\sigma^2_{mrpk}}$. To facilitate interpretation, we transform $\hat{\lambda}^b_{\sigma^2_{mrpk}}$ into the marginal effect on aggregate TFP through the misallocation channel using $-\frac{\alpha_{Kn}+\alpha^2_{Kn}(\sigma_n-1)}{2}\hat{\lambda}^b_{\sigma^2_{mrpk}}$ from Equation 11, applying an well-established conservative parameter choice of $\alpha_{Kn} = 0.35$ and $\sigma_n = 4$ across all n.[19] The right y-axis in Figure 2 then provides the scale of the implied TFP loss associated with each temperature bin.

Figure 2: Estimated impact of daily temperature shocks on annual MRPK dispersion and implied TFP loss



Notes: This figure shows the aggregate impact linking annual MRPK dispersion and TFP loss to average daily temperatures. The formula for computing TFP loss from misallocation is $-\frac{\alpha_{Kn}+\alpha^2_{Kn}(\sigma_n-1)}{2}\hat{\lambda}^b_{\sigma^2_{mrpk}}$. The estimation is normalized by setting the range of 5°C - 10°C as the reference category. Therefore, each $\lambda^b_{\sigma^2_{mrpk}}$ represents the estimated effect of an additional day in temperature bin b on annual MRPK dispersion or TFP loss, relative to a day with temperatures between 5°C - 10°C. The figure also includes the 90% confidence interval for these estimates where standard errors are clustered at the region level.

The estimated coefficients reveal that MRPK dispersion and the inferred TFP loss from temperature-induced misallocation peak at the most extreme temperatures, both coldest and hottest. This observed U-shape pattern between MRPK dispersion and temperature can also

18. Controlling for average MRPK also captures the average financial constraints across firms.
19. For the elasticity of substitution, we choose $\sigma_n = 4$ as in Bils, Klenow, and Ruane (2021). For capital share, we pick a common value of $\alpha_{Kn} = 0.35$.

be translated into an inverted U-shape pattern between TFP and temperature, a well known result in the climate econometrics literature (Burke, Hsiang, and Miguel 2015).

For temperature bins above 25°C and below -5°C, the effects on MRPK dispersion are both economically significant and statistically significant at 1% level. Specifically, the point estimates indicate that substituting a day in the 5-10°C range with a day exceeding 30°C results in an increase of 0.31 log points in MRPK dispersion, translating to a decrease of 0.11% in annual aggregate TFP due to capital misallocation, a cost equivalent to 40% of a typical day's GDP. On the cold end, we find that an additional day colder than -5°C results in approximately a 0.26 log points increase in annual MRPK dispersion and 0.09% loss in annual TFP.

Table 1: Effects of daily mean temperature bins on MRPK dispersion and TFP loss

	(1) σ^2_{mrpk}	(2) σ^2_{mrpk}	(3) σ^2_{mrpk}	(4) σ^2_{mrpk}	(5) Implied TFP Loss
< -5°C	0.0026***	0.0025***	0.0028***	0.0012	0.0935***
	(0.0010)	(0.0009)	(0.0009)	(0.0023)	(0.0342)
$-5 \sim 0$°C	0.0015**	0.0013**	0.0016***	0.0006	0.0526**
	(0.0006)	(0.0006)	(0.0006)	(0.0013)	(0.0212)
$0 \sim 5$°C	0.0004	0.0002	0.0005	-0.0019**	0.0131
	(0.0004)	(0.0004)	(0.0004)	(0.0009)	(0.0146)
$10 \sim 15$°C	0.0009**	0.0008**	0.0008**	0.0036***	0.0308**
	(0.0004)	(0.0004)	(0.0004)	(0.0010)	(0.0137)
$15 \sim 20$°C	0.0013**	0.0012**	0.0014***	0.0045***	0.0471**
	(0.0005)	(0.0005)	(0.0005)	(0.0013)	(0.0190)
$20 \sim 25$°C	0.0015**	0.0015**	0.0015**	0.0080***	0.0546**
	(0.0007)	(0.0007)	(0.0007)	(0.0020)	(0.0259)
$25 \sim 30$°C	0.0028***	0.0027***	0.0027***	0.0095***	0.1008***
	(0.0009)	(0.0009)	(0.0009)	(0.0021)	(0.0331)
> 30°C	0.0031***	0.0030***	0.0030***	0.0090***	0.1112***
	(0.0011)	(0.0011)	(0.0011)	(0.0021)	(0.0401)
Controls	No	No	Yes	No	No
Region-Sector FE	Yes	Yes	Yes	Yes	Yes
Country-Year FE	Yes	No	Yes	Yes	Yes
Country-Sector-Year FE	No	Yes	No	No	No
1995 VA Weighted	No	No	No	Yes	No
Observations	124,065	123,518	124,065	123,847	124,065
R^2	0.876	0.903	0.878	0.897	0.876

Notes: Standard errors in parentheses. We cluster standard errors at the regional level (NUTS3 level for European countries, prefecture level for China, and district level for India). Dependent variables in columns (1) to (4) represent the variance of log MRPK. Results from estimating Equation 13 are displayed in columns (1) to (4), with controls in column (3) and weighted OLS regression in column (4). Column (5) is the implied TFP loss calculated using the formula, $-\frac{\alpha_{Kn}+\alpha^2_{Kn}(\sigma_n-1)}{2}\hat{\lambda}^b_{\sigma^2_{mrpk}}$, and the regression estimates. Countries included are China, India, and 30 European countries.

* $p < 0.10$, ** $p < 0.05$, *** $p < 0.01$

Robustness. Table 1 columns (2)-(4) present results with different specifications of fixed effects, inclusions of control variables, and weighting method. We introduce country-sector-year fixed effects instead of country-year fixed effects in column (2). Column (3) adds the set of control variables, including total number of observed firms, average firm-level sales, and average level of MRPK across firms in a region-sector-year (all in logs). Column (4) reports the results of the weighted OLS using the 1995 region-sector value-added as the regression weight. Our results, in particular the "U-shaped" pattern, remain robust under various specifications.

4.3 Technology vs. Misallocation

While our main empirical focus is on identifying the causal effect of climate conditions on capital misallocation, we now turn to estimating how temperature affects the aggregate technology component of productivity. This allows us to compare the relative importance of technology versus misallocation channels in the face of climate change.

We interpret the technology effect as the shift in the physical productivity frontier of the aggregate economy due to climate conditions. Using the decomposition of aggregate TFP from Equation (11), we isolate the technology channel:

$$\frac{d\,\text{Technology}_{nt}}{d\tilde{\mathbf{T}}_{rt}} = \frac{d\log \text{TFP}_n^E(\tilde{\mathbf{T}}_{r,t},\cdot)}{d\mathbf{T}_{r,t}} = \frac{1}{\sigma_n - 1}\frac{d\log\left[\mathbb{E}_i \text{TFP}_{ni}(\tilde{\mathbf{T}}_{r,t},\cdot)^{\sigma_n-1}\right]}{d\tilde{\mathbf{T}}_{r,t}},$$

where $\text{TFP}_{ni}(\tilde{\mathbf{T}}_{r,t},\cdot) := B_{ni}(\tilde{\mathbf{T}}_{r,t},\cdot)^{\frac{1}{\sigma_n-1}} A_{ni}(\tilde{\mathbf{T}}_{r,t},\cdot)$. This expression quantifies how changes in $\mathbf{T}_{r,t}$ affect the CES aggregate of firms' physical productivity.

The semi-elasticity of interest, $\frac{d\log\left[\mathbb{E}_i \text{TFP}_{ni}(\tilde{\mathbf{T}}_{r,t},\cdot)^{\sigma_n-1}\right]}{d\tilde{\mathbf{T}}_{r,t}}$, is an "elasticity of the average" across firms.[20] It can be viewed as a productivity-share-weighted average of individual firm elasticities, where more productive firms with larger market shares have greater influence on the aggregate response. This contrasts with the "average elasticity" across all firms:

$$\underbrace{\frac{d\log \mathbb{E}_i\left[\text{TFP}_{ni}(\tilde{\mathbf{T}}_{r,t},\cdot)^{\sigma_n-1}\right]}{d\tilde{\mathbf{T}}_{r,t}}}_{\text{Elasticity of the Average}} = \mathbb{E}_i\left[\frac{\text{TFP}_{nit}^{\sigma_n-1}}{\mathbb{E}_i[\text{TFP}_{nit}^{\sigma_n-1}]}\cdot\frac{d\log \text{TFP}_{ni}(\tilde{\mathbf{T}}_{r,t},\cdot)^{\sigma_n-1}}{d\mathbf{T}_{r,t}}\right] \neq \underbrace{\mathbb{E}_i\left[\frac{d\log \text{TFP}_{ni}(\tilde{\mathbf{T}}_{r,t},\cdot)^{\sigma_n-1}}{d\mathbf{T}_{r,t}}\right]}_{\text{Average Elasticity}}.$$

A simple OLS estimation, which assigns equal weight to the observations of all firms, would yield the "average elasticity", rather than the "elasticity of the average." This approach could bias the aggregate estimate downward for heat shocks, as larger, more productive firms are likely more resilient to heat (i.e., $\text{cov}\left(\frac{\text{TFP}_{nit}^{\sigma_n-1}}{\mathbb{E}_i[\text{TFP}_{nit}^{\sigma_n-1}]}, \frac{d\log \text{TFP}_{ni}(\tilde{\mathbf{T}}_{r,t},\cdot)^{\sigma_n-1}}{d\text{Tbin}_{r,t}^{>30C}}\right) > 0$). We draw caution to the practice of using (unweighted) micro-level OLS estimates to infer aggregate impacts.

As demonstrated in Tyazhelnikov, Zhou, and Shi (2024), the elasticity of the average, $\frac{1}{\sigma_n-1}\cdot\frac{d\log\left[\mathbb{E}_i \text{TFP}_{ni}(\tilde{\mathbf{T}}_{r,t},\cdot)^{\sigma_n-1}\right]}{d\tilde{\mathbf{T}}_{r,t}}$, can be consistently estimated using a Poisson Pseudo Maximum Likeli-

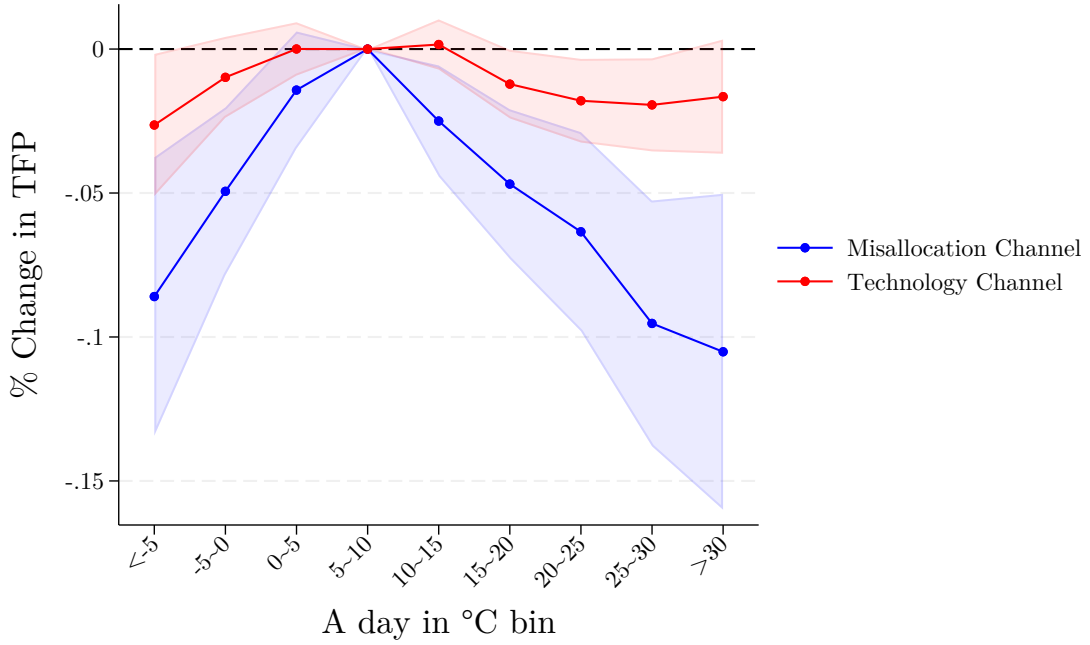
20. We slightly abuse the usage of "elasticity" to refer to semi-elasticity for expositional clarity.

hood (PPML) regression. Specifically, we impose the following moment conditions:

$$\mathrm{E}_i\left[\tfrac{1}{\sigma_n-1}\widetilde{\mathrm{TFP}}_{nit}^{\sigma_n-1} \mid \tilde{\mathbf{T}}_{rt}, \eta_i, \log(P_{nt}Y_{nt}), \kappa_{c(r)st}\right] = \exp\left[\boldsymbol{\beta}\tilde{\mathbf{T}}_{rt} + \eta_i + \delta\log(P_{nt}Y_{nt}) + \kappa_{c(r)st}\right], \tag{14}$$

where we define $\widetilde{\mathrm{TFP}}_{nit} := \frac{(P_{nit}Y_{nit})^{\frac{\sigma_n}{\sigma_n-1}}}{K_{nit}^{\alpha_{Kn}}L_{nit}^{\alpha_{Ln}}}$ as the model-consistent empirical measure of TFP from the data, up to a constant consisting of the aggregate demand and price index of n. In this specification, η_i represents firm fixed effects. The term $\log(P_{nt}Y_{nt})$, along with the country-sector fixed effect $\kappa_{c(r),s,t}$, captures differences between local and national price levels. Estimating this equation by PPML yields a theory-consistent estimate of $\boldsymbol{\beta} = \mathbb{E}\left[\frac{1}{\sigma_n-1}\frac{d\log\mathbb{E}_i[\mathrm{TFP}_{nit}^{\sigma_n-1}|\cdot]}{d\tilde{\mathbf{T}}_{rt}}\right]$, which is plotted alongside the aggregate TFP impact from the misallocation channel in Figure 3.

Figure 3: Technology vs. Misallocation



Notes: The graphs include 90% confidence intervals, and standard errors are clustered at the regional level. The reference temperature is at 5∼10°C.

We find that while the estimated effect of climate shocks through the technology channel is noticeable, it remains considerably smaller than the effect through the misallocation channel. Specifically, a cold shock of an additional day below -5°C (relative to the 5°C–10°C range) results in an annual aggregate physical productivity loss of about 0.03%, and a heat shock above 25°C or 30°C leads to a loss of approximately 0.02%. The impact of a heat shock on aggregate technology is roughly one-fifth of the corresponding loss through the misallocation channel.

4.4 Heterogeneous Effect by Climate and Development from Misallocation Channel

Our benchmark specification in Equation 13 captures the average effect of temperature on capital misallocation, $\mathbb{E}[\boldsymbol{\lambda}^{s,r}_{\sigma^2_{mrpk}}]$. We now try to estimate the heterogeneous impact of temperature shocks across regions with different long-run climate conditions and levels of economic development.

It is not immediately clear whether a hot day consistently leads to more or less *misallocation* in regions that are already warm or economically thriving. This ambiguity arises from two potentially counteracting factors. For simplicity, consider two types of firms: "heat-loving" versus "heat-averse." On one hand, heat-averse firms in warmer climates may have adapted to high temperatures—by investing in heat-tolerant capital, securing more flexible financing, or adjusting production methods—such that additional heat shocks impose relatively mild disruptions on their marginal products and factor usage. On the other hand, heat-averse businesses in hotter regions might still face disproportionately large *adjustment frictions*—for example, steeper capital-investment costs or financing constraints—once temperatures surpass their adaptation threshold. Limited adaptability (Moscona and Sastry 2023) and the convexity of damage from cumulative heat exposure (Burke, Hsiang, and Miguel 2015) might still sharply widen cross-firm differences in marginal products. Similarly, in higher-income regions, while firms may, on average, possess greater resources for adaptation to heat shocks, these economies often have highly specialized productions and services and exhibit larger dispersion in firm sizes (e.g., Chen 2022; Poschke 2018). Such heterogeneity can magnify responses to climate shocks: some firms manage to shield themselves from heat shocks by making quick adjustments while others cannot, causing greater MRPK divergence and reinforcing the misallocation channel.

To more precisely account for the heterogeneous impact stemming from different long-run climate and development levels across regions, we follow the approach of Carleton et al. (2022) and Nath (2023) by interacting a time-invariant measure of climate (i.e., long-run average temperature) and GDP per capita with each temperature bin. This method allows us to capture how climate and income jointly influence the effects of temperature variations on capital misallocation. The modified regression model is formulated as follows:

$$\begin{aligned}\sigma^2_{mrpk_{s,r,t}} = &\sum_{b\in B_{/(5\sim10^\circ C)}} \lambda^b \times \text{Tbin}^b_{r,t} + \sum_{b\in B_{/(5\sim10^\circ C)}} \lambda^b_{\overline{T}} \times \text{Tbin}^b_{r,t} \times \overline{T}_r \\ &+ \sum_{b\in B_{/(5\sim10^\circ C)}} \lambda^b_{\text{GDP}_{\text{pc}}} \times \text{Tbin}^b_{r,t} \times \ln \overline{\text{GDP}_{\text{pc}}}_r + \boldsymbol{\delta}\tilde{\mathbf{X}}_{s,r,t} + \alpha_{c,t} + \eta_{s,r} + \varepsilon_{s,r,t},\end{aligned} \tag{15}$$

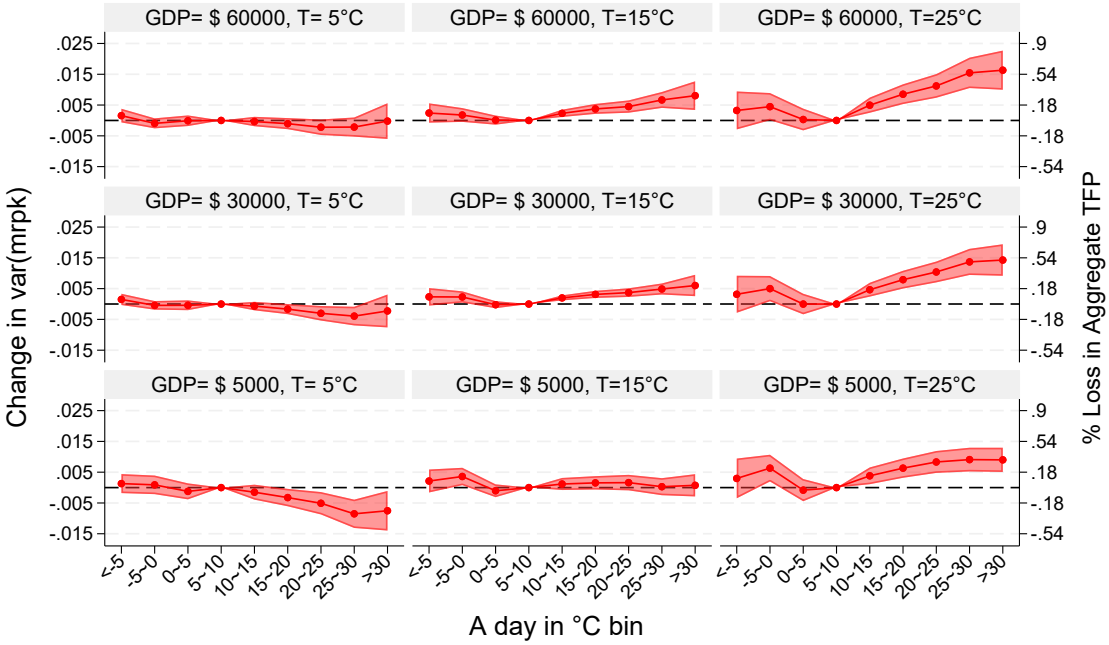
where $\overline{T}_r$ represents the long-run annual average temperature and $\ln \overline{\text{GDP}_{\text{pc}}}_r$ is the log of long-run average GDP per capita in region r.[21] Both long-run temperature and GDP per capita are computed as sample averages from 1997-2018. The coefficients $\lambda^b_{\overline{T}}$ and $\lambda^b_{\text{GDP}_{\text{pc}}}$ quantify how the impact of temperature shocks on MRPK dispersion varies across regions with different income

21. The sub-national level (PPP-adjusted) GDP per capita data is from DOSE. It is important to use sub-national level data as countries like India and China admit large income heterogeneity across the districts or prefectures. The GDP per capita data is in 2017 International Dollars.

levels and climates.[22]

Figure 4 presents the results from estimating Equation 15. We predict the impact of temperature shocks on MRPK dispersion and its equivalent TFP loss across a combination of three levels of income and three levels of long-run climate. The left y-axis indicates the projected effects of temperature shocks on MRPK dispersion, while the right y-axis shows the implied TFP loss suggested by the estimates.

Figure 4: MRPK Dispersion and TFP Loss Across Climates and Income



Notes: The graphs plot the predicted effect of exposure to daily mean temperature bins on MRPK dispersion and TFP loss at varying levels of income and climates. These predicted effects are derived from the interacted panel regression specified in Equation 15. The graphs include 90% confidence intervals, and standard errors are clustered at the regional level. The left y-axis indicates changes in MRPK dispersion, and the right y-axis shows the calculated TFP loss. The reference temperature is at 5∼10°C.

Level Effect: Hotter Regions Suffer More from the Misallocation Channel Figure 4 shows that in regions with higher baseline temperatures, an extremely hot day (above 30°C) increases MRPK dispersion more than it does in cooler areas. Among regions with comparable income levels, the adverse effects of heat on misallocation intensify as the regional climate becomes warmer. For instance, when $\overline{T}_r = 25$°C, an additional day above 30°C leads to a substantial TFP loss of about 0.3% to 0.58%, irrespective of income. In contrast, in colder climates (e.g., $\overline{T}_r \approx 5$°C), heat shocks have negligible or even negative effects on MRPK dispersion, lowering TFP losses. Interestingly, even cold shocks (below 0°C) increase misallocation more in hotter regions than in colder ones, although their overall impact is typically much smaller than that of a heat shock (above 30°C) —except in certain hot, low-income regions like India (GDP ≈ \$5,000, $\overline{T}_r = 25$°C).

22. Interacting temperature bins with the region's long-term average temperature allows us to analyze how an additional hot day has differential effects across areas with varying baseline climates. Similarly, by interacting temperature bins with a country's annual per capita income, we evaluate how the same heat shock impacts developed and developing economies differently.

The quantitative implications can be best understood by comparing two regions with similar incomes but different climates. Arizona (U.S.) and Norway both have an average per capita income of around $60,000 but vastly different average annual temperatures ($14.68°$C in Arizona vs. $0.53°$C in Norway). According to our estimates, an additional day above $30°$C compared to a $5-10°$C day in Norway *reduces* MRPK dispersion by 0.41 log points, implying a 0.14% *increase* in TFP. In Arizona, the same heat shock *increases* MRPK dispersion by 0.75 log points and lowers TFP by 0.27%. In Section 5, we discuss how these divergent responses can be explained by deviations from the "bliss-point" temperature for production, estimated to be around $13°$C.

Income Effect: Richer Economies Suffer More from the Misallocation Channel A second key finding is that wealthier economies incur greater losses through the misallocation channel in response to extreme heat—what we term the *Income Effect*. Figure 4 illustrates that for each fixed long-run temperature (each column), moving from lower to higher income levels amplifies the impact of heat shocks and makes the MRPK response more U-shaped. For instance, the Netherlands and Turkey both have an average temperature of around $9.9°$C, yet the Netherlands' per capita income ($56,784) is more than double that of Turkey ($28,150). Our estimates suggest that an additional day above $30°$C causes a 0.03% TFP loss in Turkey, but 0.11% in the Netherlands—nearly four times higher. To explain the income effect, in Section 6, we show how firm size dispersion rises with economic development, potentially resulting in greater cross-firm MRPK divergence under similar heat shocks.

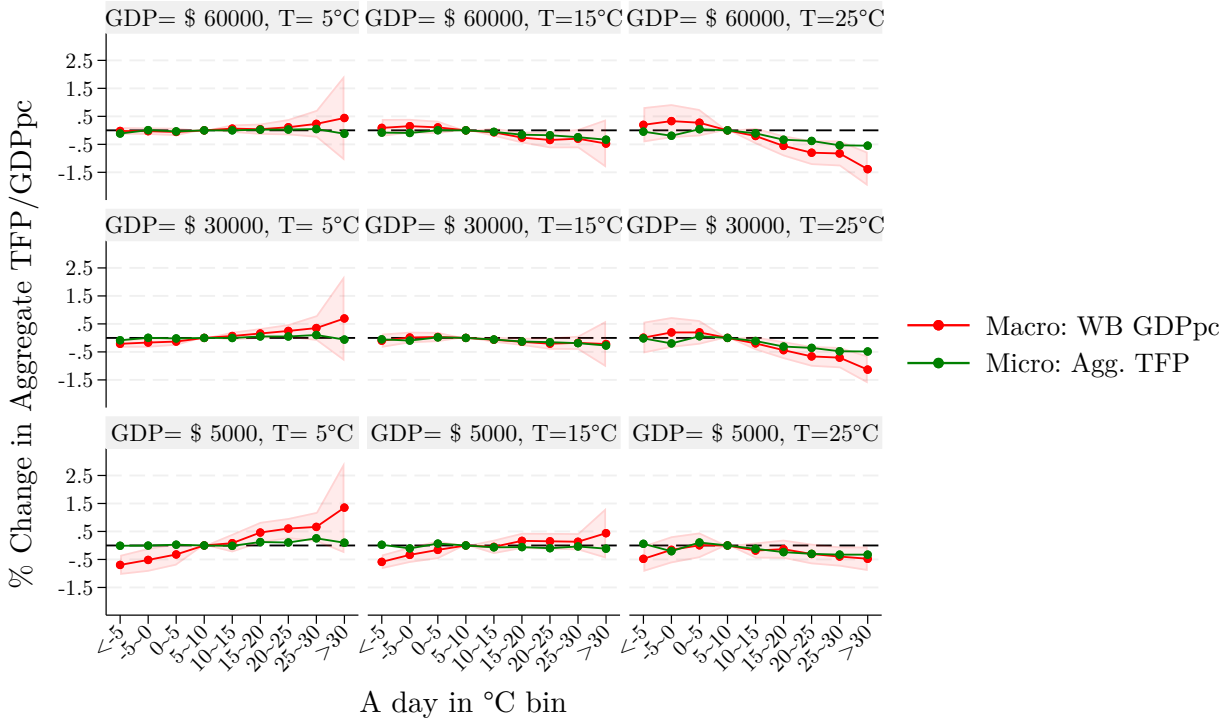
Overall, the heterogeneous effect shows that the nature of the misallocation channel of climate change may differ substantially from other channels, such as labor productivity (Nath 2023) and mortality risk (Carleton et al. 2022), where richer economies and hotter regions are often found to experience smaller heat-related losses due to long-run adaptation. The *opposite* pattern emerges here: hotter and richer regions face larger TFP losses via misallocation, suggesting that market-based adaptation may do little to curb the efficiency losses across firms.[23] As an economy develops to be more sophisticated in its techniques of production among firms, it might become more vulnerable to climate variations since achieving efficient resource allocations becomes more challenging.

Micro Estimates vs. Macro Estimates We compare our *micro estimates*, derived from firm-level data and aggregation theory, to *macro estimates* obtained from country-level aggregate data. For the micro estimates, we first apply the PPML estimator in Equation (14) with the same interaction terms used in Equation (15), thereby capturing the heterogeneous effects from the technology channel on aggregate TFP. We then combine these technology effects with the misallocation effects to form the micro estimates of the total effect of climate shocks, $\frac{d \log \text{TFP}_n(\tilde{\mathbf{T}}_{rt},\cdot)}{d\tilde{\mathbf{T}}_{rt}}$, as in Equation 11. For the macro estimates, we use World Bank annual GDP per capita data from 1990 to 2019 for all available countries, running a regression analogous to Equation (15) at the country level—now controlling for country and year fixed effects.

23. Interestingly, the *average effect* of temperature on MRPK also exhibits similar heterogeneity. Estimates can be found in Figure C.1.

We plot both sets of estimates in Figure 5 and find that the micro-based estimates closely track the macro-based estimates, except in two instances: (1) the micro estimates understate the damage of heat shocks (above 30°C) in regions with per capita GDP over $30,000 and mean temperatures above 25°C, and (2) overstate the benefits of heat shocks in colder, poorer regions. Both types of regions are infrequent in our dataset and globally. Overall, these findings suggest that our micro estimates capture the same cross-country heterogeneity in temperature sensitivity as the macro estimates, making them suitable for out-of-sample extrapolation.

Figure 5: Aggregate Impact of Climate shocks: Micro vs. Macro Estimates



Notes: The graphs include 90% confidence intervals, and standard errors are clustered at the region level. The reference temperature is at 5∼10°C.

4.5 End-of-the-century Projection of the Misallocation Channel

In this subsection, we use the estimates from Section 4.4 to project how climate-induced misallocation will affect aggregate TFP by the end of the 21st century (2081–2100) for 4,881 regions in 172 countries.[24]

Such projections require detailed region-level daily temperature distributions, average temperature levels, and GDP per capita projections at the end of the century. We use near-surface air temperature forecasts from the sixth phase of the Coupled Model Intercomparison Project (CMIP6) (Copernicus Climate Change Service 2021) under RCP 4.5, a scenario featuring moderate mitigation efforts. To project each region's daily temperature distribution, we calculate the average number of days in each temperature bin (as defined in Section 4.1) and the mean

24. For our 32-country sample, regions are defined as in Section 3. For other countries, we use GADM1-level administrative units from the GADM dataset.

annual temperature for 2081–2100, taking a 20-year average to smooth over short-term climate fluctuations. Following Carleton et al. (2022), we obtain national per capita income projections from the OECD EnvGrowth model (Dellink et al. 2017) under the SSP3 scenario. For the average region in our sample, the mean annual temperature is expected to rise by about $1.78^{\circ}\mathrm{C}$ between 2000–2014 and 2081–2100, while GDP per capita (in 2017 international dollars) is projected to increase by approximately \$20,748 relative to 2019. Figure C.2 illustrates these projected evolution in income and temperature.

Our objective is to measure how much additional aggregate TFP loss arises from climate-induced misallocation by the end of the 21st century (EOC), compared to baseline conditions near the century's start. To make these mechanisms transparent, we decompose the total effect of climate-induced misallocation into three components:

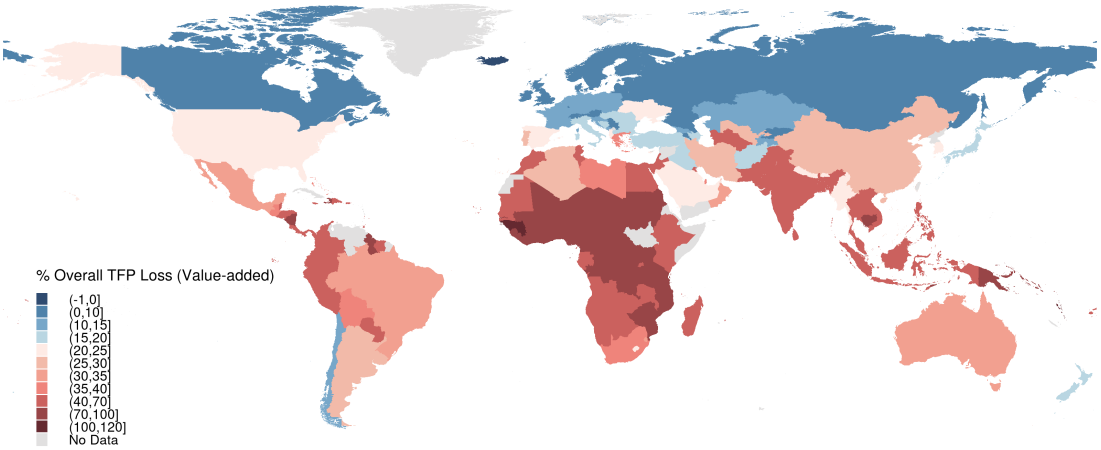
$$\begin{aligned}\underbrace{\Delta^{\text{Loss}} \ln \text{TFP}_r}_{\text{Total Effect}_r} = &\frac{\alpha_{Kn} + \alpha_{Kn}^2(\sigma_n - 1)}{2} \Bigg[\underbrace{\sum_b \left(\lambda^b + \lambda^b_{\text{GDP}_{pc}} \ln \text{GDP}_{pc,r,\text{base}} + \lambda^b_{\bar{T}} \bar{T}_{r,\text{base}} \right) \times \Delta \text{Tbin}^b_r}_{\text{Shock Effect}_r} \\ &+ \underbrace{\sum_b \lambda_{b,\bar{T}} \text{Tbin}^b_{r,\text{base}} \times \Delta T_r}_{\text{Level Effect}_r} \\ &+ \underbrace{\sum_b \lambda^b_{\text{GDP}_{pc}} \text{Tbin}^b_{r,\text{base}} \times \Delta \ln \text{GDP}_{pc,r}}_{\text{Income Effect}_r} \Bigg] + \underbrace{\varepsilon_{rt}}_{\text{Residuals}_r},\end{aligned} \tag{16}$$

where Δ denotes the difference between a variable's end-of-century (EOC) value and its baseline value. The *shock effect* refers to the change in TFP losses due to shifts in daily temperature distributions ΔTbin^b_r, conditional on the baseline income and long-run temperature; the *level effect* refers to the change in TFP losses due to the change in long-run temperature ΔT_r; and the *income effect* reflects the cost of the region's increasing misallocation arising from economic development, proxied by $\Delta \ln \text{GDP}_{pc,r}$. To render the results more interpretable, we aggregate each region's TFP losses to the country level using a weighted sum of projected regional GDP shares under SSP3.[25]

Figure 6 displays each country's projected TFP loss from the capital misallocation channel. While most countries experience substantial losses, the magnitudes vary widely. Among the most severely affected are Tanzania, Malaysia, Honduras, and India, where TFP losses exceed 40%. In India, for instance, the number of days above $30^{\circ}\mathrm{C}$ is projected to increase from 76.24 to 99.78 by 2100, accompanied by rises in average temperature (from $23.29^{\circ}\mathrm{C}$ to $25^{\circ}\mathrm{C}$) and income per capita (from \$6,608.62 to \$14,615.39). Combined, these factors yield a TFP loss of roughly 50.45%. As illustrated in Figure 4, such substantial heat-related damages become more pronounced in already-warm (tropical/subtropical), lower-income countries that simultaneously grow hotter and wealthier.

25. Grid-level SSP3 GDP data from Wang and Sun (2022) provides projected GDP shares.

Figure 6: End-of-century Projected TFP Loss Due to the Misallocation Channel

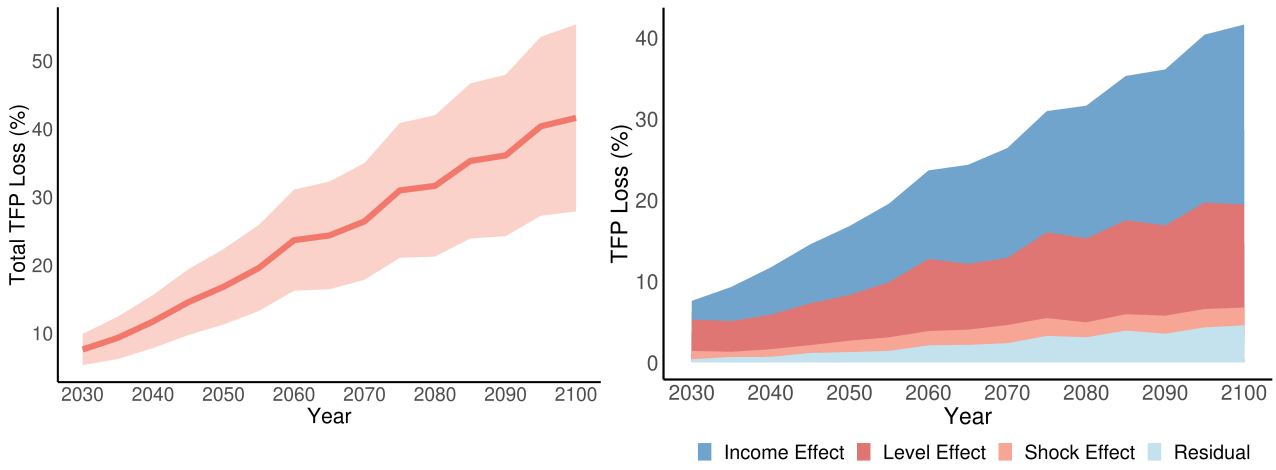


Notes: Figure shows the projected TFP losses from capital misallocation under SSP3-4.5 scenarios. The estimation follows Equation 16 where we estimate the total effect in MRPK dispersion and compute the equivalent value of TFP losses.

Figure 7: Projected Global TFP Loss and Its Decomposition: 2030-2100

(a) Total TFP Loss from the Misallocation Channel

(b) TFP Loss Decomposition



Notes: Figure 7a plots the total TFP loss across years. The dark red line plots the estimates and the shaded area is 90% confidence intervals from the parameter uncertainty. Figure 7b plots the three effects contributing to total TFP loss. All computations are under the SSP3-4.5 scenario and the percentage loss is compared to the baseline level.

In contrast, countries like the United States, Argentina, and Spain are projected to lose 20–30%. For example, in the U.S., the TFP loss is about 20.92%. Per capita income is expected to rise from \$62,478 to \$95,801, while average annual temperature increases from 10.07°C to 12.45°C, and days above 30°C grow from 3.97 to 8.94. Meanwhile, countries with milder impacts—such as France, the United Kingdom, Russia, and Canada—see losses below 15%. In the U.K., for instance, the average temperature climbs from 9.15°C to 10.16°C, with days above 25°C increasing from 0.03 to 0.37, and income per capita rising from \$47,362.27 to \$85,615.36. Taken together, these lead to a TFP loss of 8.23%. Although climate change slightly raises aver-

age temperatures in temperate, maritime climates, the incidence of extreme heat remains relatively low, moderating the misallocation losses compared to tropical regions. Figures C.4 and C.5 provide additional projections under alternative emissions scenarios and uncover similar effects.

Finally, by weighting each country's misallocation-induced TFP losses by its projected share of global GDP,[26] we estimate the worldwide cost of climate-induced misallocation to be:

$$\underbrace{\Delta^{\text{Loss}} \ln \text{TFP}}_{\text{Total Effect}=36.73\%} = \underbrace{\text{Shock Effect}}_{2.13\%} + \underbrace{\text{Level Effect}}_{11.34\%} + \underbrace{\text{Income Effect}}_{19.46\%} + \underbrace{\text{Resid.}}_{3.8\%}.$$

Relative to baseline conditions, this translates into a 36.73% decline in aggregate TFP (GDP). Specifically, shifts in the daily temperature distribution (*shock effect*) contribute 2.13%, rising average temperature (*level effect*) accounts for 11.34%, and higher income per capita (*income effect*) explains 19.46%. Figure 7a depicts the projected evolution of misallocation-driven TFP losses from 7.60% in 2030 to 41.62% by 2100, with 90% confidence intervals accounting for parameter uncertainty. Figure 7b further separates these losses into the three components over time, highlighting the dominant roles of the level and income effects.

These estimates are substantial and comparable to the overall projected impacts reported by Burke, Hsiang, and Miguel (2015) and, more recently, Bilal and Känzig (2024). Much of the total projected effect arises from the sharp increase in the marginal effect of daily temperature shocks, driven by rising temperatures and incomes. As with any century-scale forecast, our projection is subject to various caveats—most notably out-of-sample extrapolation—since income and temperature levels by the end of the century lie well beyond historical experience. However, even if we only adjust the daily temperature distribution while keeping the first-order marginal effect of temperature shocks at current levels, we still project a 2.14% global TFP loss from misallocation.[27] Overall, these results underscore the quantitative importance of the misallocation channel of climate change, which may serve as a one of the key forces driving up the social cost of carbon.

5 A Firm Dynamics Model of Temperature Shocks and MRPK Dispersion

We now turn to the question of *why* and examine how both temperature *shocks* and *levels* affect capital misallocation within a standard dynamic investment model. Given the time-to-build nature of capital inputs, a natural explanation is that temperature influences firms' ability to forecast capital returns in heterogeneous ways. We highlight two mechanisms: (i) weather forecasts are noisy and firms vary in their temperature sensitivity, leading to heterogeneous investment mistakes from a common forecast error, and (ii) firms do not have perfect foresight about their damage sensitivity, so temperature extremes can cause large, unexpected losses for

26. Under this weighting scheme, the resulting TFP losses correspond to a model-implied global TFP loss based on a Cobb-Douglas aggregator of country-level value added. This also serves as a first-order approximation under any constant-returns-to-scale aggregator for global output.

27. A detailed breakdown of each effect on the country level is presented in Figure C.3. Country-level misallocation loss projections under other climate change scenarios are provided in C.4.

certain firms. These sources of heterogeneity generate misallocation within each region-sector. Our model provides empirically testable regression equations and rich quantitative insights, which we present in Sections 6 and 7.

5.1 Setup

Similar to the accounting framework in Section 2, our model describes the action of firms and the aggregate economy within a region-sector $n = (r, s)$. We suppress the region-sector label to avoid notation burdens. Our model follows a partial equilibrium set-up similar to that of David and Zeke (2021).

Production and Demand. We begin by describing the production side of the economy. Each firm i produces a differentiated product of quantity Y_{it} with Cobb-Douglas technology, $Y_{it} = \tilde{A}_{it} K_{it}^{\tilde{\alpha}_K} N_{it}^{\tilde{\alpha}_N}$, where $\tilde{A}_{it}$ is the physical productivity, K_{it} is the capital input, N_{it} represents labor and $\tilde{\alpha}_K + \tilde{\alpha}_N = 1$. The firm's product faces a constant elasticity downward-sloping demand curve, $Y_{it} = B_{it} P_{it}^{-\sigma}$, with demand shifter B_{it}. Combing production and demand functions, we obtain the equilibrium revenue function of the form:

$$P_{it} Y_{it} = \hat{A}_{it} K_{it}^{\alpha_K} N_{it}^{\alpha_N}, \tag{17}$$

where $\alpha_F = (1 - \frac{1}{\sigma})\tilde{\alpha}_F, \forall F \in \{K, N\}$ and $\hat{A}_{it} = B_{it}^{\frac{1}{\sigma}} \left(\tilde{A}_{it}\right)^{(1-\frac{1}{\sigma})}$ is the firm's revenue-based productivity (TFPR), which we will simply call "productivity" hereafter.

Productivity and Heterogeneity in Temperature Sensitivity. We now introduce how firms' productivity is heterogeneously impacted by temperature. For parsimony, we allow the annual temperature to be a sufficient statistic for climate conditions in the structural model (as in Dell, Jones, and Olken 2012 and Cruz and Rossi-Hansberg 2023). We assume that firms' (log) productivity, $\hat{a}_{it} \equiv \ln(\hat{A}_{it})$, is determined by:

$$\hat{a}_{it} = \hat{\beta}_{it}(T_t - T^*) + \hat{z}_{it}, \tag{18}$$

where T_t is the realized temperature at year t, and T^* is the optimal temperature for firms' production. We assume that each firm i's (log) productivity changes linearly with temperature's deviation from the optimum, $T_t - T^*$, subject to the sensitivity $\hat{\beta}_{it}$.[28] $\hat{z}_{it}$ denotes the firm-specific idiosyncratic productivity, which captures all the variations apart from the effect of temperature.

We allow a firm i's temperature sensitivity $\hat{\beta}_{it}$, to be firm-specific and time-varying. There are two sources of heterogeneity in a firm's sensitivity to temperature:

$$\hat{\beta}_{it} = \underbrace{\hat{\beta}_i}_{\substack{\text{Persistent} \\ \text{sensitivity}}} + \underbrace{\hat{\xi}_{it}}_{\substack{\text{Idiosyncratic} \\ \text{sensitivity}}} + \mathcal{O}_t.$$

28. The heterogeneity of $\hat{\beta}_{it}$ reflects the composite effect of how both physical productivity and demand shifter are impacted by temperature across firms.

In our model, we distinguish between *persistent* and *idiosyncratic* temperature sensitivities. The persistent sensitivity $\hat{\beta}_i$ is assumed to be observable and known to firms, with $\hat{\beta}_i \sim \mathcal{N}(\overline{\hat{\beta}}, \sigma^2_{\hat{\beta}})$ across firms. Here, $\sigma^2_{\hat{\beta}}$ measures the dispersion of persistent sensitivity within a region-sector.[29] On the other hand, the idiosyncratic sensitivity, $\hat{\xi}_{it} \sim \mathcal{N}(0, \sigma^2_{\hat{\xi}})$, is unknown to the firm and i.i.d. across firms and time. Here, $\sigma^2_{\hat{\xi}}$ captures damage uncertainty within a region-sector. The impact of idiosyncratic sensitivity on TFP scales with $T_t - T^*$, reflecting the increased likelihood of a firm experiencing extreme events associated with extreme temperature (e.g. plant-level fire hazards are more likely to happen during heat waves). Finally, $\mathcal{O}_t$ denotes the adjustment to offset the Jensen's inequality terms when aggregating across firms; because it is common to all firms, it plays no role in cross-firm misallocation.[30]

Jointly, we model $\hat{\beta}_{it}$ to reflect the idea that a firm reacts to temperature conditions based on the firm's known characteristics.[31] Given that dynamic inputs require time to build, firms cannot fully optimize each period, as some damage sensitivity to temperature remains unknown at the time of investment.

Law of Motion for Productivity and Temperature. We assume (agents perceive that) temperature and (log) idiosyncratic productivity $\hat{z}_{it} = \log \hat{Z}_{it}$[32] follow an AR($p$) process, with persistence ρ_T and ρ_z, respectively:

$$\begin{aligned} (T_{t+1} - \bar{T}) &= \sum_{h=1}^{p} \rho_{T,h}(T_{t+1-h} - \bar{T}) + \eta^T_{t+1}, \\ \hat{z}_{it+1} &= \rho_z \hat{z}_{it} + \hat{\varepsilon}_{it+1}, \end{aligned} \tag{19}$$

where we assume that temperature oscillates around a local average $\bar{T}$. $\eta^T_{t+1} \sim \mathcal{N}\left(0, \sigma^2_\eta\right)$ is the temperature shock. The idiosyncratic productivity shocks $\hat{\varepsilon}_{it+1} \sim \mathcal{N}\left(0, \sigma^2_{\hat{\varepsilon}}\right)$ are independent across firms and time.

At the firm level, uncertainty arises from three sources: 1) idiosyncratic damage sensitivity $\hat{\xi}_{it}$, 2) aggregate temperature shocks η^T_{t+1}; and 3) idiosyncratic productivity shocks $\hat{\varepsilon}_{it+1}$. We assume firms have full information regarding all realized shocks and hold rational expectations regarding the future states of the economy. We refer to the cross-sectional variance of unexpected firm-level TFP shocks as *TFP volatility*, following Asker, Collard-Wexler, and De Loecker (2014).[33]TFP volatility in the model depends endogenously on temperature levels T_t and the temperature shocks η^T_t:

29. $\hat{\beta}_i$ can depend on a firm's products and adaptability. For example, a ski resort facing extreme heat might have a negative $\hat{\beta}_i$ because higher temperatures could hinder snowmaking, whereas a more adaptable firm—offering hot cider in cold weather and iced lemonade in hot—could have a positive $\hat{\beta}_i$. A high $\sigma^2_{\hat{\beta}}$ might reflect diverse product offerings in a region-sector, such as in service industries of developed economies.

30. This adjustment is introduced to ensure log-linearity of the aggregate economy in temperature when no marginal product dispersion exists.

31. One might naturally think that part of β_{it} is an endogenous firm choice, but we do not pursue that possibility here for simplicity. For a more general treatment of how firms might optimally pick their exposure to risk factors, see Kopytov, Taschereau-Dumouchel, and Xu (2024).

32. We use lower case to denote variables in logs, except for temperature T_t.

33. This can also be viewed as a theoretical counterpart to the cross-sectional measures of uncertainty as in Bloom (2009).

Lemma 2 *TFP volatility,* $\mathrm{Var}(\hat{a}_{it} - \mathbb{E}_{t-1}[\hat{a}_{it}])$*, can be written as:*

$$\mathrm{Var}(\hat{a}_{it} - \mathbb{E}_{t-1}[\hat{a}_{it}]) = (T_t - T^*)^2\sigma^2_{\hat{\xi}} + (\hat{\eta}^T_t)^2\sigma^2_{\hat{\beta}} + \sigma^2_{\hat{\varepsilon}}. \tag{20}$$

All else being equal, TFP Volatility is minimized when $T_t = T^*$ *and the temperature forecast for date* t *is fully accurate* ($\eta^T_t = 0$)*.*

This lemma illustrates two climate-related forces that shape TFP volatility. First, TFP volatility depends on the regional climate: if a region is significantly hotter or colder than T^*, firm-level productivity becomes too volatile to forecast accurately. We will test this empirically in Section 7.1. Second, forecast errors in temperature also matter. Even if firms share the same temperature forecast, their individual forecast errors may vary due to differences in their persistent sensitivities.

Flexible Inputs and Profits. Firms hire a composite of flexible inputs, "labor", on a period-by-period basis at a competitive wage, W_t. For simplicity in modeling the temperature-related supply- and demand-side frictions in the labor market (e.g., temperature-related disutility of work or temperature-induced loss of labor productivity), we assume the equilibrium wage is given by:

$$W_t = \overline{W} \exp\left(\chi(T_t - T^*)\right),$$

where the wage is a function of temperature (deviation from T^*) with constant elasticity χ, indicating the sensitivity of which wages respond to temperature.[34]. Optimal choice of flexible inputs is made after capital inputs are allocated and all shocks are realized. The static input choice solves

$$\max_{N_{it}} \exp\left(\hat{\beta}_{it}\left(T_t - T^*\right)\right) \hat{Z}_{it} K_{it}^{\alpha_K} N_{it}^{\alpha_N} - W_t N_{it},$$

and results in the operating profits Π_{it},

$$\Pi_{it} = GA_{it}K^{\alpha}_{it} := G\exp\left(\beta_{it}(T_t - T^*) + z_{it}\right) K^{\alpha}_{it}, \tag{21}$$

where $G := \overline{W}^{-\frac{\alpha_N}{1-\alpha_N}} \alpha_N^{\frac{\alpha_N}{1-\alpha_N}} (1-\alpha_N)$, $z_{it} = \frac{1}{1-\alpha_N}\hat{z}_{it}$, and $\alpha = \frac{\alpha_K}{1-\alpha_N}$. We define capital profitability as $A_{it} := \exp\left(\beta_{it}(T_t - T^*) + z_{it}\right)$, where $\beta_{it} = \frac{\hat{\beta}_{it} - \chi\alpha_N}{1-\alpha_N}$ is the sensitivity of capital profitability to temperature, transformed from the firm's productivity's temperature sensitivity, $\hat{\beta}_{it}$, and the wage's temperature sensitivity, χ. α is the curvature of the profit function.

Dynamic Capital Investment. Capital is a dynamic input that takes time to build. It needs to be invested one period ahead before all shocks (including temperature) are realized. Naturally, the investment problem of a firm i can be formulated into the Bellman equation of the form:

$$\begin{aligned} V\left(T_t, Z_{it}, K_{it}\right) = \max_{K_{it+1}} \quad & G\exp\left(\beta_{it}(T_t - T^*) + z_{it}\right) K^{\alpha}_{it} - K_{it+1} + (1-\delta)K_{it} \\ & + \frac{1}{1+r}\mathbb{E}_t\left[V\left(T_{t+1}, Z_{it+1}, K_{it+1}\right)\right], \end{aligned}$$

34. This assumption is commonly used in business cycle analysis. See Blanchard and Galí (2010), Alves et al. (2020), and Flynn and Sastry (2023).

where $\frac{1}{1+r}$ is the discount factor. Firms are risk-neutral and face no adjustment costs in the model.[35]. The optimal investment K_{it+1} solves the Euler equation:

$$1 = \underbrace{\frac{1}{1+r}}_{\text{Discount Factor}} \left(\underbrace{\alpha G K_{it+1}^{\alpha-1} \mathbb{E}_t \left[\exp\left(z_{it+1} + \beta_{it+1}(T_{t+1} - T^*) \right) \right]}_{\text{Expected Value of Marginal Profits of Capital}} + \underbrace{(1-\delta)}_{\substack{\text{Value of} \\ \text{Undepreciated Capital}}} \right). \tag{22}$$

Equation 22 reveals that a firm's investment is increasing in the forecast of its capital profitability, which depends on expected idiosyncratic productivity $z_{i,t+1}$, temperature sensitivity $\beta_{i,t+1}$, and future temperature T_{t+1}. Log-linearizing the solution for the firm's optimal capital choice and comparing it to the average firm's investment yields:

$$k_{i,t+1} - \overline{k_{i,t+1}} \;=\; \frac{1}{1-\alpha}\Big(\frac{\mathbb{E}_t[\hat{z}_{i,t+1}]}{1-\alpha_N} \;+\; \frac{\hat{\beta}_i - \overline{\hat{\beta}_i}}{1-\alpha_N}\, \mathbb{E}_t\big[T_{t+1} - T^*\big] \Big). \tag{23}$$

This policy equation shows that the size of a firm's persistent temperature sensitivity $\hat{\beta}_i$ governs how its investment plan responds to expected heat or cold. For a *heat-averse* firm with $\hat{\beta}_i < \overline{\hat{\beta}_i}$ (e.g., a ski resort), a higher temperature forecast $\mathbb{E}_t[T_{t+1}]$ reduces expected productivity more than for the average firm, leading to lower capital investment. Conversely, a *heat-loving* firm with $\hat{\beta}_i > \overline{\hat{\beta}_i}$ (e.g., a water park) invests more than average, owing to its relatively positive productivity response to anticipated higher temperatures.

MRPK. Once idiosyncratic productivity and temperature conditions are realized, each firm chooses its labor demand, and production takes place. From Equation 21, the realized (log) marginal revenue product of capital of firm i can be written as, $mrpk_{it} = a_{it} + (\alpha - 1)k_{it} + \log(\alpha_K \bar{G})$.[36] By substituting in the capital policy k_{it} as a function of previous expectations, we derive how $mrpk_{it}$ depends on the realized shocks:

Proposition 3 *A firm with higher unexpected change in productivity exhibit a higher MRPK relative*

35. Our benchmark model abstracts from the presence of adjustment costs in capital investment. If we introduce an adjustment cost of the form $-\frac{\kappa}{2}(\frac{I_{it}}{K_{it}} - \delta)^2$ at the time of investment, then the MRPK dispersion in the economy would take the form:

$$\sigma^2_{mrpk,(r,s),t} = \left(\frac{1}{1-\alpha_N}\right)^2 \left[(T_{r,t} - T^*)^2 \sigma^2_{\xi,(r,s)} + \eta^{T\,2}_{r,t} \sigma^2_{\beta,(r,s)} + \sigma^2_{\varepsilon,(r,s)} \right] + (\alpha-1)^2 \phi_A^2 \sigma^2_{k,t-1} + \text{Adj. Cost Channel}_{(r,s),t},$$

for some constant ϕ_A. The Adj. Cost Channel$_{(r,s),t}$ captures how adjustment costs interact with past and present climate conditions. It includes terms that are linear in $\eta^T_{r,t}$, as well as the interactions of past temperature conditions with $\eta^T_{r,t}$. The interaction between adjustment costs and climate conditions operates separately from our main mechanisms. It is unlikely to affect the identification of the damage volatility channel and climate volatility channel in the data when additional controls are added.

36. $\overline{G} = \overline{W}^{-\frac{\alpha_N}{1-\alpha_N}} \alpha_N^{\frac{\alpha_N}{1-\alpha_N}}$ is the constant associated with the revenue function $P_{it}Y_{it} = \overline{G} A_{it} K_{it}$.

to the average level:

$$mrpk_{it} - \overline{mrpk_{it}} = \frac{1}{1-\alpha_N}\Bigg\{ \underbrace{(\hat{\beta}_i - \overline{\hat{\beta}_i})\eta_t^T}_{\substack{\textit{Unexpected}\\ \textit{Temperature Shock}\\ \textit{on Productivity}}} + \underbrace{\hat{\xi}_{it}(T_t - T^*)}_{\substack{\textit{Unexpected}\\ \textit{Damage}\\ \textit{Sensitivity}}} + \hat{\varepsilon}_{it} \Bigg\}, \tag{24}$$

where the relative MRPK of heat-averse firms ($\hat{\beta}_i < \overline{\hat{\beta}_i}$) will decrease with a positive temperature shock η_t^T; while the relative MRPK of heat-loving firms ($\hat{\beta}_i > \overline{\hat{\beta}_i}$) will increase with a positive temperature shock.

Proof. See Appendix E.3. ■

Equation 24 implies that, if productivity were perfectly known at the time of investment, all firms would have identical MRPKs ex post. Otherwise, the MRPK would increase with forecast error of (revenue) productivity.

This highlights the model's key mechanism. In a region-sector facing a positive temperature shock $\eta_t^T > 0$, low-MRPK firms are those that are either (1) heat-averse ($\hat{\beta}_i < \overline{\hat{\beta}_i}$) such that the productivity suffers unexpectedly more than an average firm, or (2) unexpectedly damaged with idiosyncratic sensitivity satisfying $\hat{\xi}_{it}(T_t - T^*) < 0$. In hindsight, these firms overinvested based on overly optimistic productivity forecasts, leaving their capital underutilized compared to firms that are *heat-loving* ($\hat{\beta}_i > \overline{\hat{\beta}_i}$) or those that experienced less idiosyncratic damage ($\hat{\xi}_{it}(T_t - T^*) > 0$). This cross-firm disparity in realized returns leads directly to misallocation of capital, which is summarized by the following proposition, where we add back the notation for a region-sector pair $n = (r, s)$:

Proposition 4 *Within a region-sector pair $n = (r, s)$, the $mrpk$ dispersion across firms is increasing in TFP Volatility, $\mathrm{Var}(\hat{a}_{nit} - \mathbb{E}_{t-1}[\hat{a}_{nit}])$, and can be decomposed into:*

$$\begin{aligned}\sigma^2_{mrpk,(r,s),t} &= \left(\frac{1}{1-\alpha_N}\right)^2 \mathrm{Var}(\hat{a}_{nit} - \mathbb{E}_{t-1}[\hat{a}_{nit}]) \\ &= \left(\frac{1}{1-\alpha_N}\right)^2 \Bigg[\underbrace{(T_{r,t} - T^*)^2 \sigma^2_{\hat{\xi},(r,s)}}_{\textit{Level Effect}} + \underbrace{(\eta^T_{r,t})^2 \sigma^2_{\hat{\beta},(r,s)}}_{\textit{Forecast Error Effect}} + \sigma^2_{\hat{\varepsilon},(r,s)} \Bigg]\end{aligned} \tag{25}$$

Within $n = (r, s)$, $mrpk$ dispersion is increasing in:
(1) squared deviation from optimal temperature, $(T_{r,t} - T^*)^2$,
(2) squared (unexpected) temperature shocks $(\eta^T_{r,t})^2$.

Proposition 4 shows that MRPK dispersion scales with the dispersion of unexpected productivity shocks. As TFP volatility rises, so does the dispersion of the investment mistakes across firms. Temperature variations contribute to this misallocation via two channels:

(1) Level Effect. The *level* of temperature affects misallocation by raising the volatility of idiosyncratic damages across firms. As the temperature deviates more from the "bliss point" T^*, becoming too hot or too cold, firms who receive extreme realizations of the idiosyncratic

damage sensitivity $\hat{\xi}_{it}$ will experience larger unforeseen losses (e.g., a larger fraction of firms will experience severe factory fire). As a result, extreme returns become more prevalent, and aggregate misallocation grows with $(T_{r,t+1} - T^*)^2$.

(2) Forecast Error Effect. The *forecast error* of temperature raises capital misallocation by interacting with firms' dispersion of persistent sensitivities in the region-sector. A larger unexpected temperature shock (e.g., a sudden heatwave) makes heat-averse firms' returns unexpectedly low and heat-loving firms' returns unexpectedly high—amplifying capital misallocation. The reverse occurs under an unanticipated cold shock. Consequently, MRPK dispersion increases with the squared forecast error, $(\eta^T_{r,t})^2$.

These two effects help explain why a region-sector's geography and climate patterns may influence capital misallocation, as shown in Figure 4 in Section 4. Regions exposed to extreme climates—either too hot or too cold—or to unexpected temperature shocks are prone to higher levels of capital misallocation. Moreover, it helps us rationalize why shifting toward hotter climates is detrimental to the TFP of already hot regions ($T_{rt} > T^*$) but beneficial to colder ones ($T_{rt} < T^*$).

Equation (25) further predicts that, at a fixed climate, a region-sector's average misallocation depends on the distribution of firms' weather-related characteristics. Specifically, a region-sector with larger dispersion in persistent sensitivity $\sigma^2_{\hat{\beta},(s,r)}$ or higher damage uncertainty $\sigma^2_{\hat{\xi},(s,r)}$ suffers more from climate-induced misallocation. This framework also sheds light on the *income effect* identified in Section 4.4, namely why developed countries may incur greater losses from climate shocks. Although such economies often benefit from greater "heat preparedness" (higher $\overline{\hat{\beta}}_{(s,r)}$), they may also exhibit wider dispersion in $\sigma^2_{\hat{\beta},(s,r)}$ or $\sigma^2_{\hat{\xi},(s,r)}$, owing to broader specialization and greater product variety. Developed countries also feature a larger spread of firm sizes (Poschke 2018), implying wider variation in temperature sensitivities, as bigger firms typically hold more resources to buffer sudden climate shocks. While we do not explicitly model this latter point, Section 6 empirically explores how firm size can serve as a proxy for temperature sensitivity.

TFP Loss from Misallocation. Finally, we formalize how temperature-induced misallocation affects region-sector aggregate TFP in the model. In the Appendix, we show that under a CES aggregator,[37] the economy admits an aggregate production function of the form:

$$y_{nt} = a_{nt} + \tilde{\alpha}_K k_{nt} + \tilde{\alpha}_N n_{nt},$$

where the cost of misallocation can be expressed as the deviation from the level of TFP, a^*_{nt} when MRPKs are equalized across firms:

$$a_{nt} - a^*_{nt} = -\frac{\tilde{\alpha}_K + \tilde{\alpha}^2_K(\sigma - 1)}{2}\sigma^2_{mrpk,nt} \tag{26}$$

37. Following Midrigan and Xu (2014), in a partial equilibrium context, one can define aggregate production and misallocation by considering the problem of a planner with a CES aggregator and faces no restrictions on how to reallocate inputs across firms.

This formula is reminiscent of Equation 7 in the accounting framework and shows that the intuitions behind the cost of misallocation are similar in the firm dynamics model.

6 Firm-level Evidence: Heterogeneous Sensitivity, Temperature Shocks, and MRPK Divergence

Our model builds on the assumption that firms respond heterogeneously to extreme temperature shocks. In this section, we identify two sources of firm temperature sensitivity $\hat{\beta}_{it}$ and show how such differing levels of sensitivity lead to heterogeneous responses of MRPK under heat shocks.[38] Since directly measuring each firm's $\hat{\beta}_{it}$ for each firm is challenging, we instead explore two potential major factors leading to this heterogeneity: firm size and adaptability (notably, the use of air conditioning, or AC). We examine whether firms of different sizes and adaptability levels (with AC vs. without AC) exhibit distinct MRPK responses to identical temperature shocks. Our choice of firm size and AC installation as proxies for temperature sensitivity is guided by prior empirical work. Regarding size, studies (e.g., Ponticelli, Xu, and Zeume 2023) show that larger firms are less sensitive to temperature shocks and more adaptable than smaller firms, implying a higher $\hat{\beta}_{it}$. Concerning AC, Somanathan et al. (2021) finds that hot days suppress output at plants without climate-control facilities, whereas plants with AC remain unaffected.

We test whether identical heat shocks within a region-sector lead to heterogeneous MRPK responses for firms with different levels of temperature sensitivity. In line with the model's key prediction from Equation 24, a more heat-averse firm (i.e. lower $\hat{\beta}_i$) would see a lower-than-average MRPK from an unexpected heat shock, as its productivity is more affected, thus reducing capital returns.

$\hat{\beta}_i$ and MRPK: Empirical Implementation We run the following regression, an empirical counterpart to Equation 24, to see if our two heat-sensitivity proxy variables—firm size and AC installation—result in different (log) MRPK responses to temperature shocks:

$$\begin{aligned}\log(\text{MRPK}_{r,s,i,t}) = &\sum_{b \in B/\{5-10^\circ C\}} \lambda_b \times \text{Tbin}^b_{r,t} \\ &+ \sum_{b \in B/\{5-10^\circ C\}} \lambda_{b,\hat{\beta}\text{-proxy}} \times \text{Tbin}_{r,t} \times \hat{\beta}\text{-proxy}^{r,s}_{it} + \boldsymbol{\delta}\mathbf{X}_{i,t} \\ &+ \delta_i + \alpha_{s,c(r),t} + \varepsilon_{s,c(r),i,t}, \qquad \hat{\beta}\text{-proxy}^{r,s}_{it} \in \{\text{Relative Size}^{r,s}_{it-1}, \text{AC}^{r,s}_{it}\}.\end{aligned} \tag{27}$$

Here, r represents the region, s the sector, i the firm, and t the year. $\hat{\beta}\text{-proxy}^{r,s}_{it}$ is a firm-level proxy for $\hat{\beta}_i$, given by either $\text{Relative Size}^{r,s}_{it-1}$ or $\text{AC}^{r,s}_{it}$. We include firm fixed effects η_i, removing time-invariant firm-level heterogeneity, and country-sector-year fixed effects $\alpha_{s,c(r),t}$ to capture aggregate fluctuations in the same region-sector. Our coefficients of interest, $\lambda_{b,\hat{\beta}\text{-proxy}}$

38. This also serves to identify climate-induced misallocation directly using firm-level regression, without assuming log-normality.

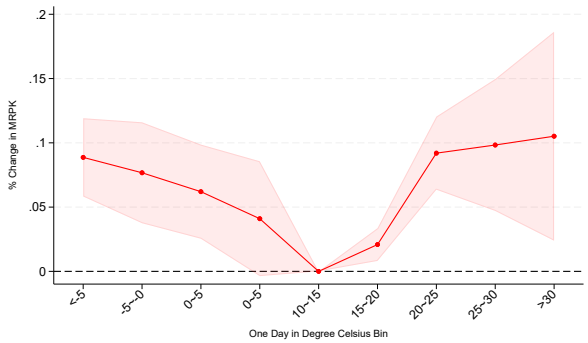
are identified by comparing how larger vs. smaller firms (or AC-equipped vs. non-AC-equipped firms) respond differently to the same temperature shock within a given country-sector. For instance, if $\lambda_b < 0$, a positive $\lambda_{b,\hat{\beta}\text{-proxy}}$ indicates that high-$\hat{\beta}_i$ firms suffer a smaller MRPK decline than low-$\hat{\beta}_i$ firms under the same shock.

Heterogeneous Effect of Temperature Shocks from Firm Size. Following Bau and Matray (2023), we characterize a firm's size based on its lagged book value of capital. We measure a firm's relative size using Relative Size$^{s,r}_{it-1} \equiv \log K^{s,r}_{it-1} - \mathbb{E}^{s,r}_i[\log K_{it-1}]$, which compares a firm's lagged (log) capital stock $\log K^{s,r}_{it-1}$ to the cross-sectional average of log capital across firms in the same region-sector-year, $\mathbb{E}^{s,r}_i[\log K_{it-1}]$. We then standardize Relative Size$^{r,s}_{it}$ over the entire sample. Figure 8a shows the differential impact of temperature shocks on MRPK across firms of varying sizes, $\lambda_{b,\text{Relative Size}}$, for each temperature bin b. Larger firms tend to experience higher MRPK in response to temperature extremes than smaller firms. Specifically, between two firms differing in size by one standard deviation, an extra day above 30°C or below -5°C (relative to a day in the 10-15°C range) incurs less decline in the MRPK of the larger firm by around 0.1%. Detailed results of the estimation are presented in Table D.2.

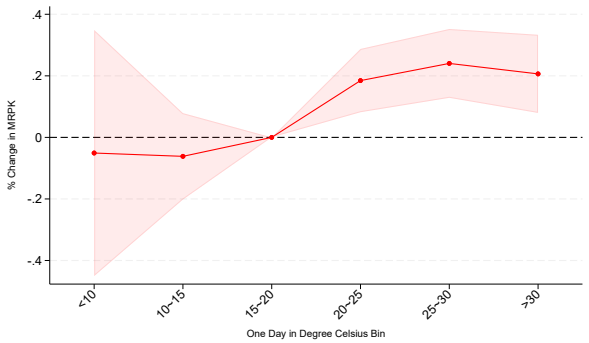
These findings imply that difference in firm sizes is a potential source of $\hat{\beta}_i$ heterogeneity and larger firms appear more heat-tolerant. Moreover, in Figure 9, we document higher dispersion in firm sizes in more developed economies, consistent with Poschke (2018). This larger size dispersion could translate to a larger spread in temperature sensitivities across firms and exacerbating capital misallocation, which help us rationalize the *wealth effect* in Figure 4, where we recover stronger increase in misallocation from extreme heat in wealthier economies.

Figure 8: Effects of daily temperature shocks on log MRPK for firms of different sizes and adaptability

(a) Heterogeneous Effect from Firm Size



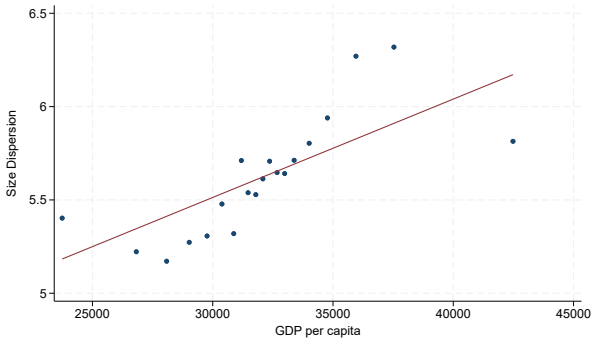
(b) Heterogeneous Effect from Firm Adaptability (AC)



Notes: Graph plots the effects of daily mean temperature bins on firm-level log MRPK. Figure 8a plots the interaction terms of relative firm size and temperature bins. Each point measures the estimated effect on a large firm relative to a firm that is 1 SD smaller. We include firm and country-sector-year fixed effects. Figure 8b plots the estimated effect on firms with and without AC separately. We include firm and sector-year fixed effects (since AC data only covers the India ASI sample). Standard errors are clustered at the regional level. Shaded areas indicate a 90% confidence interval.

Heterogeneous Effect of Temperature Shocks from Adaptability. Another source of $\hat{\beta}_i$ heterogeneity could be the firm's ability to cope with temperature extremes. Firms with better

Figure 9: Firm Size Dispersion and GDP per Capita



Notes: The graph presents the bin-scatter plots illustrating the relationship between firm size dispersion (measured as the variance of log fixed assets across firms) and annual GDP per capita at the region-sector-year level.

adaptation measures should be more resilient to heat shocks, implying a higher $\hat{\beta}_i$. We measure adaptability via the installation of computerized air conditioning (AC) systems, a variable collected annually in the Indian Annual Survey of Industries (ASI) since 2001. Therefore, our analysis for this part focuses on the sample from the Indian ASI.

We run Equation 27 with $\hat{\beta}\text{-proxy}_{it}^{s,r} = \text{AC}_{it}^{s,r}$, a dummy variable indicating whether the firm reports having AC.[39] Figure 8b depicts, $\lambda_{b,\text{AC-equipped}}$, the impact of temperature shocks on MRPK for AC-equipped firms relative to non-AC firms for each temperature bin b. We find that cold shocks produce little difference in MRPK between the two groups, but heat shocks lead to significantly smaller MRPK declines for AC-equipped firms compared to the non-AC ones. Our findings reveal that cold temperature shocks creates a negligible difference in MRPK between AC-equipped and non-AC firms. However, heat shocks lead to significantly less decline inn MRPK for AC-equipped firms compared to non-AC firms. For example, an additional day with temperatures above 30°C (relative to a day of 15°C-20°C) raises the MRPK of AC-equipped firms by about 0.2% relative to firms without AC. Detailed results are presented in Table D.3.[40]

7 Quantifying the Causes and Consequences of Climate-Induced Misallocation

In this section, we empirically identify the two effects driving climate-driven misallocation: (1) the level effect increasing damage volatility, and (2) the forecast error effect that amplifies

39. A firm is defined as AC-equipped if it has reported the installation of AC at least once during the sample period.

40. Our baseline specification in Column 3 analyzes the within-firm variation on the effect of AC installation by including firm fixed effects δ_i and sector-year fixed effects $\theta_{s,t}$, and we include the AC indicator variable $\text{AC}_{it}^{s,r}$ and capital stock $\ln K_{it}$ as controls. However, installing air conditioning is a common adaptation strategy for firms to cope with extreme heat, but it also makes them subject to costs of adaptive investment (e.g. Somanathan et al. 2021), which means the investment of AC itself could change the firm's MRPK as well. Following the approach of Asker, Collard-Wexler, and De Loecker (2014), we address this in our alternative specification in Column (3) by conditioning on current capital stock to make sure that we are comparing two firms making the same capital decision, but one firm has AC while the other does not. We include sector-year fixed effects in all specifications, such that λ_b and $\lambda_{b,\text{AC}}$ are identified based on the comparison of across-firm differences caused by AC installation within each sector-year.

cross-firm investment mistakes, as suggested by the model in Equation 25, and then quantify its aggregate consequences in global economic development over the past 40 years.

We first test the level effect by empirically estimating how the temperature level nonlinearly shifts the TFP volatility and MRPK dispersion in the cross-section of firms. From this exercise, we can also identify an optimal temperature of roughly 13°C, consistent with Burke, Hsiang, and Miguel (2015). Next, we provide direct evidence of the forecast error effect by using mid-range weather forecast data from ECMWF and show that mean squared forecast errors of monthly temperature contribute to MRPK dispersion. Finally, we use these estimates to explore the critical role of the misallocation channel in accounting for cross- and within-country productivity variations, growth, and global income inequality.

7.1 Level Effect: Temperature and TFP Damage Volatility

Our theory suggests that MRPK dispersion is proportional to TFP volatility, which in turn depends nonlinearly on the level of temperature $T_{r,t}$. As the temperature deviates from the optimal level T^*—either becoming too hot or too cold—the likelihood of firm-level extreme events rises. Therefore, local temperature's deviation from T^* increases TFP volatility across firms. We now test this relationship in the data and estimate the optimal temperature T^*.

As it is difficult to directly measure unexpected TFP shocks ($\hat{a}_{nit} - \mathbb{E}_{t-1}[\hat{a}_{nit}]$) precisely due to possible mis-specifications of the law of motion of productivity and agents' information set, we adopt the approach of Asker, Collard-Wexler, and De Loecker (2014), and use the variance of 'first-differenced' TFP shocks, $\text{Var}_{(r,s)t}(\hat{a}_{it} - \hat{a}_{it-1})$, which approximates the TFP volatility.[41] Inspired by Equation 46, we identify the nonlinear impact of temperature on TFP volatility from the following reduced-form specification:

$$\text{Var}_{(r,s),t}(\hat{a}_{it} - \hat{a}_{it-1}) = \alpha + \boldsymbol{\beta}\boldsymbol{f}(T_{r,t}) + \eta_{s,r} + \delta_{c(r),t} + \varepsilon_{s,r,t}, \tag{28}$$

where $\boldsymbol{f}(T_{r,t})$ is a polynomial of annual average temperature. $\eta_{s,r}$ and $\delta_{c(r),t}$ denote region-sector and country-year fixed effects, respectively. We include only region-sector-year observations with at least 15 recurrent firms in the estimation.[42] The estimation results are reported in Columns (1)–(3) of Table 2.

Column (1) reports the estimate of the linear effects of temperature, which is negative and not statistically significant. However, including second- and third-order terms reveals a clear nonlinear U-shaped pattern that aligns with our theoretical model. Column (2) shows that the quadratic temperature term is statistically significant and economically meaningful: a 1 °C increase in the annual average temperature in a location with an average of 5°C will lead to a decrease of 2.9 log points in TFP volatility; however, the same 1 °C increase from a 20°C place will increase the TFP volatility by 2.5 log points. These effects are quantitatively large,

41. TFP can alternatively be derived as the conventional Solow residuals including labor. However, as noted in David and Venkateswaran (2019), footnote 22, TFP calculated from the Solow residual approach can no longer be directly tied to capital profitability in the presence of labor distortions, while the model-based measure of TFP remains a valid proxy for capital profitability.

42. This is to reduce measurement errors from the observations that aggregate statistics with only a few numbers of firms. The measured TFP volatility is winsorized at the top 1 percent level to avoid outliers.

Table 2: TFP Volatility and Temperature Levels

	(1) 1st Order	(2) 2nd Order	(3) 3rd Order	(4) Model-Induced
$T_{r,t}$	-0.005319	-0.023121***	-0.012380	
	(0.004573)	(0.007536)	(0.008537)	
$T_{r,t}^2$		0.000841***	-0.000447	
		(0.000303)	(0.000679)	
$T_{r,t}^3$			0.000040**	
			(0.000018)	
$(T_{r,t}^2 + T_{r,t-1}^2)$				-0.021556***
				(0.005682)
$(T_{r,t} + T_{r,t-1})$				0.000882***
				(0.000216)
$(\Delta T_{r,t})^2$				-0.003604
				(0.002233)
Estimated T^*		13.75 °C	14.64°C	12.22°C
		(3.067678)	(2.173182)	(2.216646)
Region-Sector FE	Yes	Yes	Yes	Yes
Country-Year FE	Yes	Yes	Yes	Yes
Observations	113,765	113,765	113,765	113,765
R^2	0.754	0.754	0.754	0.754

Notes: Standard errors in parentheses. We cluster standard errors at the regional level (NUTS3 level for European countries, prefecture-level for China, and district-level administrative divisions for India).
* $p < 0.10$, ** $p < 0.05$, *** $p < 0.01$

especially in the context of global warming projections.[43] The cubic specification in column (3) suggests some asymmetry, where a positive 1°C shock can cause more damage in warmer climates than benefits in cooler ones. Figure 10 illustrates the U-shaped relationship between temperature and volatility by presenting a binscatter of the two variables after residualizing all relevant fixed effects.

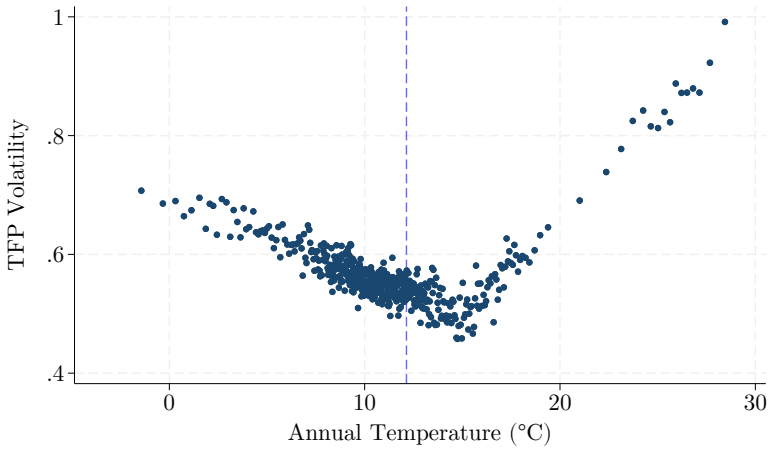
Interpreting these estimates through our model, a positive temperature shock in a colder environment will move the economy closer to the optimal temperature T^*, reducing the harmful dispersion of extreme events caused by idiosyncratic temperature sensitivity $\hat{\xi}_{it}$. In contrast, the same positive shock in a hotter climate drives the economy further away from T^*, increasing the damage volatility.[44] Next, we will identify T^*.

Identifying the Optimal Temperature T^*. While the reduced-form polynomials are intuitive, they may omit how past temperatures affect the lagged TFP $\hat{a}_{it-1}$. To address this, we

43. To illustrate, let us consider a simple back-of-the-envelope calculation using parameters from our model. Take, for example, a permanent increase from 16 °C to 20 °C, which aligns with an RCP 8.5 climate scenario projected for Southern Spain (*World Bank Climate Change Knowledge Portal* 2023). According to our model's damage uncertainty mechanism, this 4 °C increase would increase TFP Volatility by 4.24 log points. This increment translates into a 12.31 log points increase in MRPK dispersion using Equation 25. Subsequently, under standard elasticity assumptions, this dispersion translates into a 7.6% loss in TFP.

44. This temperature-volatility relationship, as depicted in our reduced-form estimate in Figure 10, also clarifies why the same hot temperature shock in cooler climates leads to a decrease in MRPK dispersion while producing an opposite effect in hotter climates as estimated in Equation 15 and depicted in Figure 4.

Figure 10: TFP Volatility and Annual Temperature



Notes: The graph plots a binned scatter of TFP Volatility against annual temperature. The variation shown is derived from residuals after controlling for region-sector fixed effects and country-year fixed effects. The blue dashed line indicates the identified optimal temperature, $T^* = 12.22°\text{C}$.

derive the exact model-consistent expression for first-differenced volatility:

$$\text{Var}_t(\hat{a}_{it} - \hat{a}_{it-1}) = \sigma^2_{\hat{\xi}}(T_t^2 + T_{t-1}^2) - 2\sigma^2_{\hat{\xi}}T^*(T_t + T_{t-1}) + 2\sigma^2_{\hat{\xi}}T^{*2} + \sigma^2_{\hat{\beta}}(\Delta T_t)^2 + \sigma^2_{\Delta z},$$

and estimate the model-induced specification:

$$\text{Var}_{(s,r),t}(\hat{a}_{it}-\hat{a}_{it-1}) = \alpha+\beta_1(T_{r,t}^2+T_{r,t-1}^2)+\beta_2(T_{r,t}+T_{r,t-1})+\gamma(\Delta T_{r,t})^2+\eta_{s,r}+\delta_{c(r),t}+\varepsilon_{s,r,t}, \quad (29)$$

where $\Delta T_{r,t} \equiv T_{r,t} - T_{r,t-1}$. Column (4) of Table 2 shows the estimates from the model-induced regression are very comparable to the quadratic specification in Column (2). By applying the Delta Method to the estimated coefficients, we find $\hat{T}^* = -\frac{\hat{\beta}_2}{2\hat{\beta}_1} = 12.22°\text{C}$ (SE: 2.21°C). The reduced-form specifications yield $\hat{T}^* = 13.75°\text{C}$ and $\hat{T}^* = 14.64°\text{C}$ for the quadratic and cubic specifications, respectively. Across specifications, estimates align closely with those found by Burke, Hsiang, and Miguel (2015), who also found that country-level productivity or GDP peaks at the "bliss point" 13°C. Our findings corroborate the literature by suggesting an additional mechanism: temperature levels contribute to aggregate MRPK dispersion and TFP (output) loss as a volatility shock.

7.2 Forecast Error Effect: Temperature Forecast Errors and Misallocation

We now identify how temperature forecast errors cause misallocation. Rather than relying on proxies from statistical models, we directly use mid-range temperature forecasts from the ECMWF (Copernicus Climate Change Service and Climate Data Store 2018). Extensive research shows that accurate daily and seasonal temperature forecasts significantly affect adaptation behaviors (e.g., Shrader 2023) and mortality (Shrader, Bakkensen, and Lemoine 2023), as agents base their decisions on these signals. We similarly assume firms incorporate monthly weather forecasts into their planning or at least process related information.

Since MRPK is reported annually while the ECMWF's mid-range temperature forecast is

released every month, we create a yearly mean-squared forecast error (MSFE) measure. Let us denote the realized average temperature in the region r at month m and year t as $T_{m,r,t}$ and the month-ahead ECMWF temperature forecast as $\mathbb{E}_{m-1}[T_{m,r,t}]$. We construct a measure of mean squared forecast errors, $\text{MSFE}_{q,r,t}$, for each time frame q in year t, where we let $q \in \{\text{summer}, \text{winter}, \text{annual}\}$,

$$\begin{aligned}
\text{MSFE}_{\text{summer},r,t} &= \frac{1}{6}\sum_{m=4}^{9}(T_{\text{m},r,t} - \mathbb{E}_{m-1}[T_{m,r,t}] - \widehat{\text{Bias}}_{m,r})^2, \\
\text{MSFE}_{\text{winter},r,t} &= \frac{1}{6}\sum_{m=\{1,2,3,10,11,12\}}(T_{\text{m},r,t} - \mathbb{E}_{m-1}[T_{m,r,t}] - \widehat{\text{Bias}}_{m,r})^2, \\
\text{MSFE}_{\text{annual},r,t} &= \frac{1}{12}\sum_{m=1}^{12}(T_{\text{m},r,t} - \mathbb{E}_{m-1}[T_{m,r,t}] - \widehat{\text{Bias}}_{m,r})^2.
\end{aligned}$$

where $\widehat{\text{Bias}}_{m,r}$ is a region-month fixed effect capturing historical forecast biases over 40 years. We split the year into two seasons: "summer" (April–September) and "winter" (October–March), reflecting how temperature forecast errors in warmer vs. colder months may affect MRPK differently. We also remove $\widehat{\text{Bias}}_{m,r}$ to reduce mechanical differences in temperature measurements due to the positioning of the weather stations and forecasting methods.

Equation 25 suggests that a larger squared forecast error in a region-sector would lead to more capital misallocation. We therefore estimate the following regression:

$$\sigma^2_{mrpk,(s,r),t} = \sum_q \theta_q \cdot \text{MSFE}_{q,r,t} + \sum_q \gamma_{1,q} T_{q,rt} + \sum_q \gamma_{2,q} T^2_{q,r,t} + \eta_{s,r} + \delta_{c(r),t} + \varepsilon_{s,r,t}, \tag{30}$$

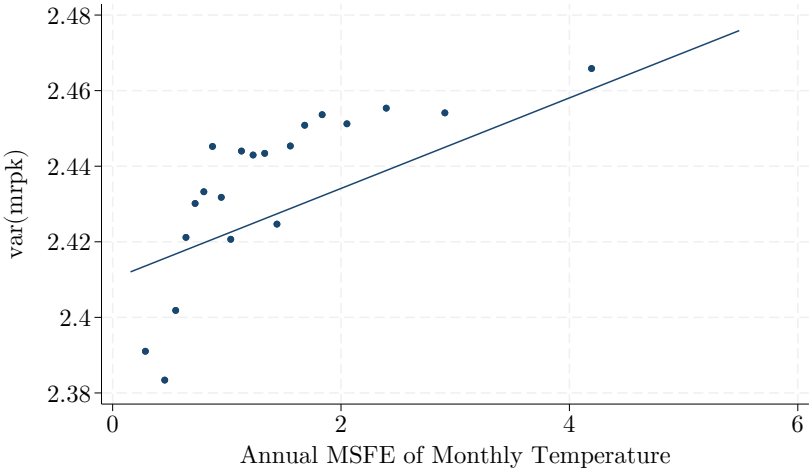
where θ_q measures how a one-unit increase in MSFE for time frame q affects annual capital misallocation. We include the linear and quadratic terms of realized temperatures in Equation 25 to ensure that identification of θ_q stems from *information* (forecast errors) rather than realized weather extremes.

Table 3 presents the results. Columns (1)–(2) show that annual MSFE (averaged over all months) significantly increases MRPK dispersion, even after controlling for the level effect of realized temperatures. Figure 11 illustrates the variations in Column (2) using a binscatter of MRPK dispersion against annual MSFE after residualizing the relevant temperature controls and fixed effects. Consistent with theoretical predictions, the graph reveals a monotonic pattern and indicates that misallocation is minimized when forecast errors approach zero. Columns (3) and (4) display the estimates using "seasonal" MSFEs from both summer and winter. We find that an MSFE increase in summer is at least twice as costly as in winter, suggesting that unexpected temperature shocks during warmer months are more damaging. Winter forecast errors become insignificant upon controlling for realized temperature.

The estimates in column (2) can be interpreted in the following way: a 1°C increase in the temperature forecast errors in all months would lead to a 1.6 log point increase in MRPK dispersion, compared to a perfect information counterfactual, equivalent to an approximate 0.58% of annual aggregate TFP loss. Obtained from a small deviation from a perfect information state, this number should be interpreted as a lower bound of the aggregate cost of

temperature forecast errors.[45] Moreover, with an average $\text{MSFE}_{\text{annual},r,t}$ of 1.39 in our sample, the average cost of forecast errors is around 0.81% of TFP. Our findings suggest that temperature forecast errors are costly: unexpected temperature shocks lead to dispersion in investment mistakes among firms due to their varying sensitivity to heat. In sum, the value of temperature forecasts is highlighted through a new channel in our context: accurate forecast increases the allocative efficiency of capital.

Figure 11: MRPK Dispersion and Annual MSFE



Notes: The graph plots a binned scatter of MRPK dispersion against the annual MSFE. The variation shown is derived from residuals after controlling for quadratic temperature terms, region-sector fixed effects, and country-year fixed effects.

Table 3: Temperature Forecast Errors and MRPK Dispersion

	(1)	(2)	(3)	(4)
$\text{MSFE}_{\text{annual},r,t}$	0.019114***	0.016249**		
	(0.006675)	(0.006561)		
$\text{MSFE}_{\text{summer},r,t}$			0.014908**	0.016592**
			(0.007115)	(0.007084)
$\text{MSFE}_{\text{winter},r,t}$			0.008536**	0.006096
			(0.004017)	(0.003882)
Quadratic Temperature Control	No	Yes	No	Yes
Region-Sector FE	Yes	Yes	Yes	Yes
Country-Year FE	Yes	Yes	Yes	Yes
Observations	124,065	124,065	124,065	124,065
R^2	0.876	0.876	0.876	0.876

Notes: Standard errors in parentheses. We cluster standard errors at the regional level (NUTS3 level for European countries, prefecture-level for China, and district-levels for India).
* $p < 0.10$, ** $p < 0.05$, *** $p < 0.01$

45. 0.58% is obtained by using the calibrated structural parameter, $-\frac{\tilde{\alpha}_K+\tilde{\alpha}_K^2(\sigma-1)}{2} = 0.359$.

7.3 Quantitative Exploration of the Model: Economic Development since 1981

Having established the empirical relevance of both channels in the data, we now revisit a classic question in development economics: how much do temperature conditions affect productivity and income inequality through the lens of the misallocation channel?

We calibrate the strength of these two channels using a model-induced regression derived directly from Equation (25), assuming a uniform across-firm dispersion of temperature sensitivities in all regions:

$$\sigma^2_{mrpk,(s,r),t} = \kappa_1 (T_{r,t} - \hat{T}^*)^2 + \kappa_2 \hat{\eta}^{T\,2}_{r,t} + \iota_{s,r} + \iota_{c(r),t} + \varepsilon_{s,r,t}, \tag{31}$$

where $(T_{r,t} - \hat{T}^*)^2$ is the squared deviation of annual temperature from the estimated optimum $\hat{T}^* = 12.22\,^\circ C$, and $\hat{\eta}^{T\,2}_{r,t}$ (the squared unexpected temperature shocks) is measured by the annual mean squared forecast error $\text{MSFE}_{\text{annual},r,t}$ in the data.

Table 4: Model-induced Regressions: Calibrating the Sensitivity Dispersions

	(1)	(2)
$(T_{r,t} - \hat{T}^*)^2$	0.0045***	0.0042***
	(0.0008)	(0.0007)
$\text{MSFE}_{r,t}$	0.0120**	0.0124**
	(0.0055)	(0.0052)
Region-Sector FE	Yes	Yes
Country-Year FE	Yes	No
Country-Sector-Year FE	No	Yes
Observations	121,561	121,004
R^2	0.876	0.909

Notes: Standard errors in parentheses. We cluster standard errors at the region level (NUTS 3 level for European countries, province level for China, and first-level administrative divisions for India).
* $p < 0.10$, ** $p < 0.05$, *** $p < 0.01$

Table 4 reports the coefficients κ_1 and κ_2. Using Column (1) (our preferred specification) and referencing Equation (25), we recover $\sigma^2_\xi = \frac{\sigma^2_{\hat{\xi}}}{(1-\alpha_N)^2} = \hat{\kappa}_1 \approx 0.0023$, and $\sigma^2_\beta = \frac{\sigma^2_{\hat{\beta}}}{(1-\alpha_N)^2} = \hat{\kappa}_2 \approx 0.015$, which represent the empirical averages of the two sensitivity dispersions in our sample.

7.3.1 The Cost of Climate-Induced Misallocation

We first measure the total cost of climate-driven misallocation in our model. Precisely, we define this cost as the aggregate productivity (or output) loss when comparing observed states of the world to a counterfactual in which all within-region dispersion in climate sensitivities is removed ($\sigma^2_\xi = 0$ and $\sigma^2_\beta = 0$).

To operationalize the exercise, we pair our estimates with gridded climate data (ERA5) and weather forecast data (ECMWF) for all countries worldwide, partitioning the globe into roughly 4,000 regions. For China, India, and EU countries, we use the same regional definitions

as in our empirical analysis; for other regions, we adopt GADM level-1 partitions.

We treat the global economy under a Cobb-Douglas aggregator of country-level outputs $\log Y_t^{\text{Global}} = \sum_c \omega_{ct} \log Y_{ct}$, where ω_{ct} is each country's output share. Within each country c, we similarly write $\log Y_{ct} = \sum_{r \in R(c)} \omega_{rt}^c \log Y_{rt}$, where ω_{rt}^c is the share of region r's output in country c's total output. This implies an aggregate global production function[46] and hence a global TFP:

$$\log \text{TFP}_t^{\text{Global}} = \sum_r \omega_{rt} \log \text{TFP}_{rt}.$$

where $\omega_{rt} = \omega_{ct}\omega_{rt}^c$. Under this setup, the global cost of climate-induced misallocation from the two channels corresponds to output-weighted deviations from optimal temperature, $\sum_r \omega_{rt}(T_{r,t} - T^*)^2$, and from forecast errors, $\sum_r \omega_{rt}\text{MSFE}_t$, scaled by our estimated sensitivity dispersions. Formally,

$$\underbrace{\overline{\Delta^{T,\text{Mis}} \log \text{TFP}_t^{\text{Global}}}}_{\approx -8.9\%} = -\frac{\tilde{\alpha}_K + \tilde{\alpha}_K^2(\sigma - 1)}{2} \Bigg[\underbrace{\sigma_\xi^2 \Big(\overline{\sum_r \omega_{rt}(T_{r,t} - T^*)^2} \Big)}_{\substack{\text{Level Effect} \\ \approx -8.34\%}} + \underbrace{\sigma_\beta^2 \Big(\overline{\sum_r \omega_{rt}(\text{MSFE}_t)} \Big)}_{\substack{\text{Forecast Error Effect} \\ \approx -0.56\%}} \Bigg].$$

Averaging these two sufficient statistics over 1981–2019, we find that climate-induced misallocation costs the global economy about 8.9% of TFP. Of this total, 8.34% arises from the *level effect*, whereas 0.56% derives from the *forecast error effect*. Notably, the contribution of the level effect is substantially larger than that of the forecast error effect, suggesting that most climate-induced misallocation arises from persistent deviations of regional climates from the optimal temperature rather than from unpredictability of weather fluctuations in the short-run.

7.3.2 The Changing Cost: Global Warming and Weather Forecast Improvement

We then examine the changing costs of climate-induced misallocation using the evolution of regional temperature and weather forecasts from $t_0 = 1981$ to $t_1 = 2019$:

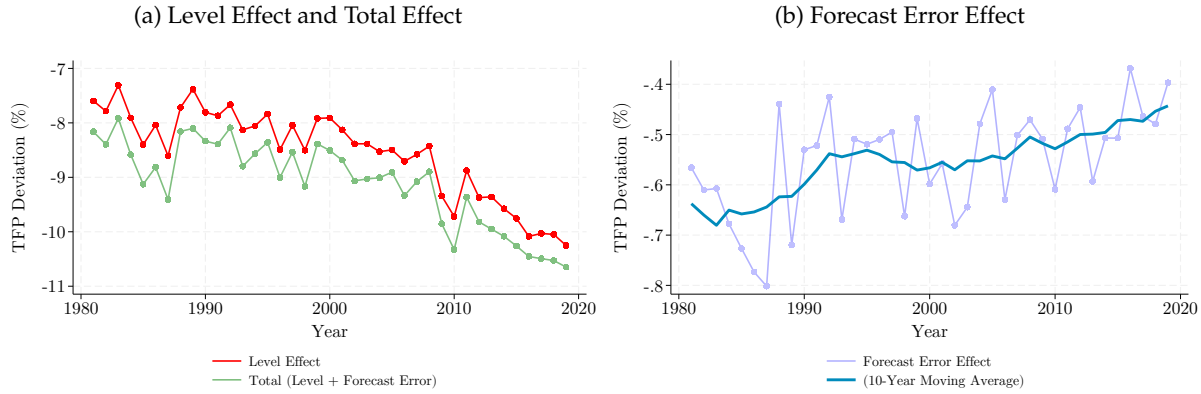
$$\underbrace{\Delta_{t,t_0}^{T,\text{Mis}} \log \text{TFP}_t^{\text{Global}}}_{-2.49\%} = -\frac{\tilde{\alpha}_K + \tilde{\alpha}_K^2(\sigma - 1)}{2} \Bigg[\underbrace{\sigma_\xi^2 \Delta_{t,t_0} \Bigg(\sum_r \omega_{rt}(T_{r,t} - T^*)^2 \Bigg)}_{\substack{\Delta \text{ Level Effect} \\ \approx -2.66\%}} + \underbrace{\sigma_\beta^2 \Delta_{t,t_0} \Bigg(\sum_r \omega_{rt}\text{MSFE}_t \Bigg)}_{\substack{\Delta \text{ Forecast Error Effect} \\ \approx +0.17\%}} \Bigg]. \tag{32}$$

We plot the evolution of the global costs of misallocation induced by the two effects in Figure 14a. Altogether, they reduce global TFP by 2.49% from 1981 to 2019. Not surprisingly, the pri-

46. This remains valid regardless of inter-regional factor mobility.

mary driver of this significant increase in costs is global warming, which moves hotter regions further away from the optimal temperature more than it brings cooler regions closer. Not surprisingly, the main driver of this large increase in costs is global warming, which pushes more hotter regions further away from the optimal temperature than the cooler regions it brings closer. This rise in the level effect makes firm-level productivity more volatile and reduces investment efficiency in the global economy, lowering TFP (and thus the average return to capital) by 2.66% after four decades of warming. In contrast, improvements in global weather forecasts have actually enhanced allocative efficiency, raising global TFP by 0.17%. Using a 10-year moving average filter to extract trends from short-term weather fluctuations, the benefits of forecast improvement is about 0.20%. Both time series are plotted in Figure 14b.

Figure 12: The Changing Cost of Climate-Induced Misallocation



Although the aggregate gains from improved forecast accuracy appears small relative to the level effect, they remain substantial in absolute terms. To the best of our knowledge, our paper is the first study to provide a quantitative evaluation of the improvements in global weather forecasts over the past four decades. These estimates can be directly compared with the costs of weather information services. For example, Georgeson, Maslin, and Poessinouw (2017) measures that the investment cost of weather information services amount to around 0.08% of global GDP in recent years, but we estimate that it can yield at least 0.2% in benefits.[47] This implies a benefit–cost ratio of exceeding 2. Our analysis implies that improving weather forecasts is a promising and effective route for climate adaptation, corroborating the argument by Shrader (2023), although it cannot fully compensate for losses due to a warming climate.

7.3.3 How much does climate matter for productivity differences and growth across countries? Macro Data vs. Model Estimates

We use our framework to revisit a central question in economic development: what explains the large productivity differences among countries? Geography and climate have long been recognized as influential factors in comparative development (Montesquieu 1748; Sachs and Warner 1997; Gallup, Sachs, and Mellinger 1999; Nordhaus 2006; Dell, Jones, and Olken 2012),

47. Our estimate is a conservative lower bound since (1) we do not consider mortality costs, only production costs, and (2) the 1981 estimates serve as a lower bound; the cost of having no weather forecasts at all is unknown but must be lower than the 1981 baseline.

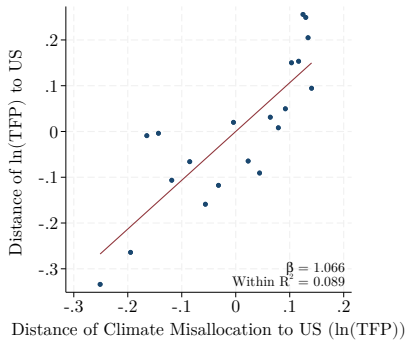
yet direct quantitative evidence on the underlying mechanisms is often limited. Here, we re-examine this question through the misallocation channel and show how our model, when combined with micro-level estimates and granular weather data, can explain a significant portion of observed macroeconomic development patterns.

We match our model-generated country-year estimates with country-level TFP data from the Penn World Table (PWT) 10.01 (Feenstra, Inklaar, and Timmer 2015). Our first goal is to gauge the extent to which cross-country productivity differences can be attributed to climate, as captured by climate-induced misallocation in our model. Specifically, we compare the measured TFP gap relative to the United States ($\ln \text{TFP}_{c,t} - \ln \text{TFP}_{\text{US},t}$) with the model-predicted climate misallocation cost relative to the United States $\left(\Delta^{T,\text{Mis}} \log \text{TFP}_{c,t} - \Delta^{T,\text{Mis}} \log \text{TFP}_{\text{US},t}\right)$ each year. The United States, often regarded as the global productivity frontier, is also geographically close to the estimated optimal temperature ($T^* \approx 12°\text{C}$), facing relatively minimal climate-induced misallocation—an "allocational frontier," in effect.

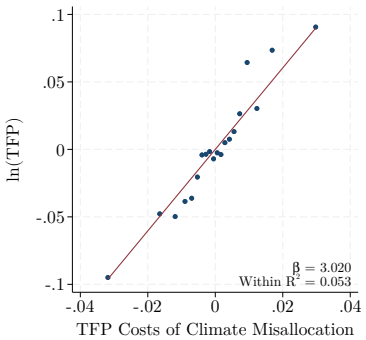
Figure 13a depicts a binned scatter plot of macro data against model-generated micro estimates, both demeaned by year fixed effects to remove average global convergence trends. A fitted regression line yields a slope coefficient near 1, which signals the quantitative success of our simple model: if a country's predicted TFP distance to the U.S. owing to climate misallocation rises by 1%, its actual measured TFP distance, on average, also increases by about 1%. This indicates that climate-induced misallocation contributes to cross-country productivity differences in a manner largely orthogonal to other potential drivers. An R^2 of 0.089 implies that about 9% of measured TFP differences can be explained by climate via the misallocation channel. Notably, the model results are derived solely from micro-data estimates and granular regional temperature and forecast information, yet they match the macro data reasonably well.

Figure 13: Macro Data vs. Model Estimates

(a) Across-country TFP Dispersion



(b) Within-country TFP Variation



Notes: Values in Panel (a) is demeaned by the year fixed effect to remove average TFP convergence. Values in Panel (b) is demeaned by the country and year fixed effect.

Next, we compare measured TFP variations *within* a country against the changes in misallocation cost due to recent climate shifts in the model. Figure 13b shows that our model also tracks the within-country patterns well, with a fitted slope of around 3. This suggests other omitted factors may correlate with climate-induced across-firm misallocation (for example, perhaps due to the spatial misallocation across regions that we do not explicitly model). The fact that both fitted slopes in Figures 13a and 13b exceed 1 also demonstrates the lower-bound

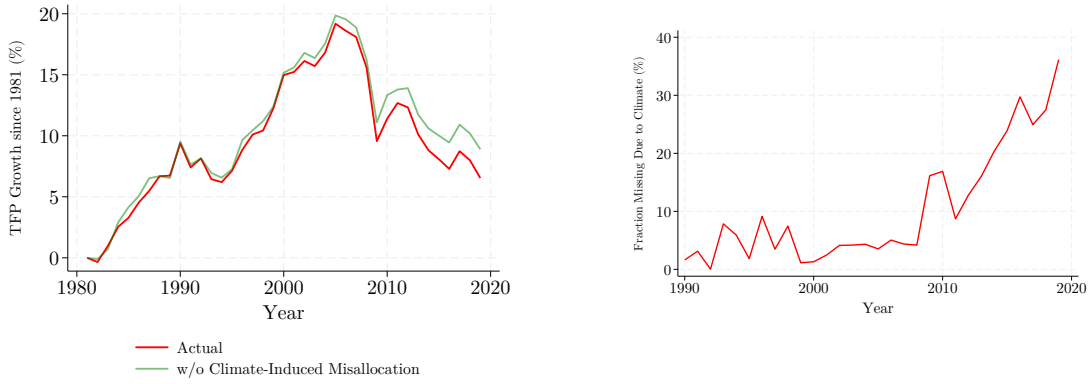
nature of our results.

Finally, we explore how rising climate-induced misallocation affects global TFP growth over time. We calculate actual cumulative global TFP growth (relative to 1981) from the PWT, along with a counterfactual path where climate-induced misallocation remains at its 1981 level. Our results show that global TFP would be about 2.36% higher in the PWT sample absent the increase in climate misallocation costs. Since cumulative global TFP growth from 1981 to 2019 is only about 8.9 percentage points, this equates to a 36% increase in cumulative growth.

Figure 14: Climate Change and Global Aggregate TFP Growth

(a) Actual vs. Counterfactual TFP

(b) Contribution to Cumulative Growth since 1981



In summary, our findings highlight that climate-induced misallocation accounts for a sizable portion of cross-country productivity differences and global growth trends. By emphasizing the role of geography and climate in shaping misallocation patterns, these results offer a fresh perspective on the longstanding question of why some nations are more productive than others.

7.3.4 Climate and Global Income Inequality

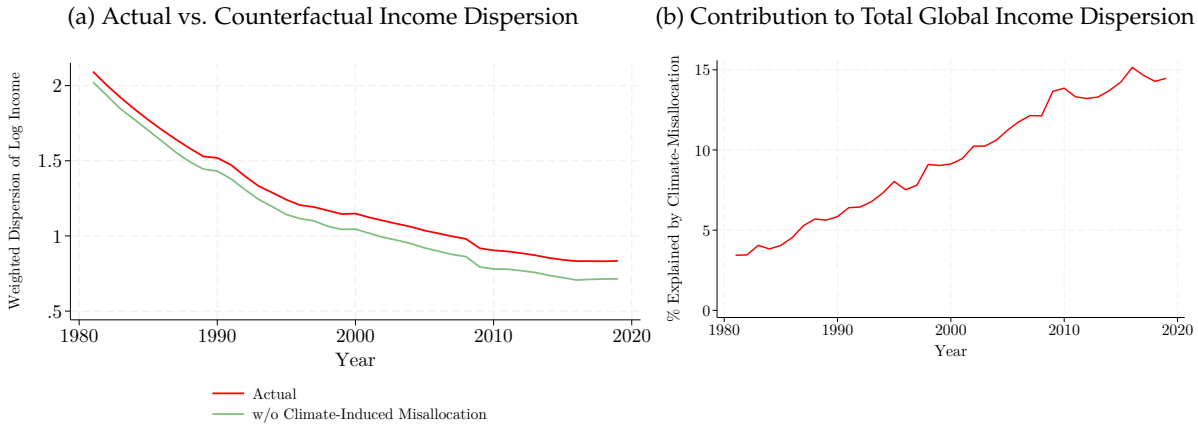
Given our model's explanatory power for productivity dispersion and growth, it is natural to extend the analysis to assess the impact of climate on global income inequality. Widespread evidence of income convergence trends has been documented in the literature (see, for example, Barro and Sala-i-Martin 1991; Barro 2015). To measure income inequality, we follow Gaubert et al. (2021) by adopting a population-weighted, between-country variance of per capita income:

$$V_{\text{Global},t} = \sum_r s_{rt}^L \left(\ln \text{GDPpc}_{rt} - \sum_r s_{rt}^L \ln \text{GDPpc}_{rt} \right)^2 \tag{33}$$

where s_{rt}^L is region r's share of the global population. This index also approximates the welfare-theoretic inequality measure proposed by Bourguignon (1979). Using World Bank data on GDP per capita and UN population statistics, we construct $V_{\text{Global},t}$ for the period 1981–2019. Figure 15a shows a consistent pattern of global income convergence since 1981: the variance of per capita income dropped by half, from about 2.09 in 1981 to 0.83 in 2019.

We then ask: What role does the misallocation channel play in global income dispersion? To

Figure 15: Climate-Induced Misallocation and Global Income Dispersion



address this, we compute a counterfactual GDP per capita $\ln(\widetilde{\text{GDPpc}}_{c,t})$ that excludes climate-induced misallocation:

$$\ln \widetilde{\text{GDPpc}}_{c,t} = \ln \text{GDPpc}_{c,t} - \Delta^{T,\text{Mis}} \log \text{TFP}_{c,t}.$$

Using these counterfactual values, we construct a counterfactual inequality index $\widetilde{V}_{\text{Global},t}$ by applying Equation (33). The green line in Figure 15a plots $\widetilde{V}_{\text{Global},t}$, revealing that, in every year, income inequality would have been lower without cross-country climate differences. Moreover, the dispersion induced by climate grows over time, causing observed inequality to fall more slowly compared to the counterfactual scenario without climate misallocation. Thus, we identify climate-induced misallocation as a potentially significant factor slowing global income convergence. According to our estimates, climate-induced misallocation accounts for a rising share of global income dispersion, from about 3% in 1981 to 14% in 2019.

8 Policies to Manage Climate-Induced Misallocation

Our results shed new light on the design and effectiveness of climate mitigation and adaptation policies. We discuss three types of policies that could potentially reduce the cost of climate-induced misallocation: (1) reducing the end-of-century temperature rise from 4°C to 2°C; (2) improving mid-range weather forecast accuracy; and (3) reducing climate sensitivity heterogeneity across firms.

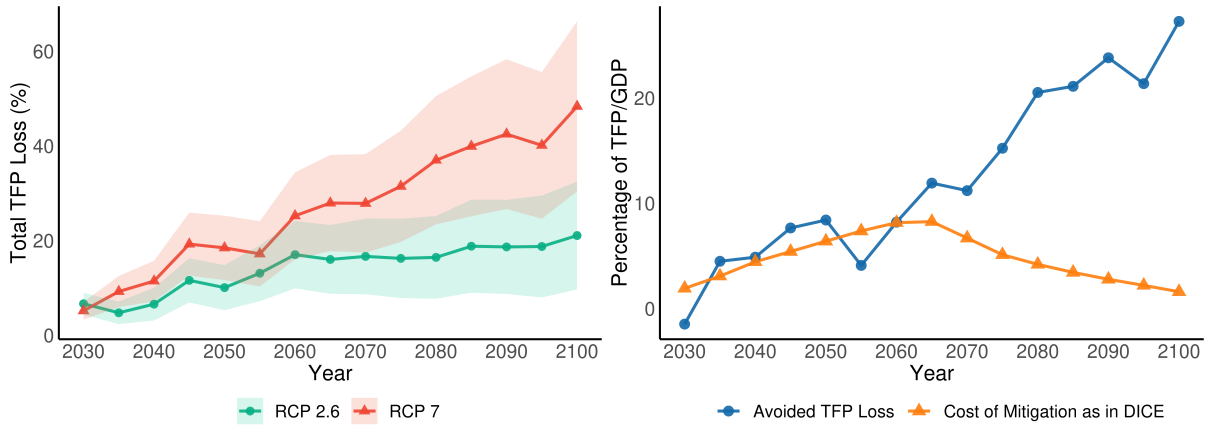
8.1 Mitigating Global Warming: RCP 7.0 vs. RCP 2.6

The most important policy to mitigate the cost of the misallocation channel is to address climate change itself. To illustrate this, we compare the projected misallocation losses between a stringent policy scenario (RCP 2.6) and a business-as-usual scenario (RCP 7.0). RCP 7.0 represents a baseline outcome with limited additional climate policies in place, resulting in a projected 4°C global warming by 2100. In contrast, the RCP 2.6 pathway aligns with the Paris Agreement goals and aims to limit global warming below 2°C.

Figure 16: The Cost and Benefit of Mitigation

(a) TFP Loss from Misallocation: RCP 2.6 vs. RCP 7.0

(b) The Cost and Benefit of RCP 2.6



Notes: In Figure 16a, the climate projection data is collected from CMIP6, and the income projection data are from the SSP database. In Figure 16b, the blue line with dot markers represents the difference in TFP losses between the RCP 2.6 and RCP 7.0 scenarios, referred to as the avoided TFP loss or benefit. This is the difference between the two lines in Figure 16a. The orange line with triangle markers shows the estimated cost of mitigation, calculated using the results from DICE-2016R, defined as the percentage difference in post-abatement potential output between the optimal policy scenario to achieve less than 2°C warming (consistent with RCP 2.6) and the baseline scenario with 4°C warming (consistent with RCP 7.0)

Our objective is to compare TFP losses between these two scenarios to assess the effectiveness of mitigation policies in avoiding misallocation losses. Using the approach developed in Section 4.5, we compute the projected TFP losses from the misallocation channel for the two scenarios, as shown in Figure 16a. By the end of the century, TFP losses are projected to be approximately 21% under RCP 2.6, compared to 43% under RCP 7.0. This suggests that a global TFP loss of 22% can be avoided by achieving the Paris Agreement goals.

Using existing estimates from the DICE-2016R model (Nordhaus 2017), we also calculate the potential costs of switching from RCP 7.0 to RCP 2.6 and compare them to our projected benefits. We define the cost of mitigation as the percentage difference in post-abatement potential output between the optimal policy scenario to achieve less than 2°C warming (consistent with RCP 2.6) and the baseline scenario with 4°C warming (consistent with RCP 7.0). Figure 16b shows that the estimated GDP cost of mitigation is moderate; it initially increases over time, peaks at 8% around 2065, and then decreases to less than 2% by 2100. More importantly, while the annual costs closely track the annual benefits from avoided misallocation loss by 2060, the benefits significantly outweigh the policy costs afterward, amounting to a 20% lead by 2100. Therefore, we argue that mitigation policy is extremely beneficial to avoid losses from climate-induced misallocation. Additionally, regardless of the choice of the discount factor, the cost of such a policy is always justified by the large estimated benefits.

8.2 Improving Mid-Range Weather Forecast Accuracy

Our model suggests that lowering mid-range weather forecast errors (i.e., reducing σ_η^2) would alleviate capital misallocation. Improvements in medium-range weather forecasting at current rates could yield an additional 0.3% gain in aggregate TFP by the end of the century. Moreover, Georgeson, Maslin, and Poessinouw (2017) highlight cross-country disparities in the quality of

weather forecast services. Subsidies and international collaboration could play a crucial role in enabling developing nations to access high-quality weather forecasts, especially those already bearing the brunt of climate change.

Our analysis also points to a potential benefit–cost ratio of more than 2 in recent years, suggesting that further investment in weather forecasting capacity could serve as a vital adaptation strategy. By improving investment efficiency and enhancing overall productivity, better weather forecasts offer a tangible path to strengthening economic resilience in a changing climate.

8.3 Reducing "Climate Inequality" Across Firms

The differential response of MRPK to shocks stems from the heterogeneity in temperature sensitivity ($\sigma^2_{\hat{\beta}}$ and $\sigma^2_{\hat{\xi}}$) across firms. We also point out that this "climate inequality" among firms could result from various factors, including size-related distortions and adaptability. Therefore, policies should be targeted to identify and subsidize firms that are productive but lack the resources to defend against heat. These policies could include targeted subsidies or credit policies for air conditioning installations and other risk control practices. By harmonizing climate sensitivity among firms, the MRPK dispersion will be less responsive to heat shocks or a warming climate. Interestingly, our results also highlight that there need not be an equity-efficiency trade-off in the context of heterogeneous firms. If more firms become more "equal" in their sensitivity to temperature, the aggregate efficiency in the economy will also increase. We will leave quantitative explorations of optimal firm-level policies for future research.

9 Conclusion

This paper provides the first causal estimates of the misallocation effect from temperature shocks using firm-level microdata from 32 countries. On average, an additional hot day with $>$ 30°C of temperature increases MRPK dispersion by 0.31 log points and contributes to a 0.11% decline in annual aggregate TFP. Intriguingly, the detrimental impact of extreme heat on capital misallocation is more severe in regions with hotter climates and higher incomes, highlighting a significant productivity cost of climate change coupled with a limited capacity for market-based adaptation. Using projected temperature and income data, we find that global warming, under the SSP3-4.5 scenario, could lead to an aggregate TFP loss of 36.73%. By writing down a firm dynamics model with heterogeneous temperature sensitivity, we use model-implied regressions to explain the differential effects among regions: regions with extreme climates and lower temperature forecast accuracy will have larger unexpected volatility in firm-level TFP and investment mistakes. Overall, our results suggest that firm-level heterogeneity matters for the aggregate effect of climate change. This paper suggests an important venue for research in understanding the impact of climate change in a distorted economy.

We conclude with a final suggestion for future research. First, the identified misallocation effect is highly heterogeneous across different geographical locations, implying a different level of TFP losses across regions and sectors globally. This will lead to shifts in comparative advantage and triggers the change in global trade patterns in the long-run. Moreover, as we

only focus on the misallocation effect within a region sector as a lower-bound estimate of the climate-induced misallocation, one could also study the misallocation that arises between sectors, regions, and even countries. On the empirical side, it would be important to understand whether demand-side or supply-side factors function as the main drivers of climate-induced misallocation. We leave these questions for future research.

References

Acharya, Viral V, Abhishek Bhardwaj, and Tuomas Tomunen. 2023. *Do Firms Mitigate Climate Impact on Employment? Evidence from US Heat Shocks.* Working Paper, Working Paper Series 31967. National Bureau of Economic Research.

Allcott, Hunt, Allan Collard-Wexler, and Stephen D O'Connell. 2016. "How do electricity shortages affect industry? Evidence from India." *American Economic Review.*

Alves, Felipe, Greg Kaplan, Benjamin Moll, and Giovanni L. Violante. 2020. "A Further Look at the Propagation of Monetary Policy Shocks in HANK." *Journal of Money, Credit and Banking* 52 (S2): 521–559.

Asker, John, Allan Collard-Wexler, and Jan De Loecker. 2014. "Dynamic Inputs and Resource (Mis)Allocation." *Journal of Political Economy* 122 (5): 1013–1063.

Bakkensen, Laura A, and Lint Barrage. 2021. "Going Underwater? Flood Risk Belief Heterogeneity and Coastal Home Price Dynamics." *The Review of Financial Studies* 35 (8): 3666–3709.

Baqaee, David Rezza, and Emmanuel Farhi. 2019. "The Macroeconomic Impact of Microeconomic Shocks: Beyond Hulten's Theorem." *Econometrica* 87 (4): 1155–1203.

Barrage, Lint, and William D Nordhaus. 2023. *Policies, Projections, and the Social Cost of Carbon: Results from the DICE-2023 Model.* Working Paper, Working Paper Series 31112. National Bureau of Economic Research.

Barro, Robert J. 2015. "Convergence and Modernization Revisited." *The Economic Journal* 125 (585): 911–942. https://doi.org/10.1111/ecoj.12247.

Barro, Robert J., and Xavier Sala-i-Martin. 1991. "Convergence Across States and Regions." *Brookings Papers on Economic Activity* 1991 (1): 107–182. https://doi.org/10.2307/2534639.

Basu, Susanto, and John G. Fernald. 2002. "Aggregate productivity and aggregate technology." *European Economic Review* 46 (6): 963–991.

Bau, Natalie, and Adrien Matray. 2023. "Misallocation and Capital Market Integration: Evidence From India." *Econometrica* 91 (1): 67–106.

Bilal, Adrien, and Diego R Känzig. 2024. *The Macroeconomic Impact of Climate Change: Global vs. Local Temperature.* Technical report. National Bureau of Economic Research.

Bils, Mark, Peter J. Klenow, and Cian Ruane. 2021. "Misallocation or Mismeasurement?" *Journal of Monetary Economics* 124:S39–S56.

Blanchard, Olivier, and Jordi Galí. 2010. "Labor Markets and Monetary Policy: A New Keynesian Model with Unemployment." *American Economic Journal: Macroeconomics* 2, no. 2 (April): 1–30.

Bloom, Nicholas. 2009. "The impact of uncertainty shocks." *econometrica* 77 (3): 623–685.

Bourguignon, Francois. 1979. "Decomposable income inequality measures." *Econometrica: Journal of the Econometric Society*, 901–920.

Brandt, Loren, Johannes Van Biesebroeck, and Yifan Zhang. 2014. "Challenges of working with the Chinese NBS firm-level data." *China Economic Review.*

Burke, Marshall, Solomon M. Hsiang, and Edward Miguel. 2015. "Global non-linear effect of temperature on economic production." *Nature* 527 (7577): 235–239.

Caggese, Andrea, Andrea Chiavari, Sampreet Goraya, and Carolina Villegas-Sanchez. 2023. "Climate Change, Firms, and the Aggregate Productivity." Working Paper.

Carleton, Tamma, Amir Jina, Michael Delgado, Michael Greenstone, Trevor Houser, Solomon Hsiang, Andrew Hultgren, et al. 2022. "Valuing the Global Mortality Consequences of Climate Change Accounting for Adaptation Costs and Benefits." *The Quarterly Journal of Economics* 137 (4): 2037–2105.

Casey, Gregory, Stephie Fried, and Matthew Gibson. 2022. "Understanding Climate Damages: Consumption versus Investment." Federal Reserve Bank of San Francisco Working Paper 2022-21.

Chen, Zhang. 2022. "Economic Growth and the Rise of Large Firms."

Christidis, Nikolaos, Dann Mitchell, and Peter A. Stott. 2023. "Rapidly increasing likelihood of exceeding 50°C in parts of the Mediterranean and the Middle East due to human influence." *npj Climate and Atmospheric Science* 6, no. 1 (May 26, 2023): 45.

Copernicus Climate Change Service. 2021. *CMIP6 climate projections.* Copernicus Climate Change Service (C3S) Climate Data Store (CDS).

Copernicus Climate Change Service and Climate Data Store. 2018. *Seasonal forecast daily and subdaily data on single levels.*

Cruz, José-Luis, and Esteban Rossi-Hansberg. 2023. *The Economic Geography of Global Warming.*

David, Joel M., Hugo A. Hopenhayn, and Venky Venkateswaran. 2016. "INFORMATION, MISALLOCATION, AND AGGREGATE PRODUCTIVITY." *The Quarterly Journal of Economics* 131 (2): 943–1006. Accessed November 27, 2023.

David, Joel M., and Venky Venkateswaran. 2019. "The Sources of Capital Misallocation." *American Economic Review* 109 (7): 2531–67.

David, Joel M., and David Zeke. 2021. *Risk-Taking, Capital Allocation and Optimal Monetary Policy.* Federal Reserve Bank of Chicago.

Dell, Melissa, Benjamin F Jones, and Benjamin A Olken. 2012. "Temperature Shocks and Economic Growth: Evidence from the Last Half Century." *American Economic Journal: Macroeconomics* 4 (3): 66–95.

Dellink, Rob, Jean Chateau, Elisa Lanzi, and Bertrand Magné. 2017. "Long-term economic growth projections in the Shared Socioeconomic Pathways." *Global Environmental Change.*

Deschênes, Olivier, and Michael Greenstone. 2011. "Climate Change, Mortality, and Adaptation: Evidence from Annual Fluctuations in Weather in the US." *American Economic Journal: Applied Economics* 3 (4): 152–185.

Dundas, Steven J., and Roger H. von Haefen. 2020. "The Effects of Weather on Recreational Fishing Demand and Adaptation: Implications for a Changing Climate." *Journal of the Association of Environmental and Resource Economists* 7 (2): 209–242.

Fan, Jingting. 2024. "Talent, Geography, and Offshore R
amp;D." *The Review of Economic Studies* (April): rdae044. ISSN: 0034-6527.

Feenstra, Robert C, Robert Inklaar, and Marcel P Timmer. 2015. "The next generation of the Penn World Table." *American economic review* 105 (10): 3150–3182.

Flynn, Joel P., and Karthik Sastry. 2023. *Attention Cycles.*

Gallup, John Luke, Jeffrey D. Sachs, and Andrew D. Mellinger. 1999. "Geography and Economic Development." *International Regional Science Review* 22 (2): 179–232.

Gaubert, Cecile, Patrick Kline, Damián Vergara, and Danny Yagan. 2021. "Trends in US spatial inequality: concentrating affluence and a democratization of poverty." In *AEA Papers and proceedings*, 111:520–525. American Economic Association 2014 Broadway, Suite 305, Nashville, TN 37203.

Georgeson, Lucien, Mark Maslin, and Martyn Poessinouw. 2017. "Global disparity in the supply of commercial weather and climate information services." *Science Advances* 3 (5): e1602632.

Ginglinger, Edith, and Quentin Moreau. 2023. "Climate risk and capital structure." *Management Science* 69 (12): 7492–7516.

Gopinath, Gita, Sebnem Kalemli-Ozcan, Loukas Karabarbounis, and Carolina Villegas-Sanchez. 2017. "Capital Allocation and Productivity in South Europe." *Quarterly Journal of Economics* 132 (4).

Gorodnichenko, Yuriy, Debora Revoltella, Jan Svejnar, and Christoph T Weiss. 2018. *Resource misallocation in European firms: The role of constraints, firm characteristics and managerial decisions.* Technical report. National Bureau of Economic Research.

Hsieh, Chang-Tai, and Peter J. Klenow. 2009. "Misallocation and Manufacturing TFP in China and India." *Quarterly Journal of Economics* 124 (4): 1403–1448.

Kala, Namrata. 2017. "Learning, adaptation, and climate uncertainty: Evidence from Indian agriculture." *MIT Center for energy and environmental policy research working paper* 23.

Kalemli- Özcan, Şebnem, Bent E. Sørensen, Carolina Villegas-Sanchez, Vadym Volosovych, and Sevcan Yeşiltaş. 2024. "How to Construct Nationally Representative Firm-Level Data from the Orbis Global Database: New Facts on SMEs and Aggregate Implications for Industry Concentration." *American Economic Journal: Macroeconomics* 16, no. 2 (April): 353–74.

Kopytov, Alexandr, Mathieu Taschereau-Dumouchel, and Zebang Xu. 2024. "The Origin of Risk." *Available at SSRN.*

Krusell, Per, and Anthony A. Smith Jr. 1998. "Income and Wealth Heterogeneity in the Macroeconomy." *Journal of Political Economy* 106 (5): 867–896.

Lemoine, Derek. 2018. *Estimating the Consequences of Climate Change from Variation in Weather.* Working Paper, Working Paper Series 25008. National Bureau of Economic Research.

Midrigan, Virgiliu, and Daniel Yi Xu. 2014. "Finance and misallocation: Evidence from plant-level data." *American economic review* 104 (2): 422–458.

Montesquieu, Baron de, Charles de Secondat. 1748. *The Spirit of Laws.* Printed for T. Evans.

Moscona, Jacob, and Karthik A Sastry. 2023. "Does directed innovation mitigate climate damage? evidence from us agriculture." *The Quarterly Journal of Economics* 138 (2): 637–701.

Nath, Ishan. 2023. "Climate Change, The Food Problem, and the Challenge of Adaptation through Sectoral Reallocation."

Nath, Ishan, Valerie Ramey, and Peter Klenow. 2023. "How Much Will Global Warming Cool Global Growth?"

Nordhaus, William D. 2006. "Geography and Macroeconomics: New Data and New Findings." *Proceedings of the National Academy of Sciences* 103 (10): 3510–3517.

———. 2017. "Revisiting the social cost of carbon." *Proceedings of the National Academy of Sciences.*

O'Neill, B. C., C. Tebaldi, D. P. van Vuuren, V. Eyring, P. Friedlingstein, G. Hurtt, R. Knutti, et al. 2016. "The Scenario Model Intercomparison Project (ScenarioMIP) for CMIP6." *Geosci. Model Dev.*

Oudin Åström, Daniel, Bertil Forsberg, Kristie L. Ebi, and Joacim Rocklöv. 2013. "Attributing mortality from extreme temperatures to climate change in Stockholm, Sweden." *Nature Climate Change* 3, no. 12 (December 1, 2013): 1050–1054.

Piao, Shilong, Philippe Ciais, Yao Huang, Zehao Shen, Shushi Peng, Junsheng Li, Liping Zhou, Hongyan Liu, Yuecun Ma, Yihui Ding, et al. 2010. "The impacts of climate change on water resources and agriculture in China." *Nature.*

Ponticelli, Jacopo, Qiping Xu, and Stefan Zeume. 2023. *Temperature and Local Industry Concentration.* Technical report w31533. National Bureau of Economic Research.

Poschke, Markus. 2018. "The Firm Size Distribution across Countries and Skill-Biased Change in Entrepreneurial Technology." *American Economic Journal: Macroeconomics* 10 (3): 1–41.

Restuccia, Diego, and Richard Rogerson. 2008. "Policy distortions and aggregate productivity with heterogeneous establishments." *Review of Economic dynamics* 11 (4): 707–720.

Rudik, I., G. Lyn, W. Tan, and A. Ortiz-Bobea. 2021. *The Economic Effects of Climate Change in Dynamic Spatial Equilibrium.*

Sabater, Joaquin Muñoz. 2019. *ERA5-Land monthly averaged data from 1950 to present.* Copernicus Climate Change Service (C3S) Climate Data Store (CDS).

Sachs, Jeffrey D., and Andrew M. Warner. 1997. "Sources of Slow Growth in African Economies." *Journal of African Economies* 6 (3): 335–376.

Schlenker, Wolfram, and Charles A. Taylor. 2021. "Market expectations of a warming climate." *Journal of Financial Economics.*

Shrader, Jeffrey. 2023. "Improving climate damage estimates by accounting for adaptation." *Available at SSRN 3212073.*

Shrader, Jeffrey, Laura Bakkensen, and Derek Lemoine. 2023. "Fatal Errors: The Mortality Value of Accurate Weather Forecasts." National Bureau of Economic Research Working Paper.

Somanathan, E., Rohini Somanathan, Anant Sudarshan, and Meenu Tewari. 2021. "The Impact of Temperature on Productivity and Labor Supply: Evidence from Indian Manufacturing" [in en]. *Journal of Political Economy* 129 (6). Accessed November 27, 2023.

Sraer, David, and David Thesmar. 2023. "How to Use Natural Experiments to Estimate Misallocation." *American Economic Review* 113 (4): 906–38.

Tyazhelnikov, Vladimir, Xinbei Zhou, and Xuetao Shi. 2024. *PPML, Gravity, and Heterogeneous Trade Elasticities.* Technical report.

Wang, Tingting, and Fubao Sun. 2022. "Global gridded GDP data set consistent with the shared socioeconomic pathways." *Scientific Data.*

Wenz, Leonie, Robert Devon Carr, Noah Kögel, Maximilian Kotz, and Matthias Kalkuhl. 2023. "DOSE – Global data set of reported sub-national economic output." *Scientific Data* 10 (1): 425.

World Bank Climate Change Knowledge Portal. 2023.

Zhang, Peng, Olivier Deschenes, Kyle C Meng, and Junjie Zhang. 2018. "Temperature effects on productivity and factor reallocation: Evidence from a half million Chinese manufacturing plants." *Journal of Environmental Economics and Management* 88:1–17.

Zivin, Joshua Graff, and Matthew Neidell. 2014. "Temperature and the Allocation of Time: Implications for Climate Change." *Journal of Labor Economics* 32 (1): 1–26.

Online Appendix

A Additional Derivations for Section 2

This appendix provides the derivation of the expressions and propositions featured in Section 2.

A.1 Equilibrium Allocations in Distorted Equilibrium

In this appendix, we solve the firm's profit maximization problem in Equation 4 and derive Equation 5.

Subject to the inverse demand and wedges, each firm i in region-sector n engages in monopolistic competition and optimally chooses its quantity of inputs and price to maximize profits

$$\max_{P_{nit},K_{nit},L_{nit}} \left(1-\tau_{nit}^{Y}\right) P_{nit} \underbrace{A_{nit}K_{nit}^{\alpha_{Kn}}L_{nit}^{\alpha_{Ln}}}_{Y_{nit}} - \left(1+\tau_{nit}^{K}\right) R_{nt}K_{nit} - \left(1+\tau_{nit}^{L}\right) W_{nt}L_{nit}$$
$$\text{subject to : } Y_{nit} = B_{nit}Y_{nt}\left[\frac{P_{nit}}{P_{nt}}\right]^{-\sigma_n}.$$

After substituting the demand curve $P_{nit}Y_{nit} = P_{nt}Y_{nt}^{\frac{1}{\sigma_n}}B_{nit}^{\frac{1}{\sigma_n}}Y_{nit}^{\frac{\sigma_n-1}{\sigma_n}}$ into the objective function, we derive the first-order condition with respect to any factor input F_{nit} used (where F_{nit} can be either K_{nit} or L_{nit})

$$MRPF_{nit} = \alpha_{F_n}\frac{\sigma_n-1}{\sigma_n}\frac{P_{nit}Y_{nit}}{F_{nit}} = \frac{1+\tau_{ni}^{F}(\tilde{\mathbf{T}}_{rt},\cdot)}{1-\tau_{ni}^{Y}(\tilde{\mathbf{T}}_{rt},\cdot)}P_{nt}^{F},$$

where P_{nt}^{F} denotes the factor price, specifically W_{nt} for labor and R_{nt} for capital. $\frac{\sigma_n-1}{\sigma_n}$ is the optimal CES markup. This is Equation 5 in the main text.

Next, we will derive the allocation in the distorted equilibrium. We rewrite the demand curve as

$$P_{nit} = \left(\frac{Y_{nit}}{B_{nit}Y_{nt}}\right)^{-\frac{1}{\sigma_n}}P_{nt} = \left(\frac{\frac{Y_{nit}}{F_{nit}}F_{nit}}{B_{nit}Y_{nt}}\right)^{-\frac{1}{\sigma_n}}P_{nt}. \tag{34}$$

Combining with Equation 5 yields

$$\alpha_{F_n}\frac{\sigma_n-1}{\sigma_n}\left(\frac{\frac{Y_{nit}}{F_{nit}}F_{nit}}{B_{nit}Y_{nt}}\right)^{-\frac{1}{\sigma_n}}P_{nt}\frac{Y_{nit}}{F_{nit}} = \frac{1+\tau_{ni}^{F}(\tilde{\mathbf{T}}_{rt},\cdot)}{1-\tau_{ni}^{Y}(\tilde{\mathbf{T}}_{rt},\cdot)}P_{nt}^{F}.$$

We can rewrite the previous equation as

$$F_{nit} = \alpha_{F_n}^{\sigma_n}\left(\frac{\sigma_n-1}{\sigma_n}\right)^{\sigma_n}\left(\frac{P_{nt}}{P_{nt}^{F}}\right)^{\sigma_n}\frac{(1-\tau_{nit}^{Y})^{\sigma_n}}{(1+\tau_{nit}^{F})^{\sigma_n}}\left(\frac{Y_{nit}}{F_{nit}}\right)^{\sigma_n-1}B_{nit}Y_{nt},$$

and combining with

$$\frac{Y_{nit}}{F_{nit}} = A_{nit}\frac{(1+\tau_{nit}^{F})}{(1+\tau_{nit}^{K})^{\alpha_{Kn}}(1+\tau_{nit}^{L})^{\alpha_{Ln}}}(\frac{\alpha_L}{W_{nt}})^{\alpha_L}(\frac{\alpha_K}{R_{nt}})^{\alpha_K}(\frac{\alpha_F}{P_{nt}^{F}})^{-1},$$

we can derive an expression for F_{nit} as

$$\begin{aligned} F_{nit} = \frac{1}{\left(1+\tau_{nit}^{F}\right)}\left(\frac{\alpha_{F_n}}{P_{nt}^{F}}\right)\frac{B_{nit}A_{nit}^{\sigma_n-1}\left(1-\tau_{nit}^{Y}\right)^{\sigma_n}}{\left(1+\tau_{nit}^{K}\right)^{\alpha_{Kn}(\sigma_n-1)}\left(1+\tau_{nit}^{L}\right)^{\alpha_{Ln}(\sigma_n-1)}} \\ \cdot\left(\frac{\sigma_n-1}{\sigma_n}\right)^{\sigma_n}\left(\frac{\alpha_{Kn}}{R_{nt}}\right)^{\alpha_{Kn}(\sigma_n-1)}\left(\frac{\alpha_{Ln}}{W_{nt}}\right)^{\alpha_{Ln}(\sigma_n-1)}P_{nt}^{\sigma_n}Y_{nt}, \end{aligned} \tag{35}$$

where $F \in \{K, L\}$. Substituting this expression into the production function of firm i for each factor F yields

$$\begin{aligned} Y_{nit} = A_{nit}K_{nit}^{\alpha_{Kn}}L_{nit}^{\alpha_{Ln}} = \frac{B_{nit}A_{nit}^{\sigma_n}\left(1-\tau_{nit}^{Y}\right)^{\sigma_n}}{\left(1+\tau_{nit}^{Kn}\right)^{\alpha_{Kn}\sigma_n}\left(1+\tau_{nit}^{Ln}\right)^{\alpha_{Ln}\sigma_n}} \\ \cdot\left(\frac{\sigma_n-1}{\sigma_n}\right)^{\sigma_n}\left(\frac{\alpha_{Kn}}{R_{nt}}\right)^{\alpha_{Kn}\sigma_n}\left(\frac{\alpha_{Ln}}{W_{nt}}\right)^{\alpha_{Ln}\sigma_n}P_{nt}^{\sigma_n}Y_{nt} \end{aligned} \tag{36}$$

Similarly, we can write the sales of firm i as

$$\begin{aligned} P_{it}Y_{it} &= P_{nt}Y_{nt}^{\frac{1}{\sigma_n}}B_{nit}^{\frac{1}{\sigma_n}}Y_{nit}^{\frac{\sigma_n-1}{\sigma_n}} \\ &= P_{nt}^{\sigma_n}Y_{nt}\frac{B_{nit}A_{nit}^{(\sigma_n-1)}\left(1-\tau_{nit}^{Y}\right)^{(\sigma_n-1)}}{\left(1+\tau_{nit}^{Kn}\right)^{\alpha_{Kn}(\sigma_n-1)}\left(1+\tau_{nit}^{Ln}\right)^{\alpha_{Ln}(\sigma_n-1)}} \\ &\cdot\left(\frac{\sigma_n-1}{\sigma_n}\right)^{(\sigma_n-1)}\left(\frac{\alpha_{Kn}}{R_{nt}}\right)^{\alpha_{Kn}(\sigma_n-1)}\left(\frac{\alpha_{Ln}}{W_{nt}}\right)^{\alpha_{Ln}(\sigma_n-1)}. \end{aligned} \tag{37}$$

Then the sales share of firm i in region-sector n, θ_{nit}, can be expressed in closed form of the fundamentals as:

$$\theta_{nit} = \frac{P_{nit}Y_{nit}}{\int_0^{J_n}P_{nit}Y_{nit}di} = \frac{\frac{B_{nit}A_{nit}^{(\sigma_n-1)}\left(1-\tau_{nit}^{Y}\right)^{(\sigma_n-1)}}{\left(1+\tau_{nit}^{Kn}\right)^{\alpha_{Kn}(\sigma_n-1)}\left(1+\tau_{nit}^{Ln}\right)^{\alpha_{Ln}(\sigma_n-1)}}}{\int_0^{J_n}\frac{B_{nit}A_{nit}^{(\sigma_n-1)}\left(1-\tau_{nit}^{Y}\right)^{(\sigma_n-1)}}{\left(1+\tau_{nit}^{Kn}\right)^{\alpha_{Kn}(\sigma_n-1)}\left(1+\tau_{nit}^{Ln}\right)^{\alpha_{Ln}(\sigma_n-1)}}di} \tag{38}$$

Finally, by combining 35 and 38, we derive the equilibrium allocation of factors in the distorted economy as

$$F_{nit} = \frac{F_{nit}}{F_{nt}}F_{nt} = \frac{\frac{1}{1+\tau_{nit}^{F}}\theta_{nit}}{\int_0^{J_n}\frac{1}{1+\tau_{nit}^{F}}\theta_{nit}di}F_{nt} = \frac{1+\tau_{nt}^{F}}{1+\tau_{nit}^{F}}\theta_{nit}F_{nt}, \tag{39}$$

where $1+\tau_{nt}^{F} := \left(\int_0^{J_n}\frac{1}{\left(1+\tau_{nit}^{F}\right)}\theta_{nit}di\right)^{-1}$ is a measure of aggregate factor distortion. Mathematically, it is a sales-weighted harmonic mean of all firm-level distortions of input F. Equation 39 states that a firm would use more of input F if it faces smaller distortion than the region-sector aggregate distortion. Moreover, a firm with a larger equilibrium sales share, θ_{it}, is, loosely speaking, more productive and less distorted in production, and will thus use more inputs.

A.2 Proof of Proposition 1

Proposition 1. Equilibrium (Mis)Allocation. The (log) ratio of firm i's distorted and efficient equilibrium allocation of factor, $\frac{F_{nit}}{F^*_{nit}}$,

$$\log(\frac{F_{nit}}{F^*_{nit}}) = \underbrace{-\log(\frac{1+\tau^F_{nit}}{1+\tau^F_{nt}})}_{\substack{\text{relative wedge}\\ \text{effect}}} + \underbrace{\log(\frac{\theta_{nit}}{\theta^*_{nit}})}_{\substack{\text{size}\\ \text{effect}}}$$

is decreasing in the ratio of firm i's own factor wedge comparing to the aggregate factor wedge $1+\tau^F_{nt} \equiv \left(\int_0^{J_n} \frac{1}{(1+\tau^F_{nit})}\theta_{nit}di\right)^{-1}$, and increasing in the ratio of the firm's sales share θ_{nit} comparing to its efficient counterfactual θ^*_{nit}. Moreover, the efficient allocation of inputs, $\frac{F^*_{nit}}{F_{nt}} = \theta^*_{nit} = \frac{B_{nit}A^{\sigma_n-1}_{nit}}{\int_0^{J_n} B_{nit}A^{\sigma_n-1}_{nit}di}$, is entirely determined by firm i's relative preference shifter and physical productivity within the region-sector and aligns with sales share θ^*_{nit}.

Proof. Substituting the expression of θ_{it} from 38 into 39 yields an explicit expression of $\frac{F_{nit}}{F_{nt}}$ in terms of micro fundamentals

$$\frac{F_{nit}}{F_{nt}} = \frac{\frac{1}{1+\tau^F_{nit}}\theta_{nit}}{\int_0^{J_n}\frac{1}{1+\tau^F_{nit}}\theta_{nit}di} = \frac{B_{nit}A^{\sigma_n-1}_{nit}\left(1-\tau^Y_{nit}\right)^{\sigma_n}}{\left(1+\tau^F_{nit}\right)\left(1+\tau^K_{nit}\right)^{\alpha_{Kn}(\sigma_n-1)}\left(1+\tau^L_{nit}\right)^{\alpha_{Ln}(\sigma_n-1)}} \cdot \frac{1}{\int_0^{J_n}\frac{B_{nit}A^{\sigma_n-1}_{nit}\left(1-\tau^Y_{nit}\right)^{\sigma_n}}{\left(1+\tau^F_{nit}\right)\left(1+\tau^K_{nit}\right)^{\alpha_{Kn}(\sigma_n-1)}\left(1+\tau^L_{nit}\right)^{\alpha_{Ln}(\sigma_n-1)}}di}$$

where it is more transparent that for factor $F \in \{K, L\}$, any increase in input distortion has two effects on the equilibrium allocation: (1) it brings down the sales share of the firm in the economy, limiting the usage of all inputs, and (2) it brings up the cost of the specific factor F.

We can evaluate this expression at the efficient equilibrium (quantities and prices in the efficient allocations are marked with *) where all distortions are eliminated and get

$$\frac{F^*_{nit}}{F_{nt}} = \frac{\theta^*_{nit}}{\int_0^{J_n}\theta^*_{nit}di} = \theta^*_{nit} = \frac{B_{nit}A^{\sigma_n-1}_{nit}}{\int_0^{J_n}B_{nit}A^{\sigma_n-1}_{nit}di}$$

To obtain a more intuitive expression , we use equation 35 to get

$$\frac{F_{nit}}{F^*_{nit}} = \frac{1}{1+\tau^F_{nit}} \cdot (1+\tau^F_{nt}) \cdot \frac{\theta_{nit}}{\theta^*_{nit}}$$

where we used the fact that $\tau^{F*}_{nit} = 0$ and $\tau^{F*}_{nt} = 0$ in the efficient equilibrium. Writing this in logs yields the desired expression,

$$\log(\frac{F_{nit}}{F^*_{nit}}) = \underbrace{-\log(\frac{1+\tau^F_{nit}}{1+\tau^F_{nt}})}_{\substack{\text{relative wedge}\\ \text{effect}}} + \underbrace{\log(\frac{\theta_{nit}}{\theta^*_{nit}})}_{\substack{\text{size}\\ \text{effect}}}.$$

■

A.3 Proof of Proposition 2

Proposition 2. Aggregation and TFP Decomposition. Under the log-normality assumption, each region-sector n admits an aggregate production function of the form

$$Y_{nt} = \text{TFP}_{nt} K_{nt}^{\alpha_{Kn}} L_{nt}^{\alpha_{Ln}},$$

where the region-sectoral aggregate Total Factor Productivity $\text{TFP}_{nt} := \text{TFP}_n\left(\tilde{\mathbf{T}}_{rt}, \tilde{\mathbf{X}}_{nt}\right)$ can be decomposed as follows:

$$\begin{aligned}
\log \text{TFP}_n(\tilde{\mathbf{T}}_{rt}, \cdot) = & \underbrace{\frac{1}{\sigma_n - 1} \log \left[J_n \mathbb{E}_i \left[B_{ni}(\tilde{\mathbf{T}}_{rt}, \cdot) \left(A_{ni}(\tilde{\mathbf{T}}_{rt}, \cdot) \right)^{\sigma_n - 1} \right] \right]}_{\text{Technology}(\log \text{TFP}_n^E)} - \underbrace{\frac{\sigma_n}{2} \text{var}_{\log\left(1-\tau_{ni}^Y\right)}(\tilde{\mathbf{T}}_{rt}, \cdot)}_{\text{Output Wedge Dispersion}} \\
& \underbrace{- \sum_{F \in \{K,L\}} \frac{\alpha_{Fn} + \alpha_{Fn}^2(\sigma_n - 1)}{2} \text{var}_{\log\left(1+\tau_{ni}^F\right)}(\tilde{\mathbf{T}}_{rt}, \cdot)}_{\text{Factor Wedge Dispersion}} \\
& \underbrace{+ \sigma_n \sum_{F \in \{K,L\}} \alpha_{Fn} \, \text{cov}_{\log\left(1-\tau_{ni}^Y\right), \log\left(1+\tau_{ni}^F\right)} \left(\tilde{\mathbf{T}}_{rt}, \cdot \right)}_{\text{Output-Factor Mixed Distortion}} \\
& \underbrace{- (\sigma_n - 1) \alpha_{Kn} \alpha_{Ln} \, \text{cov}_{\log\left(1+\tau_{ni}^K\right), \log\left(1+\tau_{ni}^L\right)} \left(\tilde{\mathbf{T}}_{rt}, \cdot \right)}_{\text{Factor Mixed Distortion}}
\end{aligned} \tag{40}$$

Proof. Using 35, we can derive an expression for the equilibrium aggregate factor demand F_{nt} as

$$\begin{aligned}
F_{nt} = \int_0^{J_n} F_{nit} di = & \left(\frac{\sigma_n - 1}{\sigma_n} \right)^{\sigma_n} \left(\frac{P_{nt}^F}{\alpha_{F_n}} \right)^{-1} \left(\frac{R_{nt}}{\alpha_{Kn}} \right)^{\alpha_{Kn}(1-\sigma_n)} \left(\frac{W_{nt}}{\alpha_{Ln}} \right)^{\alpha_{Ln}(1-\sigma_n)} P_{nt}^{\sigma_n} Y_{nt} \\
& \cdot \int_0^{J_n} \frac{B_{nit} A_{nit}^{\sigma_n - 1} \left(1 - \tau_{nit}^Y\right)^{\sigma_n}}{\left(1 + \tau_{nit}^F\right) \left(1 + \tau_{nit}^K\right)^{\alpha_{Kn}(\sigma_n - 1)} \left(1 + \tau_{nit}^L\right)^{\alpha_{Ln}(\sigma_n - 1)}} di.
\end{aligned} \tag{41}$$

Substituting the expression of F_{nt} into $\text{TFP}_{nt} := \frac{Y_{nt}}{K_{nt}^{\alpha_{Kn}} L_{nt}^{\alpha_{Ln}}}$ yields

$$\begin{aligned}
\text{TFP}_{nt} = & \left\{ \frac{1}{P_{nt}} \frac{\sigma_n}{\sigma_n - 1} \left(\frac{R_{nt}}{\alpha_{Kn}} \right)^{\alpha_{Kn}} \left(\frac{W_{nt}}{\alpha_{Ln}} \right)^{\alpha_{Ln}} \right\}^{\sigma_n} \\
& \cdot \frac{1}{\left(\int_0^{J_n} \frac{B_{nit} A_{nit}^{\sigma_n - 1} \left(1 - \tau_{nit}^Y\right)_n^{\sigma}}{\left(1+\tau_{nit}^K\right)^{\alpha_{Kn}(\sigma_n - 1)+1} \left(1+\tau_{nit}^L\right)^{\alpha_{Ln}(\sigma_n - 1)}} di \right)^{\alpha_{Kn}}} \\
& \cdot \frac{1}{\left(\int_0^{J_n} \frac{B_{nit} A_{nit}^{\sigma_n - 1} \left(1 - \tau_{nit}^Y\right)_n^{\sigma}}{\left(1+\tau_{nit}^K\right)^{\alpha_{Kn}(\sigma_n - 1)} \left(1+\tau_{nit}^L\right)^{\alpha_{Ln}(\sigma_n - 1)+1}} di \right)^{\alpha_{Ln}}}
\end{aligned} \tag{42}$$

Using 37 and the fact that $\int P_{nit}Y_{nit}di = P_{nt}Y_{nt}$, we can derive the aggregate price index as

$$P_{nt} = \left(\frac{\sigma_n}{\sigma_n - 1}\right)\left(\frac{R_{nt}}{\alpha_{Kn}}\right)^{\alpha_{Kn}}\left(\frac{W_{nt}}{\alpha_{Ln}}\right)^{\alpha_{Ln}} \cdot \left[\int_0^{J_n}\left(\frac{B_{nit}^{\frac{1}{\sigma_n}}A_{nit}\left(1-\tau_{nit}^{Y}\right)}{\left(1+\tau_{nit}^{Ks}\right)^{\alpha_{Kn}}\left(1+\tau_{nit}^{Ln}\right)^{\alpha_{Ln}}}\right)^{\sigma_n-1} di\right]^{\sigma_n-1} \tag{43}$$

Substituting this back into equation 42 and taking logs to both sides yields

$$\begin{aligned}\log \text{TFP}_{nt} = {} & \frac{\sigma_n}{\sigma_n-1}\log\int_0^{J_n}\left(\frac{B_{nit}^{\frac{1}{\sigma_n}}A_{nit}\left(1-\tau_{nit}^{Y}\right)}{\left(1+\tau_{nit}^{Ks}\right)^{\alpha_{Kn}}\left(1+\tau_{nit}^{Ln}\right)^{\alpha_{Ln}}}\right)^{\sigma_n-1} di \\ & - \alpha_{Kn}\log\int_0^{J_n}\frac{B_{nit}A_{nit}^{\sigma_n-1}\left(1-\tau_{nit}^{Y}\right)_n^{\sigma}}{\left(1+\tau_{nit}^{K}\right)^{\alpha_{Kn}(\sigma_n-1)+1}\left(1+\tau_{nit}^{L}\right)^{\alpha_{Ln}(\sigma_n-1)}}di \\ & - \alpha_{Ln}\log\int_0^{J_n}\frac{B_{nit}A_{nit}^{\sigma_n-1}\left(1-\tau_{nit}^{Y}\right)_n^{\sigma}}{\left(1+\tau_{nit}^{K}\right)^{\alpha_{Kn}(\sigma_n-1)}\left(1+\tau_{nit}^{L}\right)^{\alpha_{Ln}(\sigma_n-1)+1}}di\end{aligned} \tag{44}$$

Under the assumption that B_{nit}, A_{nit} , $1+\tau_{nit}^{K}$ and $1+\tau_{nit}^{L}$ follow a joint log-normal distribution, and all firm-level fundamentals $\left\{B_{nit}, A_{nit}, \tau_{nit}^{Y}, \tau_{nit}^{F}\right\}$ to be firm-specific and smooth functions of $(\tilde{\mathbf{T}}_{rt}, \tilde{\mathbf{X}}_{nt}, \tilde{\mathbf{Z}}_{nit})$, expanding all the terms in 44 yields

$$\begin{aligned}\log \text{TFP}_n(\tilde{\mathbf{T}}_{rt},\cdot) = {} & \underbrace{\frac{1}{\sigma_n-1}\log\mathbb{E}_i\left[B_{ni}(\tilde{\mathbf{T}}_{rt},\cdot)\left(A_{ni}(\tilde{\mathbf{T}}_{rt},\cdot)\right)^{\sigma_n-1}\right]}_{\text{Technology}(\log \text{TFP}_n^{E})} \underbrace{-\frac{\sigma_n}{2}\operatorname{var}_{\log\left(1-\tau_{ni}^{Y}\right)}(\tilde{\mathbf{T}}_{rt},\cdot)}_{\text{Output Wedge Dispersion}} \\ & \underbrace{-\sum_{F\in\{K,L\}}\frac{\alpha_{Fn}+\alpha_{Fn}^2(\sigma_n-1)}{2}\operatorname{var}_{\log\left(1+\tau_{ni}^{F}\right)}(\tilde{\mathbf{T}}_{rt},\cdot)}_{\text{Factor Wedge Dispersion}} \\ & \underbrace{+\sigma_n\sum_{F\in\{K,L\}}\alpha_{Fn}\operatorname{cov}_{\log\left(1-\tau_{ni}^{Y}\right),\log\left(1+\tau_{ni}^{F}\right)}\left(\tilde{\mathbf{T}}_{rt},\cdot\right)}_{\text{Output-Factor Mixed Distortion}} \\ & \underbrace{-(\sigma_n-1)\alpha_{Kn}\alpha_{Ln}\operatorname{cov}_{\log\left(1+\tau_{ni}^{K}\right),\log\left(1+\tau_{ni}^{L}\right)}\left(\tilde{\mathbf{T}}_{rt},\cdot\right)}_{\text{Factor Mixed Distortion}}\end{aligned} \tag{45}$$

which is the Equation 9 in the text.

■

B Data Sources and Variable Construction

This appendix provides details on data sources and variable constructions.

B.1 Orbis Data

Our data of firms from the European countries comes from the Orbis historical Disk Product. We use the sample period 1995-2018 for our analysis. We detail the cleaning process below.

Sample Cleaning. Following the procedure of Kalemli- Özcan et al. (2024), we link multiple vintages of Orbis products over time and link the firm's descriptive information with its financial information via the unique BVD firm identifier (BVDID). We then apply the following standard cleaning procedure:

1. We restrict our analysis to firms that satisfy the following criteria: the country they reside in from their latest address matches with their ISO codes in their BVDID identifier. For example, if the firm's ISO-2 code in BVDID is FR while its latest address is in Spain, then we exclude this firm from our sample.

2. For some firms that lack address information but have other identifiers such as postcodes, we manually map the postcodes to NUTS3 for each country.

3. We harmonize each firm's fiscal year with the calendar year based on the closing date: if the closing date is on or after July 1st, we use the current year as the calendar year; otherwise, we use the previous year.

4. Firms may report multiple sales figures from different sources (like local registries, annual reports, etc.) for consolidated or unconsolidated accounts. Following Fan (2024), we use the unconsolidated accounts to avoid double-counting that can occur with consolidated accounts.

5. We only keep firms with non-missing and positive sales (`operating_revenue_turnover`) and fixed assets (`fixed_assets`).

6. We calculate firm-level MRPK_{it} for firm i in year t as $\log \text{MRPK}_{it} = \log(\alpha_{Kn} \frac{\sigma_n - 1}{\sigma_n} \frac{P_{it} Y_{it}}{K_{it}})$ where $P_{it} Y_{it}$ is measured with sales and K_{it} is measured with fixed assets.

7. We winsorize the observations of MRPK_{it}, fixed assets, or sales at the top and bottom 0.1% of the distribution in the entire panel for each country. This is to prevent outliers from affecting the variance calculation and estimation.

B.2 China NBS Data

The annual firm-level data for China is derived from surveys conducted by the National Bureau of Statistics (NBS) in China. We only use the sample period of 1998-2007 due to inconsistent reporting after 2008 as discussed in Brandt, Van Biesebroeck, and Zhang (2014) and Nath (2023).

Sample Cleaning. To process the NBS data, we follow the methodology outlined in Zhang et al. (2018). We measure sales using the variable "产品销售收入" (product sales revenue) and capital using the variable "固定资产合计" (total fixed assets). Each firm in the dataset is categorized using a four-digit Chinese Industry Classification (CIC) code and is harmonized to the USSIC division level. Each firm's reported location can be mapped into a prefecture-level division. The rest of the cleaning follows the same procedure as items 5-7 in Appendix B.1.

B.3 India ASI Data

Our data for India are drawn from India's Annual Survey of Industries (ASI). We use the sample period of 1998 to 2018.

Sample Cleaning. We match the plants to the Indian districts following the approach of Somanathan et al. (2021) and harmonize the industries first to the NIC-04 classification, and then to the SIC division level. We measure sales using the gross sale value of all products and capital using an average of the opening and closing gross book value of total capital, as in Bils, Klenow, and Ruane (2021). The rest of the cleaning follows the same procedure as items 5-7 in Appendix B.1.

B.4 Additional Descriptive Statistics

The table below lists out the countries, year coverage, number of regions in each country, and the total number of firm-year pair observations in the final sample we used for the empirical analysis.

Table B.1: Descriptive Table of Dataset by Country

Dataset	Country	Coverage	Number of Regions	Number of Firm-Year Obs
NBS China Industrial	China	1998-2007	325	2069100
India ASI	India	1998-2017	267	473646
	Austria	2004-2018	34	185029
	Belgium	1998-2018	44	781322
	Bulgaria	1998-2018	28	1439871
	Switzerland	2003-2018	3	1701
	Cyprus	2005-2018	1	17356
	Czech Republic	1998-2018	14	1425901
	Germany	1998-2018	346	765981
	Denmark	1999-2018	11	392015
	Estonia	1998-2018	5	791340
	Greece	1998-2018	44	342636
	Spain	1998-2018	52	12210663
	Finland	1998-2018	19	1909080
	France	1998-2018	96	15151185
	Croatia	1998-2018	21	1202515
BvD Orbis	Hungary	2004-2018	20	3095326
	Ireland	2000-2018	8	115344
	Italy	1998-2018	107	12083926
	Lithuania	1998-2018	10	129442
	Luxembourg	1998-2018	1	74287
	Latvia	2010-2018	6	533640
	Malta	2000-2018	1	21249
	Netherlands	1998-2018	36	201182
	Norway	1998-2018	12	2462277
	Poland	1998-2018	73	1207428
	Portugal	1998-2018	24	3882515
	Romania	1998-2018	42	4636047
	Sweden	1998-2018	21	3934403
	Slovenia	1998-2018	12	744495
	Slovakia	1998-2018	8	1008353
	United Kingdom	1998-2018	178	3537701

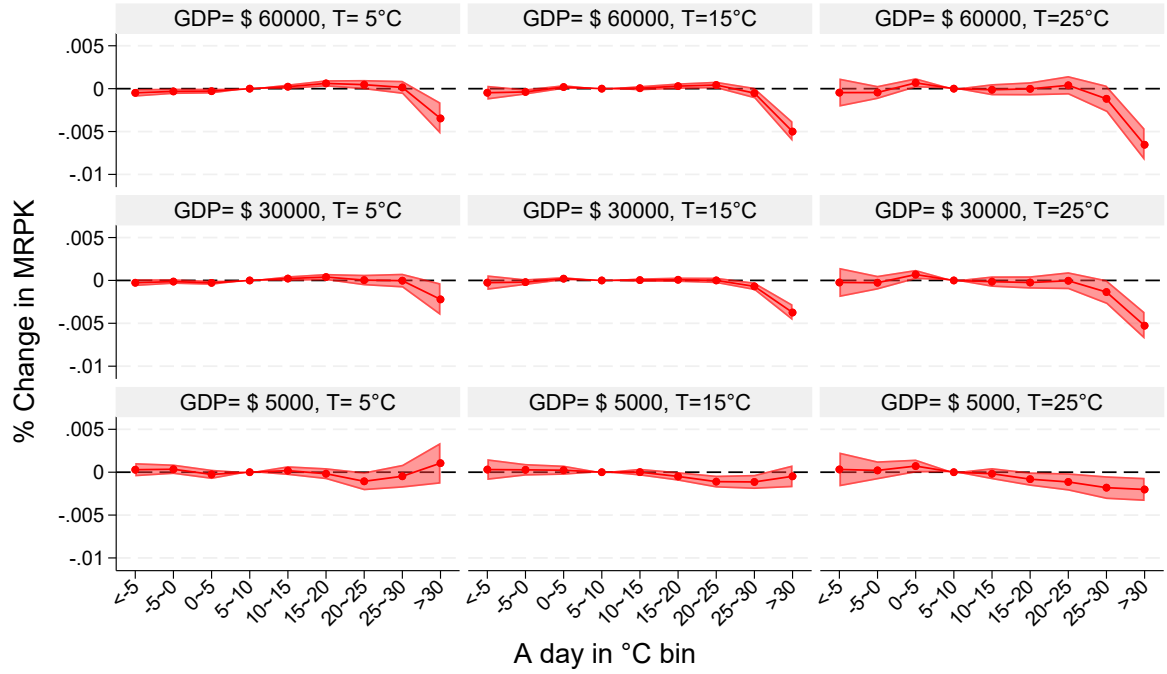
C Additional Figures for Section 4

This appendix provides additional results and figures to complement the main analysis in Section 4.

C.1 Firm-level MRPK and Temperature

Here we present the *average* effect of temperature on firm-level MRPK across climates and income. We show that heat shocks negatively affect firm-level MRPK across almost all climates and income. As an economy becomes more developed or traditions into a hotter climate, the negative effect of heat shocks on MRPK becomes larger.

Figure C.1: Average Effect of Temperature on firm-level MRPK Across Climates and Income



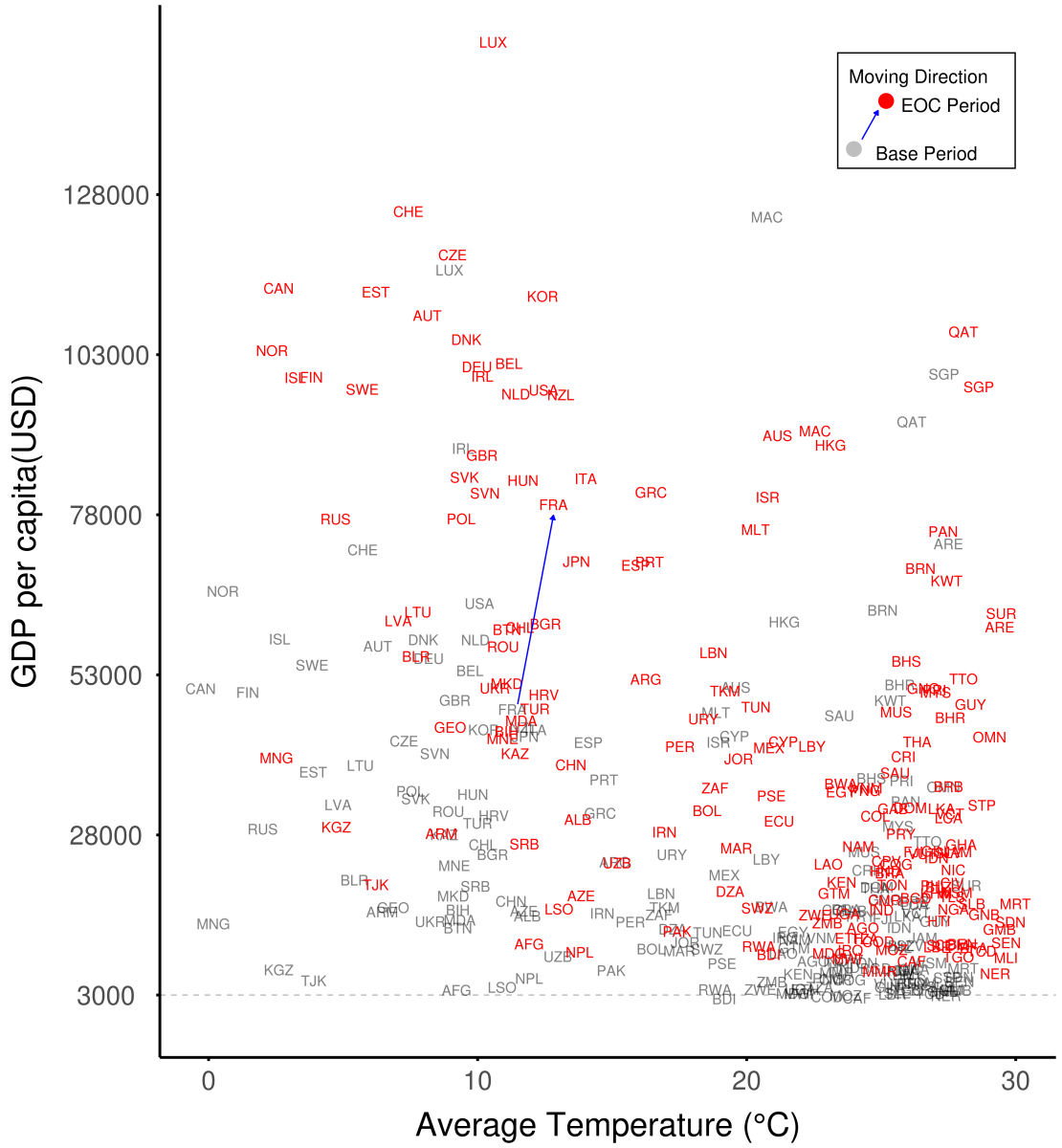
Notes: The graph plots the estimated effect of exposure to daily mean temperature bins on the level of MRPK at varying levels of income and climates. The regression is at the firm-level with firm and country-year fixed effect. The graph includes 90% confidence intervals and standard errors are clustered at the regional level. The reference temperature is at 5-10°C.

C.2 Projected Evolution of Income and Temperature under SSP3-4.5

The figure illustrates the projected evolution of income and average temperature from the 2000-2014 baseline to the end of the century (2081-2100) under the SSP3-4.5 scenarios. Among the 172 countries, All 172 countries show a rightward shift (indicating an increase in temperature), and 96% of them also show an upward shift (indicating an increase in per-capita income). In the baseline period, average temperatures are below 5°C in 11 countries, between 5-15°C in 49 countries, between 15-25°C in 62 countries, and above 25°C in 50 countries. Baseline per capita income is below $5000 in 41 countries, between $5000-$30000 in 83 countries, between

$30000-$60000 in 38 countries and above $60000 in 10 countries. The blue arrow exemplifies the joint evolution of income and temperature.

Figure C.2: Joint Evolution of Income and Average Temperature from Base Period to End of Century (under SSP3-4.5)



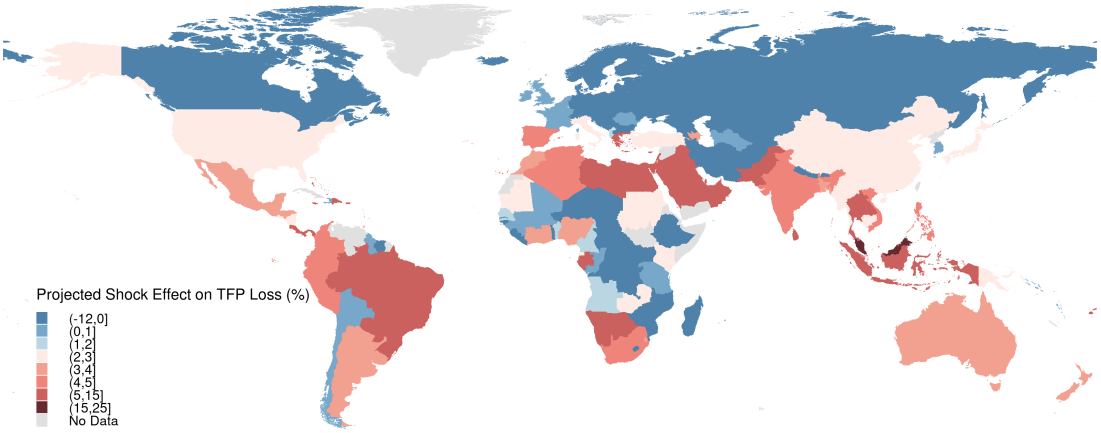
Notes: Grey texts represent the baseline period from 2000 to 2014, and the red texts represent the end of the century (2081 - 2100). End-of-century projection comes from SSP3-4.5 projection. The graph shows the joint evolution of income per capita and average temperature for each country.

C.3 Projection Components

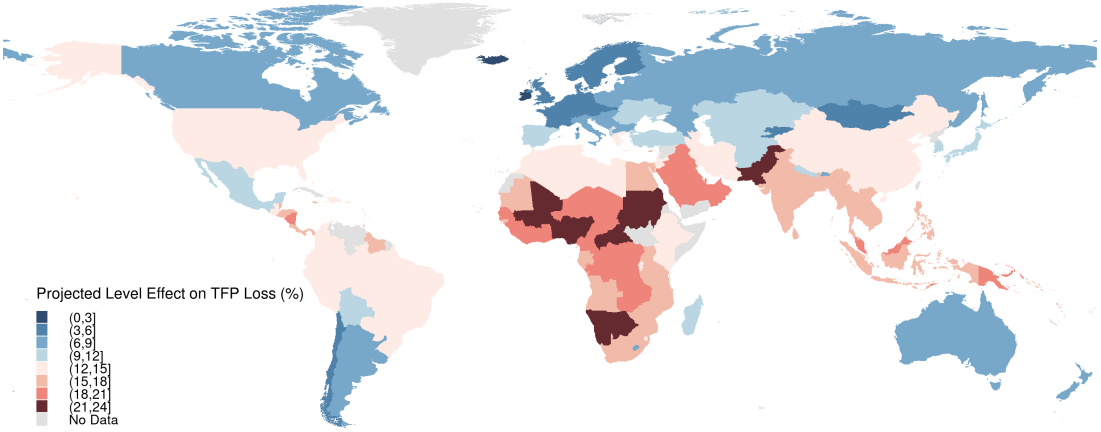
The graph shows a breakdown of the three effects contributing to the total projected TFP loss under SSP3-4.5 scenarios in Section 4.5.

Figure C.3: Three Effects Contribution to Projected TFP Loss (SSP3-4.5)

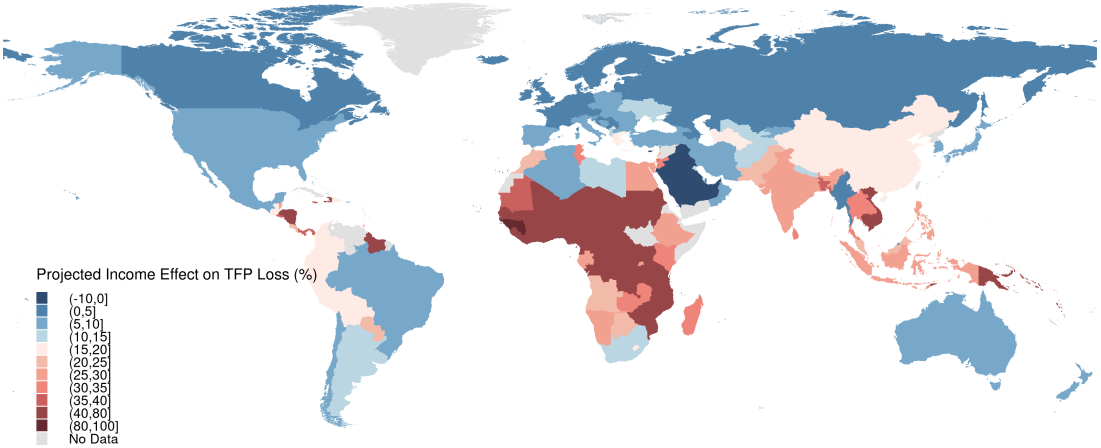
(a) Shock Effects Projection



(b) Level Effects Projection



(c) Income Effects Projection

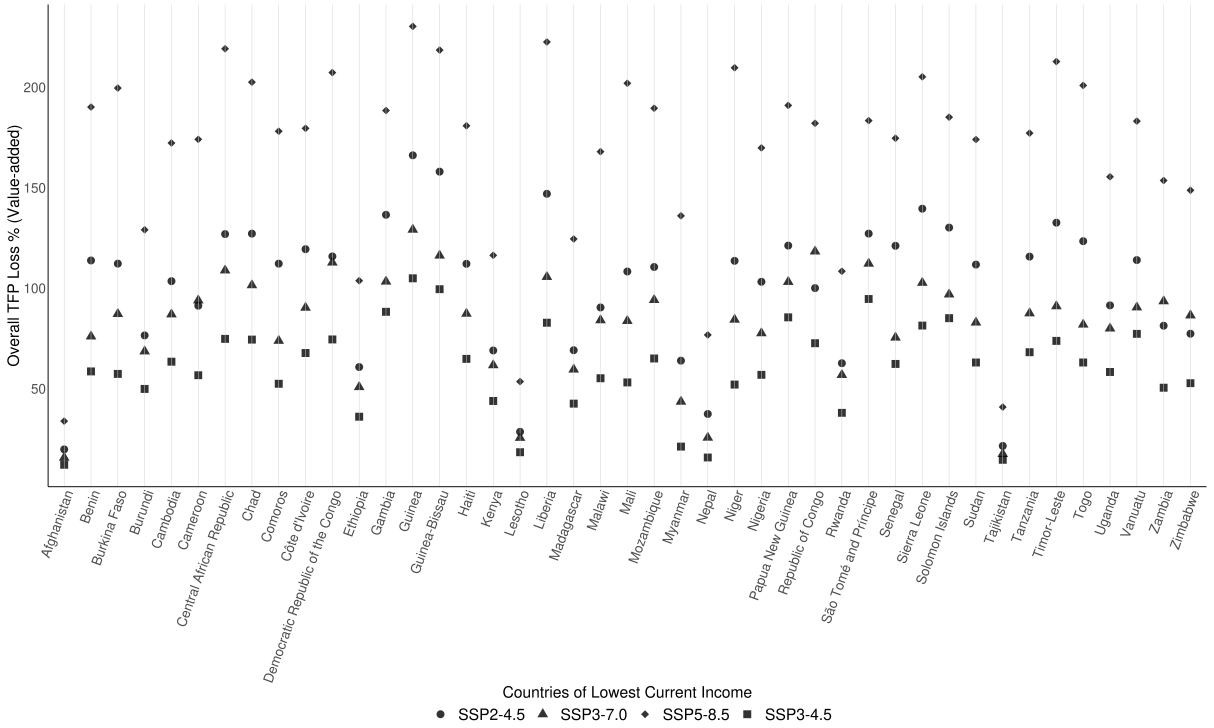


C.4 Projections from Other Scenarios

This appendix presents global TFP loss projections by current income levels under different scenarios. We categorize the countries into four groups based on current GDP per capita quantiles: below the 25th percentile (less than $5149.8), 25th-50th percentile ($5149.8-$13968.3), 50th-75th percentile ($13968.3-$32776.8), and above the 75th percentile (greater than $32776.8). The four scenarios considered are SSP2-4.5, SSP3-7.0, SSP3-4.5, and SSP5-8.5.

Figure C.4: Global TFP Loss Projection By Current Income Levels from Other Scenarios (Part 1)

(a) Income Below 25% Percentile



(b) Income at 25% to 50% Percentile

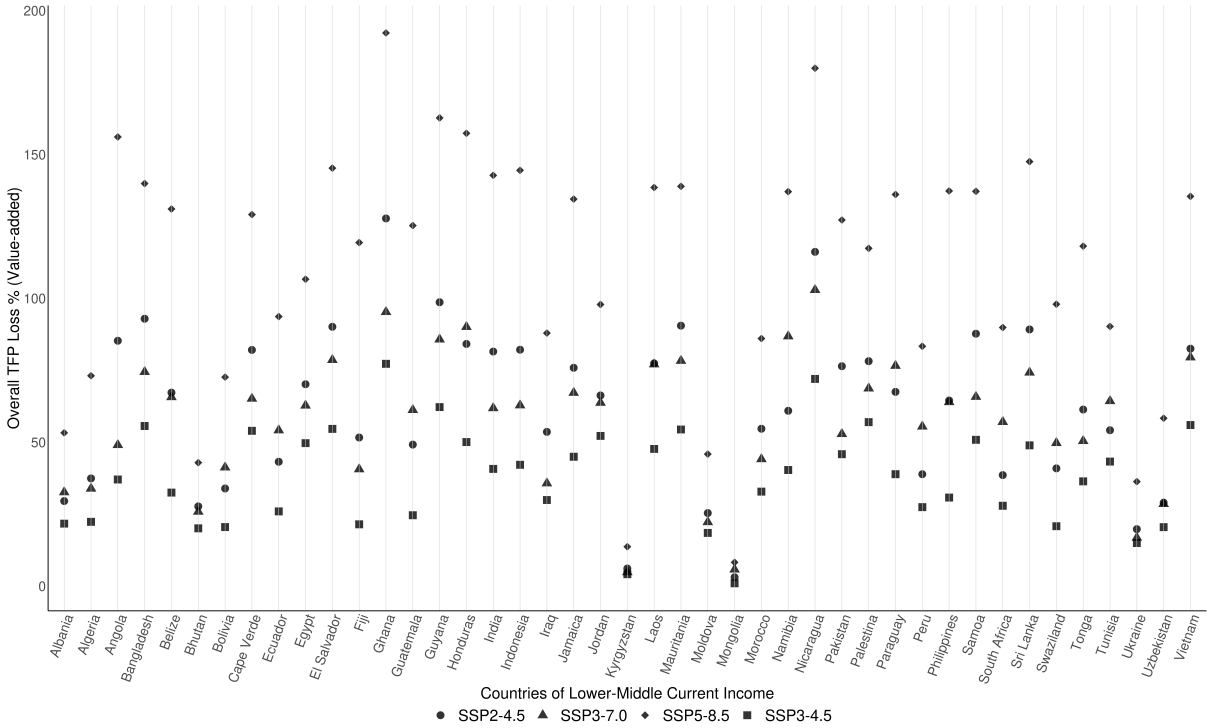
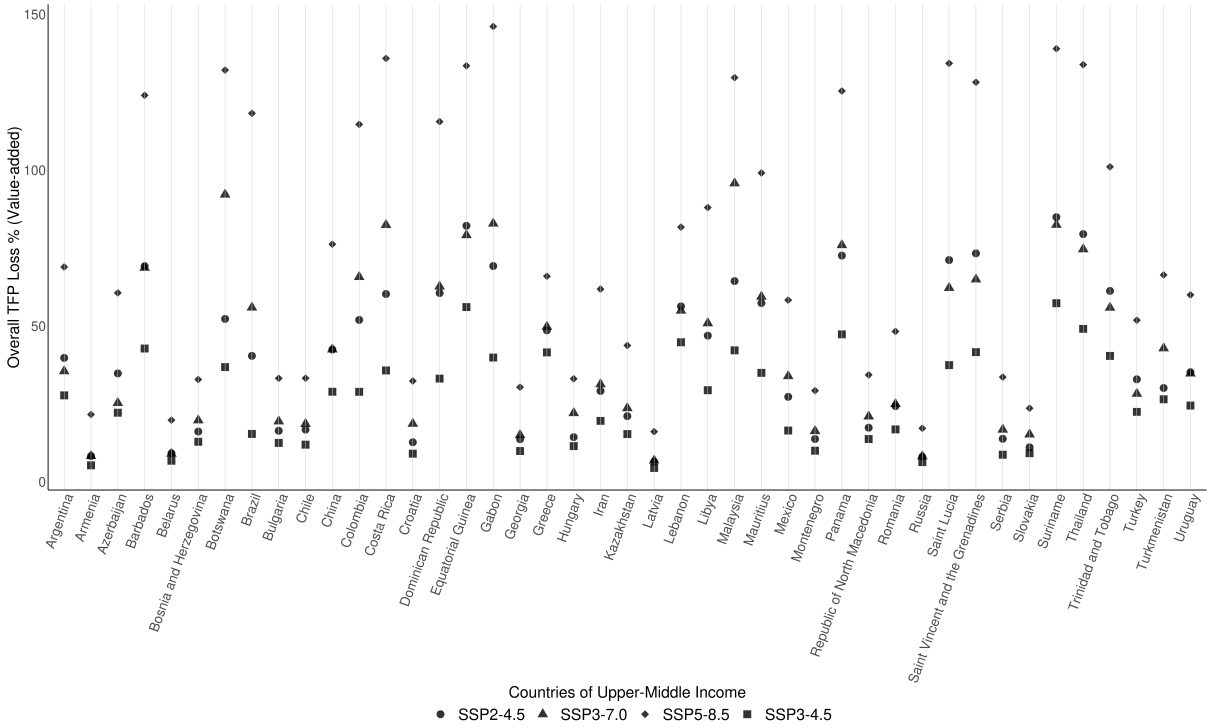
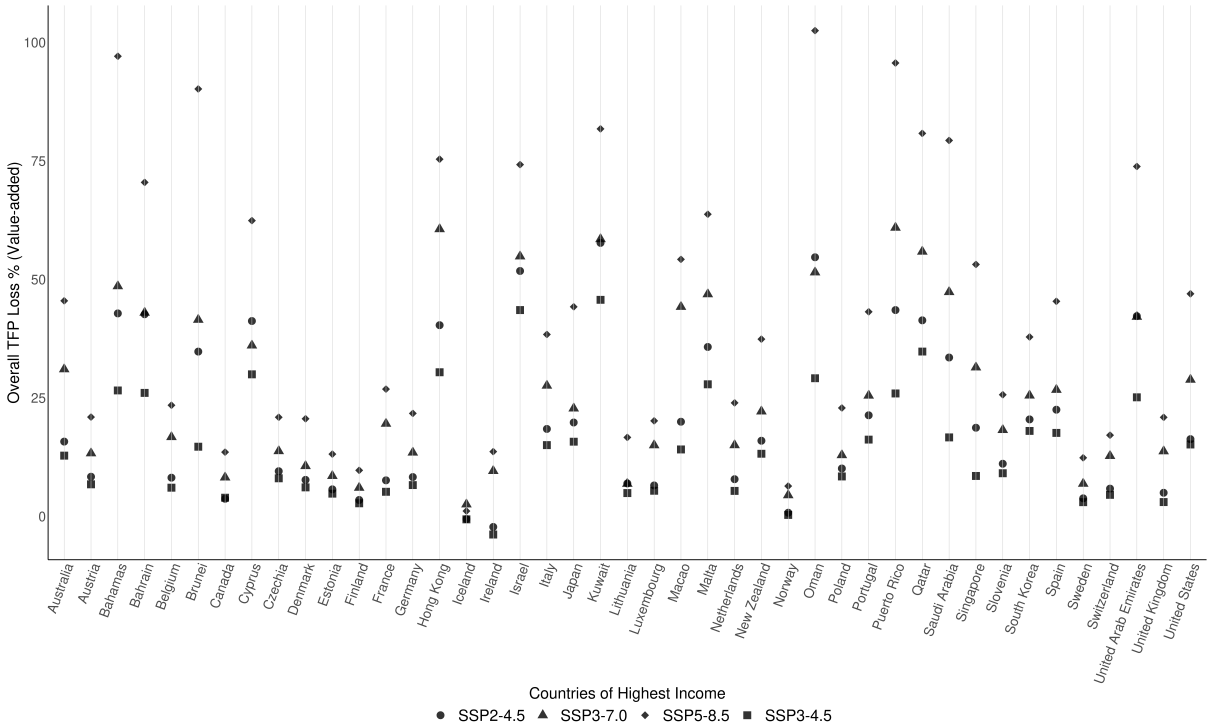


Figure C.5: Global TFP Loss Projection By Current Income Levels from Other Scenarios (Part 2)

(a) Income at 50% to 75% Percentile



(b) Income above 75% Percentile



D Additional Tables for Regressions in Section 6

This appendix reports the estimates in Section 6, corresponding to Figures 8b and 8a.

Table D.2: Relative Firm Size and Firm MRPK

	(1)	(2)
< -5°C	0.00056**	0.00046*
	(0.00027)	(0.00027)
$-5 \sim 0$°C	0.00019	0.00012
	(0.00016)	(0.00015)
$0 \sim 5$°C	0.00015	0.00010
	(0.00013)	(0.00013)
$5 \sim 10$°C	0.00005	0.00001
	(0.00014)	(0.00013)
$15 \sim 20$°C	0.00004	0.00002
	(0.00011)	(0.00011)
$20 \sim 25$°C	-0.00016	-0.00024
	(0.00016)	(0.00016)
$25 \sim 30$°C	-0.00019	-0.00028
	(0.00024)	(0.00024)
> 30°C	-0.00119***	-0.00133***
	(0.00045)	(0.00044)
< -5°C $\times$ Relative Size		0.00089***
		(0.00019)
$-5 \sim 0$°C $\times$ Relative Size		0.00077***
		(0.00024)
$0 \sim 5$°C $\times$ Relative Size		0.00062***
		(0.00022)
$5 \sim 10$°C $\times$ Relative Size		0.00041
		(0.00027)
$15 \sim 20$°C $\times$ Relative Size		0.00021***
		(0.00008)
$20 \sim 25$°C $\times$ Relative Size		0.00092***
		(0.00017)
$25 \sim 30$°C $\times$ Relative Size		0.00098***
		(0.00031)
> 30°C $\times$ Relative Size		0.00105**
		(0.00049)
Control: Relative Size	Yes	Yes
Firm FE	Yes	Yes
Country-Sector-Year FE	Yes	Yes
Observations	73350226	73350226
R^2	0.880	0.880

Notes: Standard errors in parentheses. We cluster standard errors at the region level (NUTS3 level for European countries, province level for China, and first-level administrative divisions for India). The dependent variables are the log MRPK. These results are obtained by estimating Equation 27. Column 2 presents results that interact with relative firm size, $\text{Relative Size}_{it}^{r,s} := \log K_{it}^{s,r} - \overline{\log K_{it}}^{s,r}$, which is standardized over the entire sample.

* $p < 0.10$, ** $p < 0.05$, *** $p < 0.01$

Table D.3: AC Installation and Firm MRPK

	(1)	(2)	(3)	(4)
< 10°C	0.00156	0.00124	0.00083	0.00178
	(0.00105)	(0.00101)	(0.00268)	(0.00202)
$10 \sim 15$°C	0.00032	0.00075	-0.00064	0.00131*
	(0.00051)	(0.00051)	(0.00085)	(0.00075)
$20 \sim 25$°C	-0.00037	-0.00015	-0.00226***	-0.00175***
	(0.00027)	(0.00024)	(0.00080)	(0.00061)
$25 \sim 30$°C	-0.00060*	-0.00035	-0.00286***	-0.00245***
	(0.00031)	(0.00028)	(0.00083)	(0.00065)
> 30°C	-0.00068*	-0.00044	-0.00249**	-0.00224***
	(0.00040)	(0.00035)	(0.00099)	(0.00075)
< 10°C $\times$ AC Installation			0.00089	-0.00051
			(0.00305)	(0.00243)
$10 \sim 15$°C $\times$ AC Installation			0.00110	-0.00062
			(0.00095)	(0.00085)
$15 \sim 20$°C $\times$ AC Installation			0.00218***	0.00185***
			(0.00081)	(0.00062)
$20 \sim 25$°C $\times$ AC Installation			0.00259***	0.00240***
			(0.00087)	(0.00068)
$25 \sim 30$°C $\times$ AC Installation			0.00208**	0.00206***
			(0.00102)	(0.00077)
Control: lnK	No	Yes	No	Yes
Firm FE	Yes	Yes	Yes	Yes
Sector-Year FE	Yes	Yes	Yes	Yes
Observations	532,425	532,425	532,425	532,425
R^2	0.748	0.815	0.748	0.815

Notes: Standard errors in parentheses. We cluster standard errors at the districts level. The dependent variables are the log MRPK. These results are obtained by estimating Equation 27. Column 1 and 3 present results that do not include control variables $\log K$.
* $p < 0.10$, ** $p < 0.05$, *** $p < 0.01$

E Additional Derivations for Section 5

This appendix provides the derivations of the expressions and propositions featured in Section 5.

E.1 Proof of Lemma 1

Lemma 1. TFP Volatility, $\text{Var}(\hat{a}_{it} - \mathbb{E}_{t-1}[\hat{a}_{it}])$, and can be written as:

$$\text{Var}(\hat{a}_{it} - \mathbb{E}_{t-1}[\hat{a}_{it}]) = (T_t - T^*)^2 \sigma^2_{\hat{\xi}} + \hat{\eta}_t^{T\,2} \sigma^2_{\hat{\beta}} + \sigma^2_{\hat{\varepsilon}}. \tag{46}$$

TFP volatility reaches its minimum when the temperature is at its optimum, $T_t = T^*$, and when there is no unexpected change in temperature, $\eta_t^T = 0$.

Proof. We can write a firm's (log) TFP, $\hat{a}_{it}$, as

$$\begin{aligned} \hat{a}_{it} &= \hat{\beta}_{it}(T_t - T^*) + \hat{z}_{it} \\ &= \left(\hat{\beta}_i + \hat{\xi}_{it} + \mathcal{O}_t\right)(T_t - T^*) + \rho_z \hat{z}_{it-1} + \hat{\varepsilon}_{it}. \end{aligned} \tag{47}$$

where $\mathcal{O}_t$ is defined as

$$\mathcal{O}_t = c(T_t - T^*), \quad \text{with } c = \frac{(\sigma^2_{\hat{\beta}} + \sigma^2_{\hat{\xi}})\sigma}{2}.$$

hen the expected TFP, $\mathbb{E}_{t-1}[\hat{a}_{it}]$, can be expressed as

$$\begin{aligned} \mathbb{E}_{t-1}[\hat{a}_{it}] &= \hat{\beta}_i \mathbb{E}_{t-1}[T_t - T^*] + \mathbb{E}_{t-1}[\hat{\xi}_{it}(T_t - T^*)] + \mathbb{E}_{t-1}[\mathcal{O}_t(T_t - T^*)] + \rho_z \hat{z}_{it-1} \\ &= \hat{\beta}_i \mathbb{E}_{t-1}[T_t - T^*] + c\mathbb{E}_{t-1}[(T_t - T^*)^2] + \rho_z \hat{z}_{it-1} \end{aligned} \tag{48}$$

where we have used that $\mathbb{E}_{t-1}[\hat{\xi}_{it}(T_t - T^*)] = \mathbb{E}_{t-1}[\hat{\xi}_{it}]\mathbb{E}_{t-1}[(T_t - T^*)] = 0$. Using Equations 47 and 48, we can write the forecast error of a firm's TFP as

$$\hat{a}_{it} - \mathbb{E}_{t-1}[\hat{a}_{it}] = \underbrace{\hat{\beta}_i \hat{\eta}_t^T + c\left((T_t - T^*)^2 - \mathbb{E}_{t-1}\left[(T_t - T^*)^2\right]\right)}_{\text{from Temperature FE}} + \underbrace{\hat{\xi}_{it}(T_t - T^*)}_{\text{from Sensitivity FE}} + \hat{\varepsilon}_{it}, \tag{49}$$

where the first term stems from the firm's forecast error on temperature, the second term represents the firm's unexpected sensitivity shock, and the third term represents the firm's idiosyncratic productivity.

We define TFP Volatility, $\text{Var}(\hat{a}_{it} - \mathbb{E}_{t-1}[\hat{a}_{it}])$, to be the cross-sectional variance of the TFP forecast error across firms. Taking the variance of 49 across i yields

$$\text{Var}(\hat{a}_{it} - \mathbb{E}_{t-1}[\hat{a}_{it}]) = (T_t - T^*)^2 \sigma^2_{\hat{\xi}} + \eta_t^{T\,2} \sigma^2_{\hat{\beta}} + \sigma^2_{\hat{\varepsilon}}. \tag{50}$$

We thus obtain Equation 46 in the text. ■

E.2 Solving the Model

This appendix provides additional derivations for solving the model in Section 5. Specifically, we will derive the optimal capital investment policy function in Equation 22.

Flexible Input Choice and Profits. Optimal choice of flexible inputs is made after capital inputs are allocated and all shocks are realized. The static input choice solves

$$\max_{N_{it}} P_{it}Y_{it} - W_t N_{it},$$

where $P_{it}Y_{it} = \hat{A}_{it}K_{it}^{\alpha_K}N_{it}^{\alpha_N}$. Taking the first-order condition of N_{it} gives

$$N_{it} = \left(\frac{W_t}{\hat{A}_{it}\alpha_N K_{it}^{\alpha_K}}\right)^{\frac{1}{\alpha_N - 1}}. \tag{51}$$

Plugging in the equilibrium wage, $W_t = \overline{W}\exp\left(\chi(T_t - T^*)\right)$, into this equation yields the optimal labor choice

$$N_{it} = \left(\frac{\overline{W}\exp\left(\chi(T_t - T^*)\right)}{\hat{A}_{it}\alpha_N K_{it}^{\alpha_k}}\right)^{\frac{1}{\alpha_N - 1}}. \tag{52}$$

Also, notice that $W_t N_{it} = \alpha_N P_{it}Y_{it}$, so the firm's profits can be written as

$$\begin{aligned}\Pi_{it} &= P_{it}Y_{it} - W_t N_{it} \\ &= (1-\alpha_N)\hat{A}_{it}K_{it}^{\alpha_K}N_{it}^{\alpha_N},\end{aligned} \tag{53}$$

Plugging in the expression of optimal labor, we obtain

$$\Pi_{it} = G\exp\left(\chi(T_t - T^*)\right)^{-\frac{\alpha_N}{1-\alpha_N}}\hat{A}_{it}^{\frac{1}{1-\alpha_N}}K_{it}^{\alpha_K\frac{1}{1-\alpha_N}}, \tag{54}$$

where $G = (1-\alpha_N)\overline{W}^{-\frac{\alpha_N}{1-\alpha_N}}\alpha_N^{\frac{\alpha_N}{1-\alpha_N}}$. To simplify notations, we define a firm's *profitability*, A_{it}, as

$$A_{it} = \exp\left(\chi(T_t - T^*)\right)^{-\frac{\alpha_N}{1-\alpha_N}}\hat{A}_{it}^{\frac{1}{1-\alpha_N}} = \exp\left(\beta_{it}(T_t - T^*) + z_{it}\right),$$

where $z_{it} = \frac{1}{1-\alpha_N}\hat{z}_{it}$, and $\beta_{it} = \frac{\hat{\beta}_{it} - \chi\alpha_N}{1-\alpha_N}$ is the firm's profitability sensitivity to temperature. Therefore, we can write a firm's revenue function as

$$\Pi_{it} = G\exp\left(\beta_{it}(T_t - T^*) + z_{it}\right)K_{it}^{\alpha} := GA_{it}K_{it}^{\alpha},$$

where $\alpha = \frac{\alpha_K}{1-\alpha_N}$ is the curvature of profits. This is Equation 21 in the main text.

Dynamic Capital Investment. We now characterize the firm's investment problem. The firm's dynamic capital investment problem takes the form

$$\begin{aligned}V\left(T_t, Z_{it}, K_{it}\right) = \max_{K_{it+1}} \quad & G\exp\left(\beta_{it}(T_t - T^*) + z_{it}\right)K_{it}^{\alpha} - K_{it+1} + (1-\delta)K_{it} \\ & + \frac{1}{1+r}\mathbb{E}_t\left[V\left(T_{t+1}, Z_{it+1}, K_{it+1}\right)\right].\end{aligned} \tag{55}$$

Combining the first order condition and the envelope condition associated with Equation 55 gives the Euler equation

$$1 = \underbrace{\frac{1}{1+r}}_{\text{Discount Factor}} \left(\underbrace{\alpha G K_{it+1}^{\alpha-1} \mathbb{E}_t \left[\exp\left(z_{it+1} + \beta_{it+1}(T_{t+1} - T^*) \right) \right]}_{\text{Expected Value of Marginal Profits of Capital}} + \underbrace{(1-\delta)}_{\substack{\text{Value of} \\ \text{Undepreciated Capital}}} \right). \tag{56}$$

We then rearrange the Euler equation to get the expression for optimal capital investment

$$\begin{aligned} K_{it+1}^{1-\alpha} &= \frac{\alpha G}{r+\delta} \mathbb{E}_t \left[\exp\left(a_{it+1} \right) \right] \\ &= \frac{\alpha G}{r+\delta} \mathbb{E}_t \left[\exp\left(\frac{\hat{\beta}_i + \hat{\xi}_{it+1} + \mathcal{O}_{t+1} - \chi \alpha_N}{1-\alpha_N} (T_{t+1} - T^*) \right) \right]. \end{aligned} \tag{57}$$

Notice that a first-order approximation of a non-linear function $f(\hat{\xi}_{it+1}, T_{t+1} - T^*)$ around $(\mathbb{E}_t[\hat{\xi}_{it}], \mathbb{E}_t[T_t - T^*])$, we get:

$$\begin{aligned} f(\hat{\xi}_{it+1}, T_{t+1} - T^*) \approx & f(\mathbb{E}_t[\hat{\xi}_{it+1}], \mathbb{E}_t[T_{t+1} - T^*]) \\ & + \frac{\partial f(\hat{\xi}_{it+1}, T_{t+1} - T^*)}{\partial (T_{t+1} - T^*)} \bigg|_{(\mathbb{E}_t[\hat{\xi}_{it+1}], \mathbb{E}_t[T_{t+1} - T^*])} (T_{t+1} - \mathbb{E}_t[T_{t+1}]) \\ & + \frac{\partial f(\hat{\xi}_{it+1}, T_{t+1} - T^*)}{\partial \hat{\xi}_{it+1}} \bigg|_{(\mathbb{E}_t[\hat{\xi}_{it+1}], \mathbb{E}_t[T_{t+1} - T^*])} (\hat{\xi}_{it+1} - \mathbb{E}_t[\hat{\xi}_{it+1}]). \end{aligned} \tag{58}$$

Applying expectation on both sides of this equation yields

$$\mathbb{E}_t \left[f(\hat{\xi}_{it+1}, T_{t+1} - T^*) \right] \approx f(\mathbb{E}_t \hat{\xi}_{it+1}, \mathbb{E}_t[T_{t+1} - T^*]). \tag{59}$$

Under this first-order approximation, the optimal investment in 57 becomes

$$K_{it+1}^{1-\alpha} \approx \frac{\alpha G}{r+\delta} \exp\left(\frac{\hat{\beta}_i + \mathbb{E}_t \hat{\xi}_{it+1} + \mathbb{E}_t \mathcal{O}_{t+1} - \chi \alpha_N}{1-\alpha_N} \mathbb{E}_t[T_{t+1} - T^*] + \frac{\mathbb{E}_t[\hat{z}_{it}]}{1-\alpha_N} \right).$$

Taking logs on both sides yields the policy function

$$k_{it+1} = \frac{1}{1-\alpha} \left(\frac{\hat{\beta}_i + \mathbb{E}_t \hat{\xi}_{it+1} + \mathbb{E}_t \mathcal{O}_{t+1} - \chi \alpha_N}{1-\alpha_N} \mathbb{E}_t[T_{t+1} - T^*] + \frac{\mathbb{E}_t[\hat{z}_{it}]}{1-\alpha_N} \right) + k_0. \tag{60}$$

where $k_0 = \frac{1}{1-\alpha} \left(\log \left[\frac{\alpha G}{r+\delta} \right] \right)$. Therefore, Firm i's investment, relative to the average firm in the economy at date $t+1$, would be:

$$k_{it+1} - \overline{k_{it+1}} = \frac{1}{1-\alpha} \left(\frac{\mathbb{E}_t[\hat{z}_{it+1}]}{1-\alpha_N} + \frac{(\hat{\beta}_i - \overline{\hat{\beta}_i})}{1-\alpha_N} \mathbb{E}_t[(T_{t+1} - T^*)] \right).$$

which is Equation 23 in the main text.

To gain some intuitions, using $\mathbb{E}_t[\mathcal{O}_{t+1}(T_{t+1} - T^*)] = \mathbb{E}_t[\mathcal{O}_{t+1}] \mathbb{E}_t[(T_{t+1} - T^*)] + c\sigma_\eta^2$, we can

also write Equation 60 as

$$\begin{aligned} k_{it+1} =& \frac{1}{1-\alpha}\mathbb{E}_t[a_{it}] + k_0'. \\ =& \frac{1}{1-\alpha}\left(\frac{1}{1-\alpha_N}\mathbb{E}_t[\hat{a}_{it+1}] - \frac{\alpha_N}{1-\alpha_N}\mathbb{E}_t[w_{t+1}-\overline{w}]\right) + k_0' \\ =& \frac{1}{1-\alpha}\left(\frac{1}{1-\alpha_N}\left(\mathbb{E}_t[\hat{z}_{it+1}] + \mathbb{E}_t[\hat{\beta}_{it+1}(T_{t+1}-T^*)]\right) - \frac{\alpha_N\chi}{1-\alpha_N}\mathbb{E}_t[T_{t+1}-T^*]\right) + k_0', \end{aligned} \tag{61}$$

where $k_0' = \frac{1}{1-\alpha}\left(\log\left[\frac{\alpha G}{r+\delta}\right] - \frac{c\sigma_\eta^2}{1-\alpha_N}\right)$. The derivations illustrate the following logic: investment is proportional to the expected profitability of capital, which is increasing in expected (revenue) productivity and decreasing in expected wages. These are, in turn, dependent on the firm's expectation of future temperature sensitivity and future temperature.

E.3 Proof of Proposition 3

Proposition 3 Firms with higher unexpected changes in productivity exhibit higher MRPK relative to the average level:

$$mrpk_{it} - \overline{mrpk_{it}} = \frac{1}{1-\alpha_N}\Bigg\{ \underbrace{(\hat{\beta}_i - \overline{\hat{\beta}_i})\eta_t^T}_{\substack{\text{Unexpected} \\ \text{Temperature Shock} \\ \text{on Productivity}}} + \underbrace{\hat{\xi}_{it}(T_t - T^*)}_{\substack{\text{Unexpected} \\ \text{Damage} \\ \text{Sensitivity}}} + \hat{\varepsilon}_{it} \Bigg\}, \tag{62}$$

where the relative MRPK of heat-averse firms ($\hat{\beta}_i < \overline{\hat{\beta}_i}$) will decrease with a positive temperature shock η_t^T; while the relative MRPK of heat-loving firms ($\hat{\beta}_i > \overline{\hat{\beta}_i}$) will increase with a positive temperature shock.

Proof. Recall that $P_{it}Y_{it} = \hat{A}_{it}K_{it}^{\alpha_K}N_{it}^{\alpha_N}$ and therefore a firm's MRPK can be written as

$$\text{MRPK}_{it} = \frac{\partial P_{it}Y_{it}}{\partial K_{it}} = \alpha_K \frac{P_{it}Y_{it}}{K_{it}}. \tag{63}$$

Note that since $\alpha_K = \frac{\sigma-1}{\sigma}\hat{\alpha}_K$, this definition of MRPK is consistent with the definition in our accounting framework (see Equation 5). Using 53, we can write revenue as

$$\begin{aligned} P_{it}Y_{it} = \frac{\Pi_{it}}{1-\alpha_N} &= \frac{GA_{it}K_{it}^{\alpha}}{1-\alpha_N} \\ &= \overline{G}A_{it}K_{it}^{\alpha}, \end{aligned}$$

where $\overline{G} = \frac{G}{1-\alpha_N}$. Plugging this expression in 63 and taking logs to both sides, we obtain

$$mrpk_{it} = a_{it} + (\alpha - 1)k_{it} + \log(\alpha_K\bar{G}). \tag{64}$$

Plugging in the optimal investment policy k_{it} from 61 into this expression yields

$$\begin{aligned} mrpk_{it} =& (a_{it} - \mathbb{E}_{it-1}[a_{it}]) + \log(r+\delta) + \frac{c\sigma_\eta^2}{1-\alpha_N} \\ =& \frac{1}{1-\alpha_N}\left\{ (\hat{a}_{it} - \mathbb{E}_{it-1}[\hat{a}_{it}]) - \chi\alpha_N(T_t - \mathbb{E}_{t-1}[T_t]) \right\} + \log(r+\delta) + \frac{c\sigma_\eta^2}{1-\alpha_N} \\ =& \frac{1}{1-\alpha_N}\Bigg(\underbrace{\hat{\beta}_i \eta_t^T}_{\substack{\text{Unexpected} \\ \text{T Shock} \\ \text{on Productivity}}} + \underbrace{\hat{\xi}_{it}(T_t - T^*)}_{\substack{\text{Unexpected} \\ \text{Damage} \\ \text{Sensitivity}}} - \underbrace{\chi\alpha_N\eta_t^T}_{\substack{\text{Unexpected} \\ \text{T Shock} \\ \text{on Wage}}} + \hat{\varepsilon}_{it} \Bigg\} + \log(r+\delta) \\ &+ \frac{(\mathcal{O}_t(T_t - T^*) - \mathbb{E}_{t-1}[\mathcal{O}_t]\mathbb{E}_{t-1}[T_t - T^*])}{1-\alpha_N}. \end{aligned} \tag{65}$$

which made clear that MRPK is just the user cost $r+\delta$ in the absence of any forecast error.

To calculate the average mrpk across all firms in a given year $\overline{mrpk_{it}}$, we notice that variables without i subscript will remain the same. And thus, when calculating the difference between $mrpk_{it}$ and $\overline{mrpk_{it}}$, those terms will be canceled out. Knowing this, we achieve the following

$$mrpk_{it} - \overline{mrpk_{it}} = \frac{1}{1-\alpha_N}\left\{ (\hat{\beta}_i - \overline{\hat{\beta}_i})\eta_t^T + \hat{\xi}_{it}(T_t - T^*) + \hat{\varepsilon}_{it} \right\},$$

where $\overline{\hat{\xi}_{it}} = 0$.

■

E.4 Proof of Proposition 4

Proposition 4 Within a region-sector pair $n = (r,s)$, the $mrpk$ dispersion across firms is increasing in TFP Volatility, $\text{Var}(\hat{a}_{nit} - \mathbb{E}_{t-1}[\hat{a}_{nit}])$, and can be decomposed into:

$$\begin{aligned} \sigma^2_{mrpk,(r,s),t} &= \left(\frac{1}{1-\alpha_N}\right)^2 \text{Var}(\hat{a}_{nit} - \mathbb{E}_{t-1}[\hat{a}_{nit}]) \\ &= \left(\frac{1}{1-\alpha_N}\right)^2 \Bigg[\underbrace{(T_{r,t} - T^*)^2 \sigma^2_{\xi,(r,s)}}_{\substack{\text{Damage Volatility} \\ \text{(Level Effect)}}} + \underbrace{{\eta^T_{r,t}}^2 \sigma^2_{\beta,(r,s)}}_{\substack{\text{Climate Uncertainty} \\ \text{(Shock Effect)}}} + \sigma^2_{\varepsilon,(r,s)} \Bigg] \end{aligned} \tag{66}$$

Within $n = (r,s)$, $mrpk$ dispersion is increasing in:

(1) squared deviation from optimal temperature, $(T_{r,t+1} - T^*)^2$,

(2) squared (unexpected) temperature shocks ${\eta^T_{r,t}}^2$.

Proof. From the proof above for Proposition 3, we know that

$$mrpk_{it} = \frac{1}{1-\alpha_N}\left(\hat{a}_{it} - \mathbb{E}_{it-1}[\hat{a}_{it}]\right) + \text{constant terms}$$

We can then compute the variance and obtain the following equation:

$$\begin{aligned}\sigma^2_{mrpk,(r,s),t} &= \left(\frac{1}{1-\alpha_N}\right)^2 \mathrm{Var}(\hat{a}_{nit} - \mathbb{E}_{t-1}[\hat{a}_{nit}]) \\ &= \left(\frac{1}{1-\alpha_N}\right)^2 \Bigg[\underbrace{(T_{r,t} - T^*)^2 \sigma^2_{\xi,(r,s)}}_{\substack{\text{Damage Uncertainty} \\ \text{Channel}}} + \underbrace{\eta^{T\,2}_{r,t} \sigma^2_{\beta,(r,s)}}_{\substack{\text{Climate Uncertainty} \\ \text{Channel}}} + \sigma^2_{\varepsilon,(r,s)}\Bigg].\end{aligned} \tag{67}$$

Note that we have obtained $\mathrm{Var}(\hat{a}_{it} - \mathbb{E}_{t-1}[\hat{a}_{it}]) = (T_t - T^*)^2 \sigma^2_{\hat{\xi}} + \eta^{T\,2}_t \sigma^2_{\hat{\beta}} + \sigma^2_{\hat{\varepsilon}}$ from Equation 50. ■

E.5 Derivation of TFP Loss from Misallocation

This appendix provides the derivation for Equation 26. We now aggregate firm-level production and productivity to the aggregate region-sector level. Labor market clearing implies

$$\begin{aligned}N_t = \int N_{it} di &= \int \left(\frac{\hat{A}_{it} \alpha_N K_{it}^{\alpha_k}}{\overline{W} exp(\chi(T_t - T^*)}\right)^{\frac{1}{1-\alpha_N}} di \\ &= \left(\frac{\alpha_N}{\overline{W}\exp(\chi(T_t - T^*)}\right)^{\frac{1}{1-\alpha_N}} \int \left(\hat{A}_{it} K_{it}^{\alpha_k}\right)^{\frac{1}{1-\alpha_N}} di.\end{aligned}$$

Then we solve for $MRPK_{it}$ through the revenue function.

$$\begin{aligned}P_{it} Y_{it} &= \hat{A}_{it} K_{it}^{\alpha_K} N_{it}^{\alpha_N} \\ &= \hat{A}_{it} K_{it}^{\alpha_K} \left(\frac{\overline{W}\exp\left(\chi(T_t - T^*)\right)}{\hat{A}_{it}\alpha_N K_{it}^{\alpha_k}}\right)^{\frac{\alpha_N}{\alpha_N - 1}}.\end{aligned}$$

Note that from the labor market clearing condition, we can get the following equation

$$\left(\frac{\overline{W}\exp(\chi(T_t - T^*))}{\alpha_N}\right)^{\frac{1}{\alpha_N - 1}} = \frac{N_t}{\int \left(\hat{A}_{it} K_{it}^{\alpha_K}\right)^{\frac{1}{1-\alpha_N}} di}.$$

We plug this back into the revenue function and get

$$\begin{aligned}P_{it} Y_{it} &= \hat{A}_{it} K_{it}^{\alpha_K} (\hat{A}_{it} K_{it}^{\alpha_K})^{\frac{\alpha_N}{1-\alpha_N}} \left(\frac{N_t}{\int \left(\hat{A}_{it} K_{it}^{\alpha_K}\right)^{\frac{1}{1-\alpha_N}} di}\right)^{\alpha_N} \\ &= \left(\hat{A}_{it} K_{it}^{\alpha_K}\right)^{\frac{1}{1-\alpha_N}} \cdot \left(\frac{N_t}{\int \left(\hat{A}_{it} K_{it}^{\alpha_K}\right)^{\frac{1}{1-\alpha_N}} di}\right)^{\alpha_N}\end{aligned} \tag{68}$$

From this, we can solve for $MRPK_{it}$. Note that $MRPK_{it} = \alpha_K \frac{P_{it}Y_{it}}{K_{it}} = \alpha_K \frac{\hat{A}_{it} K_{it}^{\alpha_K} N_{it}^{\alpha_N}}{K_{it}}$.[48] Plugging in the expression of revenue function, we get

$$MRPK_{it} = \alpha_K \hat{A}_{it}^{\frac{1}{1-\alpha_N}} K_{it}^{\theta-1} \cdot \left(\frac{N_t}{\int \left(\hat{A}_{it} K_{it}^{\alpha_K} \right)^{\frac{1}{1-\alpha_N}} di} \right)^{\alpha_N},$$

where $\theta = \frac{\alpha_K}{1-\alpha_N}$. Next we rearrange terms to find expressions for K_{it}

$$K_{it} = \left(\frac{\alpha_K \hat{A}_{it}^{\frac{1}{1-\alpha_N}}}{MRPK_{it}} \right)^{\frac{1}{1-\theta}} \cdot \left(\frac{N_t}{\int \left(\hat{A}_{it} K_{it}^{\alpha_K} \right)^{\frac{1}{1-\alpha_N}} di} \right)^{\frac{\alpha_N}{1-\theta}}$$

We now use the capital market clearing condition

$$\begin{aligned} K_t &= \int K_{it} di \\ &= \alpha_K^{\frac{1}{1-\theta}} \cdot \left(\frac{N_t}{\int \left(\hat{A}_{it} K_{it}^{\alpha_K} \right)^{\frac{1}{1-\alpha_N}} di} \right)^{\frac{\alpha_N}{1-\theta}} \int \left(\frac{\hat{A}_{it}^{\frac{1}{1-\alpha_N}}}{MRPK_{it}} \right)^{\frac{1}{1-\theta}} di \end{aligned}$$

Rearrange terms we can have

$$\left(\frac{N_t}{\int \left(\hat{A}_{it} K_{it}^{\alpha_K} \right)^{\frac{1}{1-\alpha_N}} di} \right)^{\frac{\alpha_N}{1-\theta}} = \frac{K_t}{\alpha_K^{\frac{1}{1-\theta}} \int \left(\frac{\hat{A}_{it}^{\frac{1}{1-\alpha_N}}}{MRPK_{it}} \right)^{\frac{1}{1-\theta}} di}$$

We can plug this equation to the expression for K_{it}

$$\begin{aligned} K_{it} &= \left(\frac{\alpha_K \hat{A}_{it}^{\frac{1}{1-\alpha_N}}}{MRPK_{it}} \right)^{\frac{1}{1-\theta}} \cdot \frac{K_t}{\alpha_K^{\frac{1}{1-\theta}} \int \left(\frac{\hat{A}_{it}^{\frac{1}{1-\alpha_N}}}{MRPK_{it}} \right)^{\frac{1}{1-\theta}} di} \\ &= \frac{\hat{A}_{it}^{\frac{1}{1-\alpha_N}\frac{1}{1-\theta}} MRPK_{it}^{\frac{-1}{1-\theta}}}{\int \hat{A}_{it}^{\frac{1}{1-\alpha_N}\frac{1}{1-\theta}} MRPK_{it}^{\frac{-1}{1-\theta}} di} K_t \end{aligned}$$

48. Note that it's also fine to use the derivative definition of MRPK. This term will cancel out later.

We now have solved for N_{it}, K_{it} all in terms of $MRPK_{it}$ and aggregate variables N_t and K_t. We plug N_{it}, K_{it} back into Equation 68 and get

$$\begin{aligned} P_{it}Y_{it} &= \left(\hat{A}_{it}K_{it}^{\alpha_K}\right)^{\frac{1}{1-\alpha_N}} \cdot \left(\frac{N_t}{\int \left(\hat{A}_{it}K_{it}^{\alpha_K}\right)^{\frac{1}{1-\alpha_N}} di}\right)^{\alpha_N} \\ &= \frac{\hat{A}_{it}^{\frac{1}{1-\alpha_N}\frac{1}{1-\theta}} MRPK_{it}^{\frac{-\theta}{1-\theta}}}{\left(\int \hat{A}_{it}^{\frac{1}{1-\alpha_N}\frac{1}{1-\theta}} MRPK_{it}^{\frac{-\theta}{1-\theta}} di\right)^{\alpha_N} \left(\int \hat{A}_{it}^{\frac{1}{1-\alpha_N}\frac{1}{1-\theta}} MRPK_{it}^{\frac{-1}{1-\theta}} di\right)^{\alpha_K}} K_t^{\alpha_K} N_t^{\alpha_N} \end{aligned}$$

Using $P_{it}Y_{it} = B_{it}^{\frac{1}{\sigma}} Y_{it}^{\frac{\sigma-1}{\sigma}}$, we can write aggregate output as

$$\begin{aligned} Y_t &= \left(\int B_{it}^{\frac{1}{\sigma}} Y_{it}^{\frac{\sigma-1}{\sigma}} di\right)^{\frac{\sigma}{\sigma-1}} = \left(\int P_{it}Y_{it} di\right)^{\frac{\sigma}{\sigma-1}} \\ &= \left[\frac{\int \hat{A}_{it}^{\frac{1}{1-\alpha_N}\frac{1}{1-\theta}} MRPK_{it}^{\frac{-\theta}{1-\theta}} di}{\left(\int \hat{A}_{it}^{\frac{1}{1-\alpha_N}\frac{1}{1-\theta}} MRPK_{it}^{\frac{-\theta}{1-\theta}} di\right)^{\alpha_N} \left(\int \hat{A}_{it}^{\frac{1}{1-\alpha_N}\frac{1}{1-\theta}} MRPK_{it}^{\frac{-1}{1-\theta}} di\right)^{\alpha_K}}\right]^{\frac{\sigma}{\sigma-1}} K_t^{\alpha_K \frac{\sigma}{\sigma-1}} N_t^{\alpha_N \frac{\sigma}{\sigma-1}} \\ &= \tilde{A}_t^{\frac{\sigma}{\sigma-1}} K_t^{\tilde{\alpha}_K} N_t^{\tilde{\alpha}_N}, \end{aligned} \tag{69}$$

where we define $\tilde{A}_t := \frac{\left(\int \hat{A}_{it}^{\frac{1}{1-\alpha_N}\frac{1}{1-\theta}} MRPK_{it}^{\frac{-\theta}{1-\theta}} di\right)^{1-\alpha_N}}{\left(\int \hat{A}_{it}^{\frac{1}{1-\alpha_N}\frac{1}{1-\theta}} MRPK_{it}^{\frac{-1}{1-\theta}} di\right)^{\alpha_K}}$. We take logs to $\tilde{A}_t$ and get

$$\tilde{a}_t = (1-\alpha_N)\left[\log\left(\int \mathring{A}_{it}^{\frac{1}{1-\theta}} MRPK_{it}^{-\frac{\theta}{1-\theta}}\right) - \theta \log\left(\int \mathring{A}_{it}^{\frac{1}{1-\theta}} MRPK_{it}^{-\frac{1}{1-\theta}}\right)\right],$$

where $\mathring{A}_{it} = \hat{A}_{it}^{\frac{1}{1-\alpha_N}}$. Now, assuming log-normality, the first term is equal to

$$\begin{aligned} \log\left(\int \mathring{A}_{it}^{\frac{1}{1-\theta}} MRPK_{it}^{-\frac{\theta}{1-\theta}}\right) &= \frac{1}{1-\theta}\overline{\mathring{a}_{it}} - \frac{\theta}{1-\theta}\overline{mrpk_{it}} \\ &\quad + \frac{1}{2}\left(\frac{1}{1-\theta}\right)^2 \sigma_{\mathring{a},t}^2 + \frac{1}{2}\left(\frac{\theta}{1-\theta}\right)^2 \sigma_{mrpk,t}^2 - \frac{\theta}{(1-\theta)^2}\sigma_{mrpk,\mathring{a},t} \end{aligned}$$

The second term is equal to

$$\begin{aligned} \theta \log\left(\int \mathring{A}_{it}^{\frac{1}{1-\theta}} MRPK_{it}^{-\frac{1}{1-\theta}}\right) &= \frac{\theta}{1-\theta}\overline{\mathring{a}_{it}} - \frac{\theta}{1-\theta}\overline{mrpk_{it}} \\ &\quad + \frac{1}{2}\theta\left(\frac{1}{1-\theta}\right)^2 \sigma_{\mathring{a},t}^2 + \frac{1}{2}\theta\left(\frac{1}{1-\theta}\right)^2 \sigma_{mrpk,t}^2 - \frac{\theta}{(1-\theta)^2}\sigma_{mrpk,\mathring{a},t} \end{aligned}$$

Combining them together, we have the following equation for aggregate productivity

$$\tilde{a}_t = (1-\alpha_N)\left[\overline{\mathring{a}_t} + \frac{1}{2}\frac{1}{1-\theta}\sigma_{\mathring{a},t}^2 - \frac{1}{2}\frac{\theta}{1-\theta}\sigma_{mrpk,t}^2\right]$$

Using Equation 69, we write the log aggregate output as

$$\begin{aligned} y_t &= \frac{\sigma}{\sigma-1}\tilde{a}_t + \tilde{\alpha}_K k_t + \tilde{\alpha}_N n_t \\ &= \frac{\sigma}{\sigma-1}(1-\alpha_N)\left[\overline{\mathring{a}_t} + \frac{1}{2}\frac{1}{1-\theta}\sigma^2_{\mathring{a},t} - \frac{1}{2}\frac{\theta}{1-\theta}\sigma^2_{mrpk,t}\right] + \tilde{\alpha}_K k_t + \tilde{\alpha}_N n_t \\ &= a_t + \tilde{\alpha}_K k_t + \tilde{\alpha}_N n_t, \end{aligned}$$

where the total factor productivity is defined as

$$\begin{aligned} a_t =& \frac{\sigma}{\sigma-1}(1-\alpha_N)\left[\overline{\mathring{a}_{it}} + \frac{1}{2}\frac{1}{1-\alpha}\sigma^2_{\mathring{a},t} - \frac{1}{2}\frac{\alpha}{1-\alpha}\sigma^2_{mrpk,t}\right] \\ =& \frac{\sigma}{\sigma-1}\overline{\hat{a}_{it}} + \frac{1}{2}\frac{\sigma}{\sigma-1}\frac{1}{(1-\alpha)(1-\alpha_N)}\sigma^2_{\hat{a},t} \\ & - \frac{1}{2}\frac{\sigma}{\sigma-1}\frac{\alpha_K}{1-\alpha}\sigma^2_{mrpk,t} \end{aligned}$$

Finally, we plug in the definition for $\overline{\hat{a}_{it}}$ and $\sigma^2_{\hat{a},t}$, and we can write the TFP as

$$\begin{aligned} a_{nt} =& \frac{\sigma}{\sigma-1}\left[\overline{\hat{\beta}_i}(T_t - T^*) + c(T_t - T^*)^2\right] \\ & + \frac{\sigma}{2}\frac{\sigma}{\sigma-1}\left[\left(\sigma^2_{\hat{\beta}} + \sigma^2_{\hat{\xi}}\right)(T_t - T^*)^2 + \frac{\sigma^2_{\hat{\varepsilon}}}{1-\rho^2_z}\right] \\ & - \frac{\tilde{\alpha}_K + \tilde{\alpha}^2_K(\sigma-1)}{2}\left(\frac{1}{1-\alpha_N}\right)^2\left[(T_t - T^*)^2\sigma^2_{\hat{\xi}} + \eta_t^{T^2}\sigma^2_{\hat{\beta}} + \sigma^2_{\hat{\varepsilon}}\right] \end{aligned} \tag{70}$$

Under the parametrization that $c = -\frac{\sigma}{2}\left(\sigma^2_{\hat{\beta}} + \sigma^2_{\hat{\xi}}\right)$, we will have

$$\begin{aligned} a_t =& a^*_t - \text{Misallocation Loss}_t \\ =& \frac{\sigma}{\sigma-1}\left[\overline{\hat{\beta}_i}(T_t - T^*)\right] + \frac{\sigma}{2}\frac{\sigma}{\sigma-1}\left[\frac{\sigma^2_{\hat{\varepsilon}}}{1-\rho^2_z}\right] \\ & - \frac{\tilde{\alpha}_K + \tilde{\alpha}^2_K(\sigma-1)}{2}\left(\frac{1}{1-\alpha_N}\right)^2\left[(T_t - T^*)^2\sigma^2_{\hat{\xi}} + \eta_t^{T^2}\sigma^2_{\hat{\beta}} + \sigma^2_{\hat{\varepsilon}}\right] \end{aligned} \tag{71}$$

E.6 General Solution of the Firm's Investment Problem

This Appendix outlines the general solution of the firm's investment problem without using the first-order approximation method in Section 5. We will discuss why our first-order approximation is valid for both the theoretical analysis and the empirical identification of key model parameters.

We rearrange the Euler equation in equation 22 to get the expression for optimal capital

$$\begin{aligned} K_{it}^{1-\alpha} =& \frac{\alpha G}{r+\delta}\mathbb{E}_{t-1}\left[\exp\left(a_{it}\right)\right] \\ =& \frac{\alpha G}{r+\delta}\frac{1}{\sqrt{d}}e^{\left(\frac{\left(\frac{(\hat{\beta}_i-\chi\alpha_N)}{(1-\alpha_N)}\mathbb{E}_{t-1}[(T_t-T^*)]+\frac{1}{2}\frac{(\hat{\beta}_i-\chi\alpha_N)^2\sigma_\eta^2}{(1-\alpha_N)^2}+\frac{c}{(1-\alpha_N)}(\mathbb{E}_{t-1}[(T_t-T^*)])^2+\frac{1}{2}\frac{\sigma_{\hat{\xi}}^2}{(1-\alpha_N)^2}(\mathbb{E}_{t-1}[(T_t-T^*)])^2}{d}\right)} \\ & \cdot e^{\left(\frac{\rho_z\hat{z}_{it-1}}{1-\alpha_N}+\frac{\sigma_{\hat{\varepsilon}}^2}{2(1-\alpha_N)^2}\right)} \end{aligned} \tag{72}$$

where $d = 1 - 2\frac{c\sigma_\eta^2}{1-\alpha_N} - \frac{\sigma_\eta^2\sigma_{\hat{\xi}}^2}{(1-\alpha_N)^2}$. Notice that the risk-adjusted terms are small (as shown by our estimation), so empirically we have that $d \approx 1$.

Taking logs on both sides yields the investment decision:

$$\begin{aligned} k_{it} =& \frac{1}{(1-\alpha)d}\left(\frac{(\hat{\beta}_i-\chi\alpha_N)}{(1-\alpha_N)}\mathbb{E}_{t-1}[(T_t-T^*)] + \frac{c}{(1-\alpha_N)}(\mathbb{E}_{t-1}[(T_t-T^*)])^2 + \frac{1}{2}\frac{\sigma_{\hat{\xi}}^2}{(1-\alpha_N)^2}(\mathbb{E}_{t-1}[(T_t-T^*)])^2\right. \\ & \left. + \frac{1}{2}\frac{(\hat{\beta}_i-\chi\alpha_N)^2\sigma_\eta^2}{(1-\alpha_N)^2}\right) + \frac{1}{1-\alpha}\left(\rho_z z_{it-1} + \frac{1}{2}\sigma_\varepsilon^2\right) + \frac{1}{1-\alpha}\log\left(\frac{\alpha G}{(r+\delta)\sqrt{d}}\right) \\ =& \frac{1}{(1-\alpha)d}\left(\mathbb{E}_{t-1}[a_{it}-z_{it}] - \frac{c\sigma_\eta^2}{1-\alpha_N} + \frac{1}{2}\frac{\sigma_{\hat{\xi}}^2}{(1-\alpha_N)^2}(\mathbb{E}_{t-1}[(T_t-T^*)])^2 + \frac{1}{2}\frac{(\hat{\beta}_i-\chi\alpha_N)^2\sigma_\eta^2}{(1-\alpha_N)^2}\right) \\ & + \frac{1}{1-\alpha}\left(\rho_z z_{it-1} + \frac{1}{2}\sigma_\varepsilon^2\right) + \frac{1}{1-\alpha}\log\left(\frac{\alpha G}{(r+\delta)\sqrt{d}}\right). \end{aligned} \tag{73}$$

The $mrpk$ of a firm can be then expressed as:

$$\begin{aligned} mrpk_{it} =& \beta_i\left(\frac{d-1}{d}(T_t-T^*) + \frac{1}{d}(T_t-\mathbb{E}[T_t])\right) + \frac{1}{2}\frac{\beta_i^2\sigma_\eta^2}{d} + \xi_{it}(T_t-T^*) + \varepsilon_{it} \\ & + \frac{(\mathcal{O}_t(T_t-T^*) - \mathbb{E}_{t-1}[\mathcal{O}_t]\mathbb{E}_{t-1}[T_t-T^*])}{1-\alpha_N} \\ & + \left(\frac{1}{2}\frac{\sigma_{\hat{\xi}}^2}{d}(\mathbb{E}_{t-1}[(T_t-T^*)])^2\right) \\ & - \frac{1}{2}\sigma_\varepsilon^2 + \log\left(\frac{\alpha G}{(r+\delta)\sqrt{d}}\right). \end{aligned} \tag{74}$$

We now take variance of both sides of the $mrpk$ expression and use the fact that for a standard normal variable $x \sim \mathcal{N}(\mu, \sigma^2)$, $\text{Var}(Ax + Bx^2) = (A + 2B\mu)^2\sigma^2 + 2\mu^2\sigma^4$. A few lines of algebra

yields:

$$\begin{aligned}\sigma^2_{mrpk,t} =& \Big(\frac{d-1}{d}(T_t - T^*) + \frac{1}{d}(T_t - \mathbb{E}[T_t]) + \frac{\sigma^2_\eta \bar{\beta}}{d}\Big)^2 \sigma^2_\beta + 2\bar{\beta}^2\sigma^4_\beta + (T_t - T^*)^2\sigma^2_\xi + \sigma^2_\varepsilon \\ =& \frac{(d-1)^2}{d^2}\sigma^2_\beta\,(T_t - T^*)^2 + \frac{1}{d^2}\sigma^2_\beta\,(T_t - \mathbb{E}\,[T_t])^2 + \sigma^2_\xi (T_t - T^*)^2 + 2\frac{d-1}{d^2}\sigma^2_\beta\,(T_t - T^*)\,(T_t - \mathbb{E}\,[T_t]) \\ &+ 2\frac{(d-1)\sigma^2_\eta\sigma^2_\beta\bar{\beta}}{d^2}\,(T_t - T^*) + 2\frac{\sigma^2_\eta\sigma^2_\beta\bar{\beta}}{d^2}\,(T_t - \mathbb{E}\,[T_t]) + \frac{\left(\sigma^2_\eta\bar{\beta}\right)^2\sigma^2_\beta}{d^2} + 2\bar{\beta}^2\sigma^4_\beta + \sigma^2_\varepsilon\end{aligned}$$

Lastly, notice that since $d \approx 1$, as our empirical results suggest, the above expression can be approximated as:

$$\begin{aligned}\sigma^2_{mrpk,t} \approx& \frac{1}{(1-\alpha_N)^2}\Bigg(\sigma^2_{\hat{\beta}}\eta_t^{T\,2} + \sigma^2_{\hat{\xi}}(T_t - T^*)^2 + \sigma^2_{\hat{\varepsilon}} \\ &+ 2\frac{\sigma^2_{\eta^T}\sigma^2_{\hat{\beta}}(\bar{\hat{\beta}} - \chi\alpha_N)}{(1-\alpha_N)}\eta_t^T + \frac{\bar{\hat{\beta}}^2\sigma^2_{\hat{\beta}}\sigma^4_{\eta^T}}{(1-\alpha_N)^2} + 2\frac{(\bar{\hat{\beta}} - \chi\alpha_N)^2\sigma^4_{\hat{\beta}}}{(1-\alpha_N)^4}\Bigg)\end{aligned}$$

where we have used that $\sigma^2_\beta = \frac{\sigma^2_{\hat{\beta}}}{(1-\alpha_N)^2}$, $\sigma^2_\xi = \frac{\sigma^2_{\hat{\xi}}}{(1-\alpha_N)^2}$. Notice that apart from the risk-adjusted terms in the second line, the first line of this equation yields exactly Equation 25 in the main text.

We now discuss in detail why the risk-adjusted terms in the second line do not affect our analysis. First, regarding the identification of $\sigma^2_{\hat{\beta}}$ and $\sigma^2_{\hat{\xi}}$ in the regression specification of Equation **??**, the linear term $\frac{\sigma^2_{\eta^T}\sigma^2_{\hat{\beta}}(\bar{\hat{\beta}}-\chi\alpha_N)}{(1-\alpha_N)}\eta_t^T$ does not affect the identification of $\sigma^2_{\hat{\beta}}$, given that $\eta_t^T \sim N(0, \sigma^2_{\eta^T})$. Even if we use the monthly aggregated index, $\text{MSFE}_{\text{annual},r,t} = \sum_{m=1}^{12}\eta_{m,t}^{T\,2}$, as an empirical counterpart for $\eta_t^{T\,2}$, the forecast error of any month remains uncorrelated with $\text{MSFE}_{\text{annual},r,t}$ as long as $\eta^T_{m,t} \sim N(0, \Sigma_{\eta^T_m\eta^T_m})$.

Second, regarding the analysis of the computed average misallocation, the linear term $\frac{\sigma^2_{\eta^T}\sigma^2_{\hat{\beta}}(\bar{\hat{\beta}}-\chi\alpha_N)}{(1-\alpha_N)}\eta_t^T$ has a mean of zero and does not affect the average misallocation around year τ, $\mathbb{E}_t[\sigma^2_{mrpk,t+\tau} \mid \bar{T}', \sigma'^2_{\eta^T}]$, given the temperature distribution or forecastability $(\bar{T}', \sigma'^2_{\eta^T})$. The constant term $\frac{\sigma^4_{\eta^T}\bar{\hat{\beta}}^2\sigma^2_{\hat{\beta}}}{(1-\alpha_N)^2}$ is small as it is of the fourth order in σ_{η^T}. If we are interested in analyzing a positive change in $\sigma^2_{\eta^T}$, ignoring this term would only lead to an underestimate of the welfare loss associated with MRPK dispersion; similarly, for a negative change in $\sigma^2_{\eta^T}$ (i.e., a decrease in forecast error), ignoring this term would lead to an underestimate of the benefits. Thus, we will always capture a conservative lower bound. Therefore, we conclude that the first-order approximation approach in the main text is valid for the purpose of analysis.